Universitat de Girona
Escola Politècnica Superior

Incoming Exchange Student - Master Thesis

Erasmus □ **Techno** □ **Other (specify):**

Title of master course: Master en Enginyeria Informatica

Title of master thesis: "Behavioural investigation of campus consumption against potential renewable generation for self-sustainability model"

Document: Master Thesis

Student (Name & Surname): Euan McGill

EPS Advisor: Joaquim Melendaz
Department: Eng. Elèctrica, Electrònica i Automàtica

Delivered on (month/year): 06/2015

Euan McGill

Masters Thesis

Department of electrical, electronic and automation engineering

"Behavioural investigation of campus consumption against potential renewable generation for self-sustainability model"

2015

Abstract

At present the university hosts a small commercial PV installation located on a small section of the EPS rooftop area. In this system all production is fed directly back into the utility grid through a series of small DC-AC convertors. This PV array covers only a very small portion of the overall roof top surface area which the Montilivi campus has to offer. This report aims to investigate the potential for the campus to become fully self-sufficient with regards to its energy consumption by expanding this existing system, and thus further utilising the wonderful solar resource which is available in the area. This report will use a Matlab simulation validated using the current installation in order to investigate the potential energy production capabilities of the university with the solar array expanded over the full campus. State of the art technologies which have been developed since the current systems construction will also be investigated and included in the simulation. Observing the results, it will be possible to clearly understand the further benefits in terms of production which these new technologies could propose to such a system. Other topics which will be explored include demand side management; observing how peaks in demand could be potentially altered through user behaviour in order to ensure that maximum production and consumption align throughout the day. In addition to analysing the effects of increasing the universities production capacity, a series of case studies will be examined in order to observe how campus consumption could be vastly reduced through both intelligent design and also energy saving incentives. The results from this report will provide vital data regarding both the daily and monthly "Production Vs Consumption" relationships for this newly proposed system. This data will be essential for use in a parallel study which will assess the financial feasibility of the expansion and also propose new ideas for how the energy produced should be consumed. Based or current market prices for both small scale generators feeding in and also consumers buying out from the grid, different utilisation methods will be discussed including battery storage, grid export and direct consumption in order to provide an insight into the most profitable option or combination of options for this specific investigation.

Contents

Table of Figures

Table of Tables

1. Introduction

1.1 Motivation

Recent years have seen a rapid increase in the uptake of renewable energy projects all across the globe. Within the overall umbrella term "renewables" one of the largest subcategories is that of solar power, specifically solar photovoltaics. Typical solar PV projects vary greatly in terms of both scale and application, from residential systems on individual homes to enormous solar farms feeding into the transmission grid.

There are a wide variety of reasons which have led to this increase in PV deployment across the globe. Some of the most important factors are listed below.

- Irratic nature of oil market. (long term availability, Price Etc.)
- Government incentives. (feed in tarrifs, tax breaks Etc.)
- Decrease in cost of PV technologies due to mass manufacturing.
- Increased efficiency resulting in further decreaeses in weighted costs ($/W).
- Global concerns for enviroment.
- Increasings energy costs.

As a direct result of the above factors the total number of PV installations across the globe has increased many folds over the last 10 years. The figure below represents this increase for the USA alone, showing a dramatic increase in number of new installations each year. The effective cost per watt of production is also seen, with decreases in this value corresponding to increases in new installations. This reinforces the point mentioned above regarding key drivers for increases in PV deployment. Both of these trends only serve to further substantiate the view that whilst solar PV can propose fantastic energy and cost savings at present, it is likely to become even more beneficial for generators in the future.

Figure 1: USA annual increase in solar installations [19].

Not limited to the USA alone however, global uptake in PV installations has been dramatically increasingly across all of the continents. As seen in figure 2 below 2013 seen a 35% increase in the world's total installed PV capacity, with Asian countries such as China and Japan leading the way.

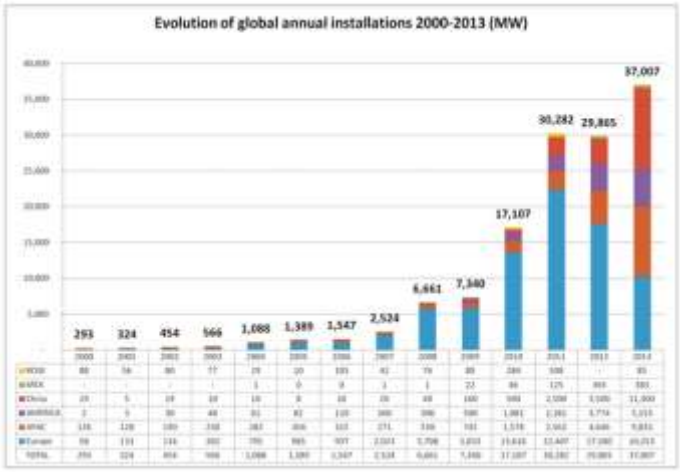

Figure 2: Global annual increase in solar installations [20].

It was seen previously that the weighted costs of solar have been declining each year. Recent figures from the Solar energy industries association (SEIA) however show that in fact weighted system costs are reducing monthly as can be seen below.

Figure 3: Quarterly reduction in weighted system costs[19].

It was noted previously that this decreases in the weighted price of PV due to increases in efficiency and cheap mass manufacturing is only one of many key reasons as to why uptake in PV has increased in recent years. In fact it is the combined effect of all the factors listed previously that has resulted in PV contributing towards an increasingly large percentage of

worldwide energy production. The extent to which solar PV is increasing its percentage of the US energy mix is highlighted below. Important to note however is that the USA represents a healthy average for the majority of developed nations as seen previously in figure 2, with the USA placing roughly mid table with regards to PV deployment.

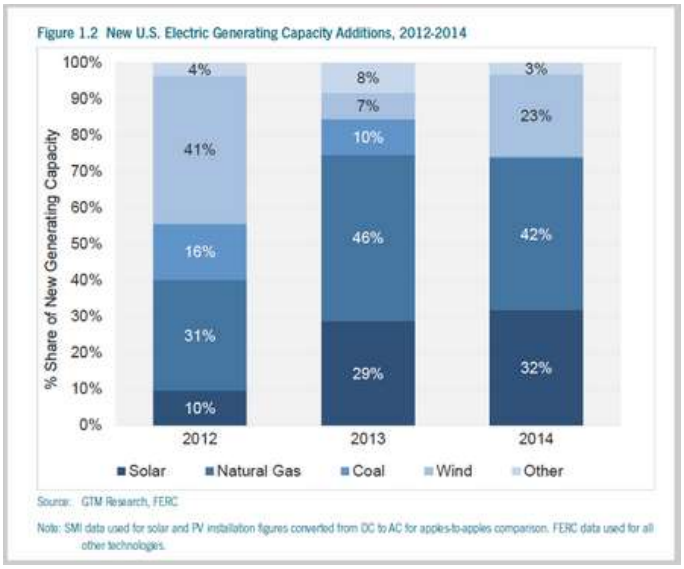

Figure 4: Yearly variation in US energy mix.[19]

To conclude, the globally installed PV capacity has dramatically increased in recent years and is set to continue to in the future. With the cost of conventional electricity increasing and the relative cost of PV energy on the decline, now is an ideal time for both residential and non-residential consumers to looks towards the idea of self-sufficient or partly self-sufficient systems in order to provide a reliable cost effective energy source for years to come. It is important to note at this stage that there is at present lots of evidence which suggest PV solutions on all scales can provide fantastic reductions in energy costs and installation payback periods well within system lifetime. However, in order to understand exactly the potential for PV production at the Montilivi campus and thus the savings which could be made, a detailed investigation of the specific site must be had. This investigation will be detailed in the following sections of this report.

1.2 Current installation configuration

The Photovoltaic Installation at the University of Girona Campus is Typical of Many systems which were deployed as a result of government incentives offering High feed in tariffs for renewable generation. Consequently all generation is exported back into the distribution grid with none being directly consumed on site.

The key components which make up the system include the following;

- 96 × 160W PV Modules
- 6 × DC-AC invertors
- A range of different protection technologies
- Metering equipment

A geometric schematic of the PV installation as well as the circuit diagram can be seen below.

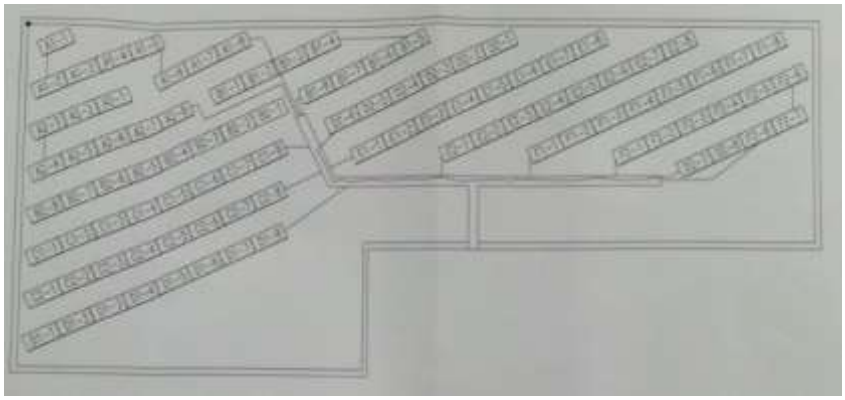

Figure 5: Geometric schematic of current installation.

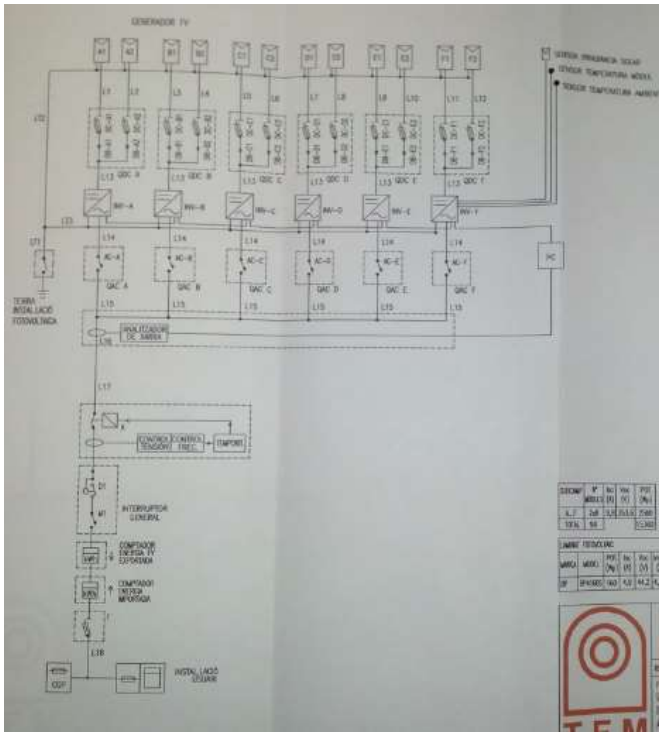

Figure 6: Current installation circuit diagram.

Each of the fore mentioned 96 solar modules are manufactured by BP solar. The exact models used on sight are the BP 4160 which has the following specification.

Potencia máxima, Pmáx. (Wp).	160
Tensión en circuito abierto, Voc (V).	44,2
Corriente de máxima potencia, Imáx (A).	4,52
Tensión de máxima potencia, Vmáx (V).	35,4
Intensidad de cortocircuito. Isc (A).	4,9

Figure 7: System solar panels technical specification.

As can be seen in Figures 6 and 7 above, the overall solar Array is subdivided into a series of smaller arrays. There are six of these smaller arrays each of which is fed into its own DC-AC inverter. For each inverter the sub array consists of 16 modules. These 16 modules are configured as 2 parallel branches of 8 series connected panels.

The inverters used in the system are SMA 2500 models. These inverters have the following specification.

Model	SMA 2500
Potencia nominal AC	2200 VA
Potencia maxima AC	2500 VA
Corrent maxim d'entrada	12A
Rang MPPT	224 - 600 V DC
Eficiencia energetica maxima	94%
Distorsio de corrent (Harmonics)	< 4%
operacio	Monofasic
pes	30kg
temperatura de funcionament	minus 25 °C a 60 °C

Figure 8: System solar inverter technical specification.

The power and voltage ratings of this inverter are ideally suited for the 16 module sub array configuration discussed above.

What can also be seen alongside the DC-AC inverters in the circuit schematic are a series of the different electrical and climatic parameters which the system measures. These include Irradiance, ambient temperature and panel temperature as well as the instantaneous power produced by the system.

In addition to the Instantaneous power measured by the PC seen in figure 6 the system also contains metering equipment for measuring the kWh energy consumption and production of the system over long periods of time.

2. System software model

The very first stage in this overall analysis of the universities potential PV capacity was to create a software model which accurately represented the system at present. Using the Local climatic conditions from the university weather station as inputs to this model, the simulation outputs could be compared with the data recorded by the system's power loggers. This comparison could then be used to identify any underlying error in the simulation, which could then be accounted for accordingly. Upon verifying a model of the existing system, the simulation could then be very simply altered in order to represent a fully expanded system over the full campus. From this the PV generation potential of the campus could be very effectively analyzed .In order to produce this model; the Matlab environment was elected. Within this software and the many different modeling libraries it contains there exists many different ways for modeling PV generation, each of which varying in its level of complexity and detail. Two of these different methods are discussed below.

2.1 Simelectronics solar cell

This is arguably the most accurate and also by far the easiest method of analyzing PV generation within the Matlab environment. Available is a predefined component block which can simulate the behavior of either the single or double diode representation of a solar cell. Already programmed into the model are a series of the parameters which effect the performance of the cell including for example; series and shunt resistances, temperature and irradiance effects, and diode quality factor to name a few. Individual cells need only be connected in series and parallel in order to produce a panel of the required rating. Seen below are the component mask and also the individual components from which it is constructed.

Figure 9: Simelectronics solar cell mask.

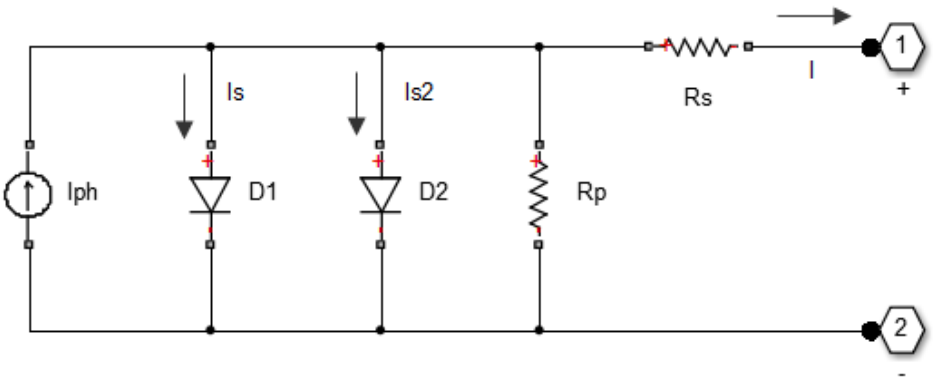

Figure 10: Solar cell equivilent circuit.

For this analysis however, this model was disregarded. This was purely down to the fact that the complexity of this predefined model results in significantly larger simulation times than some of the alternative approaches. For the long term irradiance and temperature analysis which will be carried out here, where a series of months' worth of data will be examined in one simulation a different approach would be better suited. Reduced flexibility is also another drawback compared with a user defined model. For this reason instead a user purely formulae based Simulink approach would be adopted.

2.2 Matlab equation based approach

The fundamental mathematical equations which govern the behavior of a solar cell are well known. Although there are different methods of describing this behavior the most common and widely accepted is the Shockley diode equation. This equation describes the behavior of a cell in terms of the equivalent circuit model seen previously in figure 10. It contains a range of different physical parameters; both scientific constants and parameters relevant to the specific cell technology which can be easily obtained from any manufacturer data sheet. The approach used in this thesis utilizes a method studied by Francisco M. González-Longatt [7] which uses these fundamental equations alongside a well-known numerical method in order to simulate the behavior of a single cell. Using this computational method the required parameter variations can then be made in order to construct a simulation representative of any specific cell technology. Applying some established circuit theory the simulation can then be scaled to represent either an individual panel or an overall array like that currently located at the UDG.

2.2.1 Fundamental formulae

As seen in figure 11 the equivalent circuit of the solar cell consists of current source in parallel with a diode, where the current output from the source is directly proportional on the incident irradiance (sunlight). When no sunlight is present therefor, the circuit functions exactly as a diode; producing no current or voltage. If this diode was to be connected to an external voltage however current would flow, this current is known as the "dark" current and it is this which largely determines the behavior of our cell. The cell output depends upon both the photocurrent produced due to incident light and also this "dark" current characteristic of the diode. This behavior can be seen below where the photocurrent is denoted I_l and the "dark" or diode current as D.

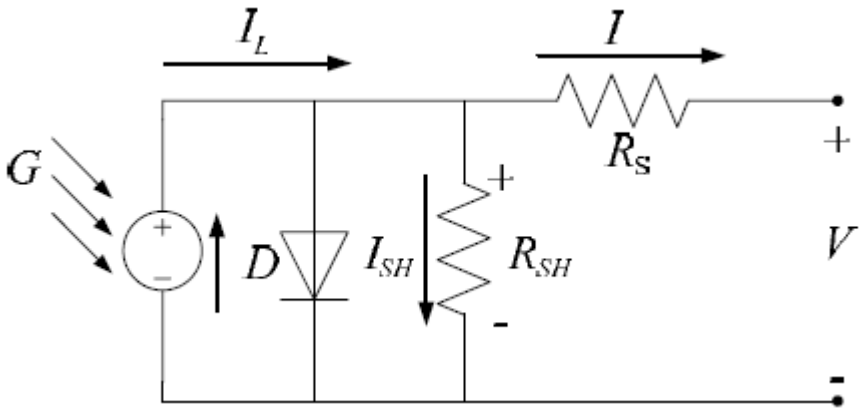

Figure 11: Equivalent circuit parameters[7].

Both R_s and R_{sh} represent parasitic effects on the cell output due to the materials from which they are constructed. Ideally R_s would be equal to zero and R_{sh} would be infinite, however in reality this is never the case. In this simulation the effects of the shunt resistance are ignored meaning the output from the cell is simply the difference between the photocurrent and the diode current. The effect of the series resistance however is considered and affects the output from the cell, denoted I as seen below.

$$I = I_l - I_o\left(e^{\left(\frac{q(V+IR_S)}{nKT}\right)} - 1\right) \quad (1)$$

Where;

- I_o = dark saturation current
- V = cell terminal voltage
- T = cell temperature in kelvin
- n = cell quality factor
- K = Boltzmann constant
- q = electron charge
- V_g = band gap of semiconductor material
- V = cell terminal voltage

In reality both the photocurrent, I_l and the dark saturation current, I_o are effected by temperature. It is therefore important that this behavior is included in the model. The effect on both I_l and I_o can be seen in equations 2 and 3 respectively.

$$I_l = I_l(T_1) + K_0(T - T_1) \quad (2)$$

$$I_0 = I_0(T_1) \times \left(\frac{T}{T_1}\right)^{\frac{3}{n}} e^{\frac{qV_g(T_1)}{nk\left(\frac{1}{T} - \frac{1}{T_1}\right)}} \quad (3)$$

K_o as seen above is the temperature-current coefficient and is characteristic of the cell material. This constant can be easily obtained via the panel data sheet.

In order to compute the functions seen in equations 2 and 3 both I_l and I_0 at reference temperature T_1 are required. Equations 4 and 5 seen below describe how both the light generated current and also the dark saturation current at reference temperature are calculated.

$I_l(T_1)$ is directly proportional to the incident sunlight. G_{nom} and T_{nom} are the incident irradiance and cell temperature for what are known as standard test conditions [2]. $I_{sc(Tnom)}$, is the short circuit current for the cell (under standard test conditions) and is defined manufacturer in the data sheet. G_{nom} is 1000 W/m^2 meaning the photocurrent will vary between 0 and $I_{sc(Tnom)}$ as the irradiance varies between 0 W/m^2 and 1000 W/m^2. As can be seen in equation 5 the incident irradiance has no effect on the dark saturation current; this is somewhat intuitive given its definition provided previously.

$$I_l(T_1) = I_{sc}(T_{nom}) \times \frac{G}{G_{nom}} \quad (4)$$

$$I_0(T_1) = \frac{I_{sc}(T_1)}{\left(e^{\frac{qV_{oc}(T_1)}{nkT_1}} - 1\right)} \quad (5)$$

As mentioned previously many different models exist for the solar cell offering a wide range of complexity levels. This inherent tradeoff between complexity and accuracy is one which must be considered when developing any software model of a real life system. The model considered here is concluded to provide a sufficient level of detail in order to accurately describe the system under investigation. The extent of this accuracy will be examined in more detail in later sections. As mentioned previously however only the effect of the series resistance is considered to affect the cell output. The value of R_s was calculated as follows.

$$R_s = -\frac{dV}{dI_{V_{oc}}} - \frac{1}{X_v} \quad (6)$$

$$X_v = I_0(T_1)\frac{q}{nkT_1}e^{\frac{qV_{oc}(T_1)}{nkT_1}} - \frac{1}{X_v} \quad (7)$$

Important to note here is an important assumption within the model. The derivative noted in equation 6 is obtained from testing on a monocrystalline silicon cell panel [7]. Testing on the polycrystalline panels used within the UDG installation may provide a slightly different

value, however within the context of this simulation the error can be considered to be reasonable. This value determines the exact shape of the cells I-V characteristic, through from short circuit to open circuit operating conditions .The slight consequences of this assumption will be confirmed later when the discrepancies between the simulated panel parameters and those found in the data sheet are analyzed (Table 1).

This concludes all of the required equations to represent the solar cell in terms of the single diode method described previously. The code provided in the supplementary document shows how all of the above combined with a simple numerical method can be used in order to obtain the output for any number of these series or parallel connected cells. The numerical method used is the Newton Raphson method. This is required due to the fact that the overall current output from the cell (as seen in equation 1) is a non-linear expression due to the inclusion of the series resistance, R_s. The method uses an iterative approach to provide an estimate to the true solution to the equation. The accuracy of which is based on the number of iterations. Here 5 iterations are used, providing sufficient accuracy as required for this investigation. The equation for the Newton Raphson method can be seen below, where x_{n+1} is the subsequent value of x after another iteration.

$$X_{n+1} = X_1 - \frac{f(X_1)}{f\prime(X_1)} \quad (8)$$

2.2.2 Panel Construction

In order to create each of the 160W panels which are present in the UDG installation the first stage was to create a simulation for each individual cell within the panels themselves. This would allow for the most flexible bottom up approach. Each of the 96 panels used in the installation contained a total of 72 cells in series. This was specified in the installation handbook. This combined with the panel characteristics seen in figure 7 and the theory that series connected cells result in an increase in voltage only (parallel connected cells increase current) [8] makes it possible to calculate the open circuit voltage for each individual cell in the system. The short circuit current for each cell was equivalent to that for each individual panel since all cells were connected in series. Both the open circuit voltage and short circuit current for the individual cells used in the installation were thus concluded to be as follows.

- V_{oc} = 0.6139V
- I_{sc} = 4.9A

In order to further adapt the model to represent the UDG installation the cell quality factor, n and temperature-current coefficient, k_0 were altered. The value of n was set to 1.9. Anywhere In the range of 1.8- 2 is typical for crystalline silicon [7] however by iterating through a range of values and analyzing the I-V characteristic observed, 1.9 was chosen to be the value which resulted in the output closest to that seen in the panel data sheet.
The value of k_0 (denoted TC in supplementary code) was also set to the exact value defined in the panel data sheet, as seen below in figure 12.

Temperature coefficient of Isc	(0.065± 0.015)%/°C

Figure 12: Installation pannel technology coefficient of temperature.

The above parameters along with the list of physical constants seen in section 2.2.1 are all required in the simulation in order to calculate the cell output using the formulae discussed in the previous section. What is also seen in the computational code are the three inputs variables required by the function used to calculate the cell output current. These are the operating voltage, irradiance and cell temperature; V, G, and T respectively. Setting a value for each of these three inputs it was now possible to simulate the behavior of one panel. This is achieved by first simulating the behavior of a single cell, and then simply manipulating the output accordingly based on the specified number of series and parallel connected cells per module. Comparing the output from the simulation alongside the panel characteristic in the data sheet, it was be possible to begin to validate the behavior of the software model. The outputs from the single panel model, due to a wide range of varying inputs will be discussed in the next section and their accuracy analyzed.

2.2.3 Panel simulation

Both the I-V and P-V characteristics of solar cells and panels are well known. They tend to follow the shape shown in figure 13 below, with slight variations in shape depending on the quality of the cells (quality factor, series resistance, shunt resistance etc.).

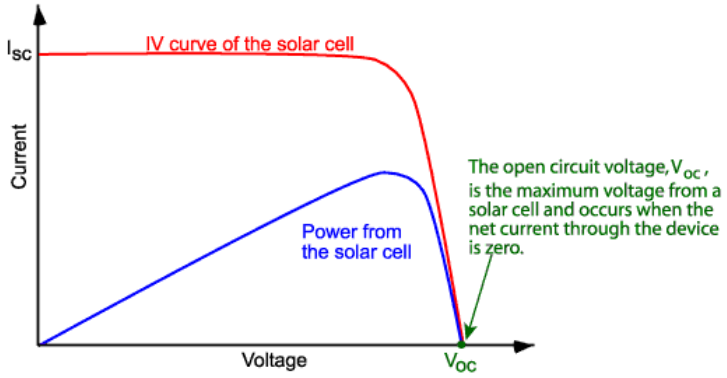

Figure 13: Typical I-P-V relationships for PV cell.[1]

The above traces could be obtained for the simulation model created here by setting constant values for both the irradiance and temperature whilst varying the voltage though a range of values from 0 up to the open circuit voltage. Characteristics from manufacture data sheets are always recorded under standard test conditions as seen previously. By setting both the irradiance and the temperature to the values defined by standard test conditions it was possible to compare exactly the characteristics given in the data sheet with those obtained from the simulation. These results can be seen below.

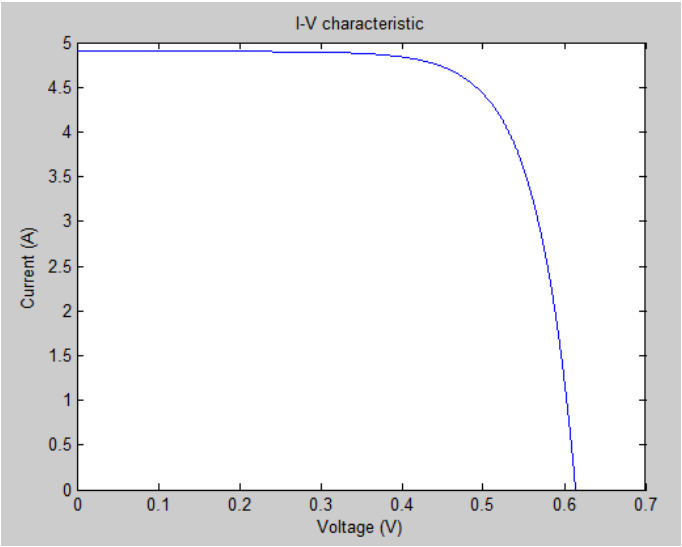

Figure 14: simulated I-V curve.

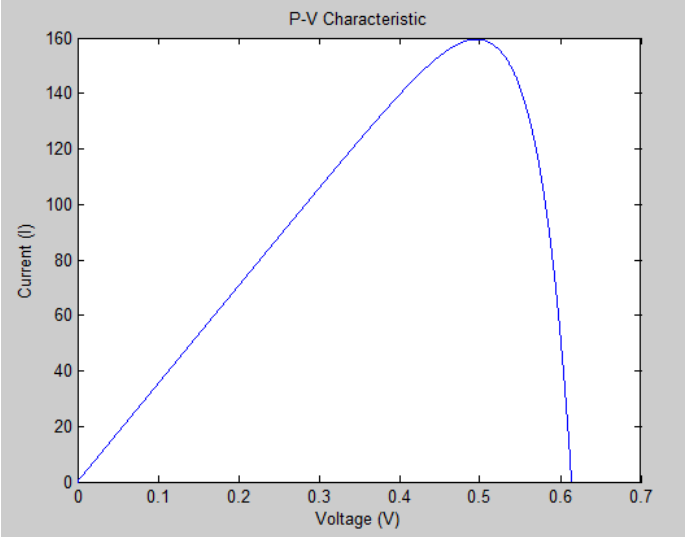

Figure 15: simulated P-V curve.

Table 1: Simulated Vs Data sheet panel characteristics

	Data sheet	Simulation	% Error
Maximum power	160W	159.53W	0.29
Maximum power voltage	35.4V	35.76V	1.02
I_{SC}	4.9A	4.9A	0
V_{OC}	44.2V	44.2V	0

As can be seen above to within a reasonable level of accuracy the simulated solar panel model represents the exact hardware used in the UDG installation. Slight errors were concluded to be a consequence of a complex combination of model assumptions and inaccuracies. These include the following:

- The absence of the shunt resistance in the model.
- Non-exact cell quality factor, n for specific technology (not given in data sheet)
- Estimation of series resistance R_s

Now that the panel has been confirmed to operate accurately under standard test conditions, the next stage was to observe the legitimacy of the models response to temperature and irradiance variations. The theoretical temperature and irradiance responses can be seen below. Increased irradiance produces a linear increase in short circuit current and a slight increase in open circuit voltage. Increased temperature causes a linear decrease in open circuit voltage and a slight increase in the short circuit current.

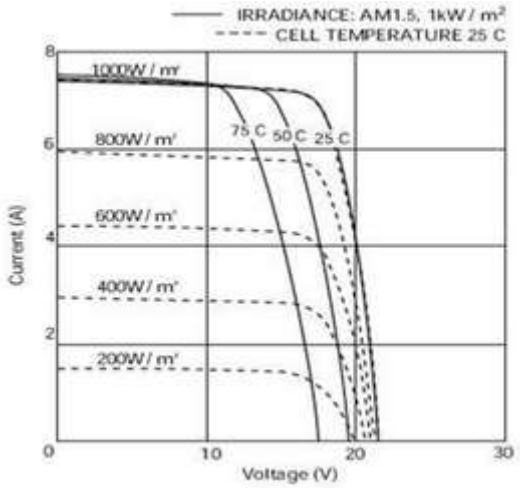

Figure 16: Theoretical temperature and irradiance behaviour.[10]

The results obtained from the simulation accurately portray this theoretical behavior. This can be seen below in figures 17, 18, 19 and 20.

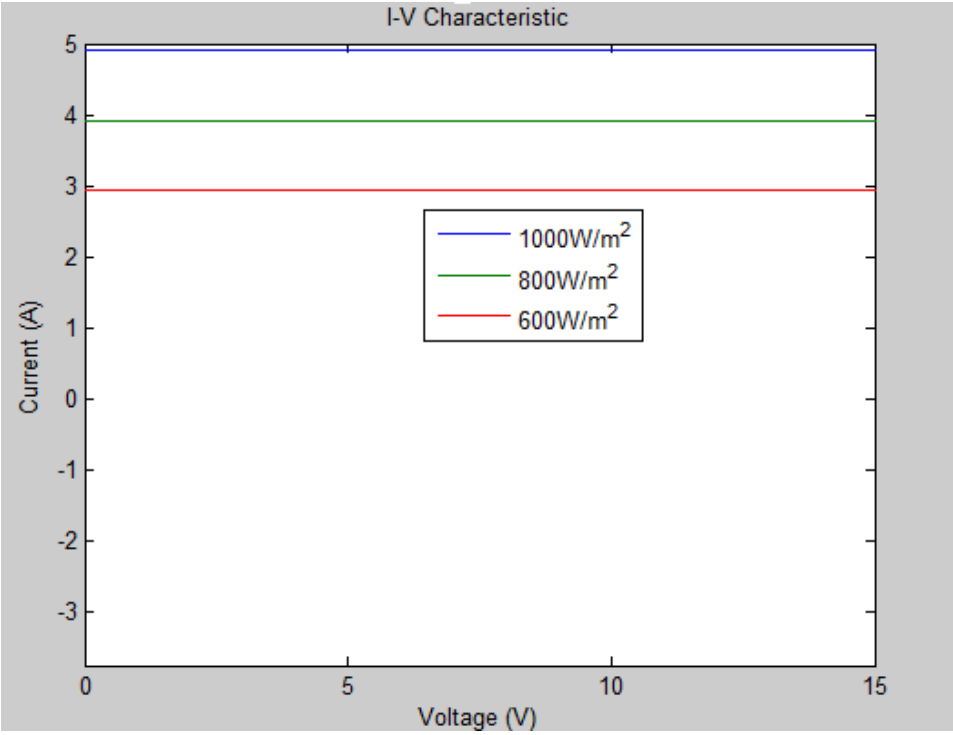

Figure 17: simulated irradiance behaviour (1).

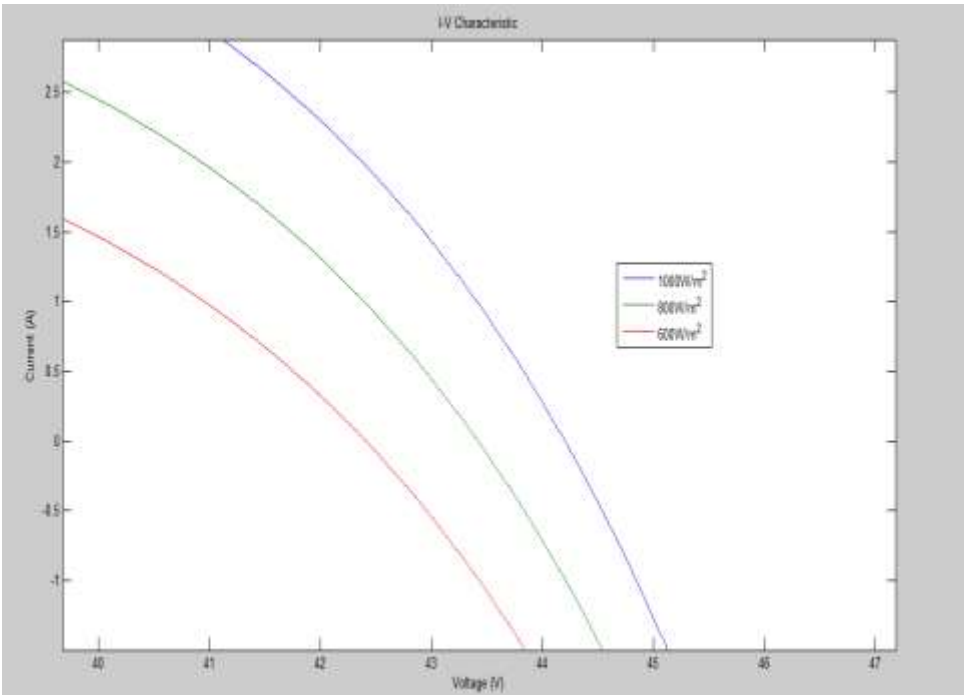

Figure 18: simulated irradiance behaviour (2).

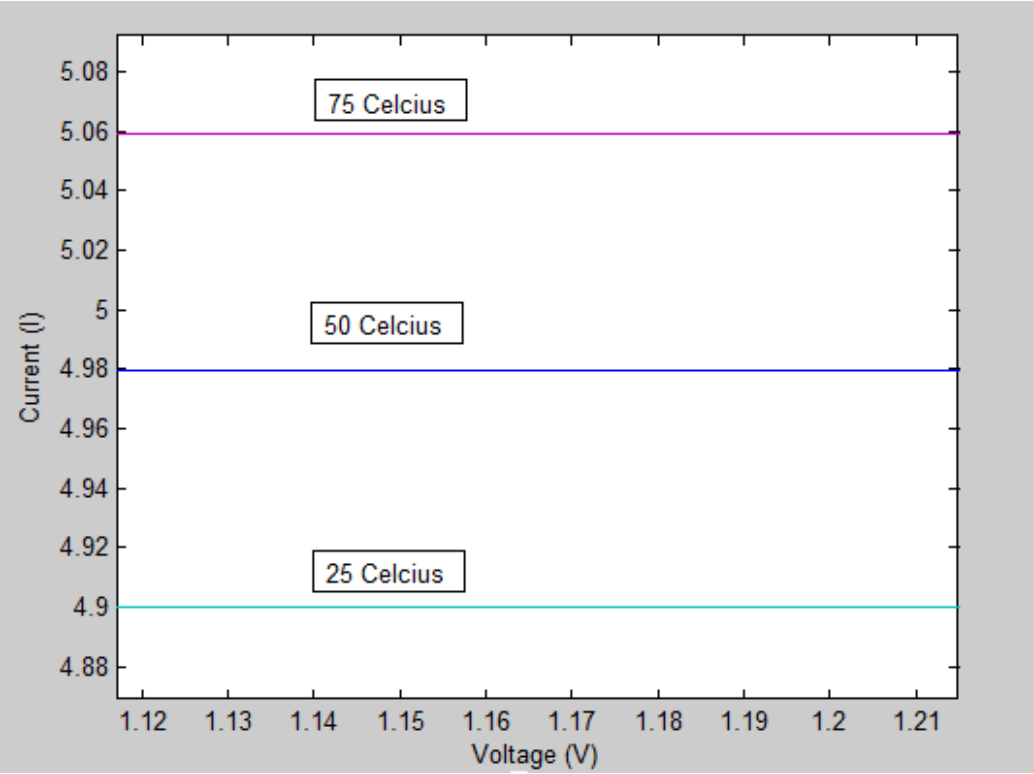

Figure 19: simulated temperature behaviour (1).

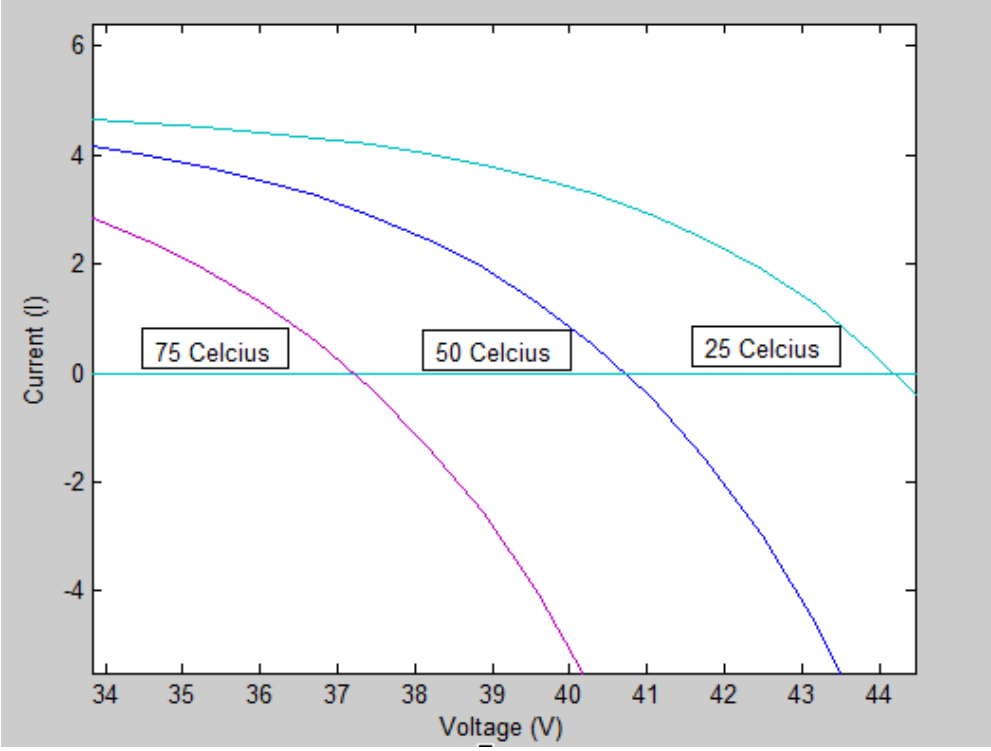

Figure 20: simulated temperature behaviour (2).

As mentioned previously in order to design a software model for the UDG installation the approach was to first design a model to accurately represent each of the cells in the system and there after construct increasingly larger sections of the installation based on the known configuration as specified in section 1. Thus far accurate software models have been created for both the individual cells and panels used in the system. The next stage therefor was to correctly create a further software model based on the known configuration of panels in order to simulate the behavior of the system as a whole.

2.2.4 Array construction

As mentioned previously when discussing the configuration of individual cells within each solar panel different arrangements of series and parallel cells result in very different system characteristics; even if the total number of cells present in each is the same. To reiterate, series connected cells act to increase the overall voltage output whilst parallel connected cells increase the current. This theory also extends to series and parallel combinations of solar panels within larger solar arrays. This behavior is portrayed simply below [8].

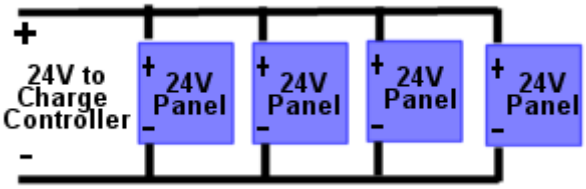

Figure 21: Parallel arrangement.[8]

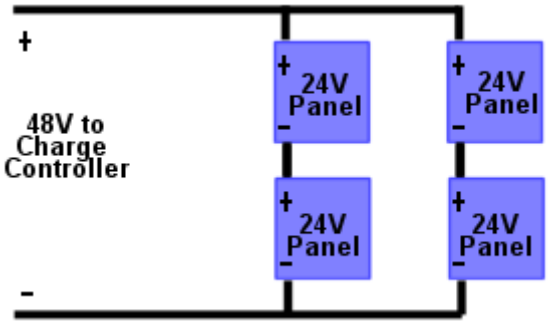

Figure 22: series/parallel configuration.[8]

It is very simple therefor to extend the panel model to one which accurately represents the overall system. Observing the system schematic in figure 6 the number of series and parallel connected panels in the system can be obtained. The 96 panel installation at the UDG was found to be configured as follows. The overall array is split into 6 separate sub arrays, each of which feed into a separate invertor. Each sub array consists to 2 parallel strings of 8 series connected panels. Furthermore each sub array is then connected in parallel. Knowing this it is thus very simple to create a working software model of the overall system by adjusting the current, voltage and thus power output using the relationships mentioned above. The exact

process of extending the model from that of a single cell through to the overall array can be seen in the supplementary annexed code.

2.3 Maximum power point extraction

Maximum power point tracking is crucial part of almost all modern day PV systems. The SMA2500 inverter model used at the UDG installation is the device in this case which carries out the MPPT operation. It is therefore important in order to ensure accurate results that this behavior is replicated in the software model. Whilst this software model will simply replicated the behavior of the MPPT device it is also important to have a brief understanding of the how the behavior is implemented in reality. Two main methods dominate the field of MPPT; these are the P&O and incremental conductance methods. P&O works by making continual changes in the operating voltage until the observed change in output power changes direction. This way it constantly homes in on the voltage which maximizes power output. Since the maximum power voltage will be constantly changing with climactic conditions the process must run constantly. The incremental conductance method computes $\Delta I/\Delta V$ comparing it to the array conductance I/V [18]. When the condition $\Delta I/\Delta V = - I/V$ is met, the maximum power voltage has been found. Again as with P&O the process must continually repeat. Flow charts for both methods can be seen below.

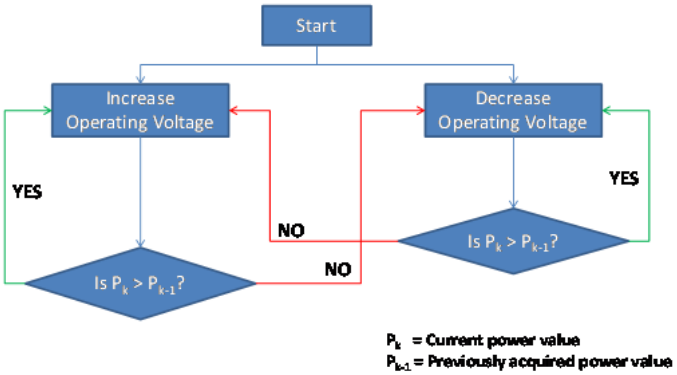

Figure 23:P&O algorithm [18].

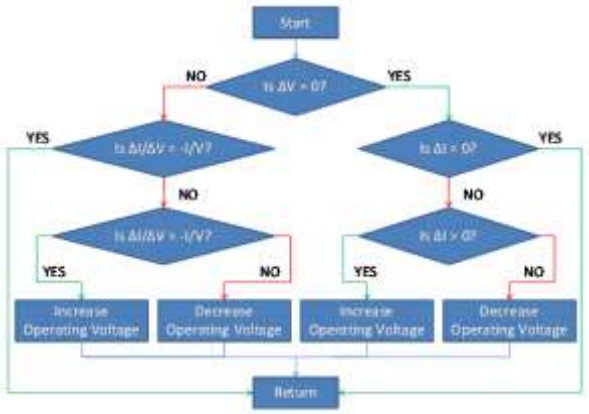

Figure 24: Incremental conductance algorithm.[18]

As can be seen above MPPT algorithms are by nature very iterative. Therefor incorporating their exact behavior in the simulation would result in vast increases to the simulation run time. Instead the behavior of the maximum power point tracking software was implemented sufficiently accurately and simply using the method discussed below. Seen below in figure 25 are the I-V and P-V characteristics for a solar cell under certain conditions. Noted by the dotted line, is the specific point on both curves which corresponds to maximum power extraction. In order to extract maximum power from the cell, the operating voltage (previously discussed as one of the simulation inputs) must therefore be set to the value of voltage corresponding to the turning point of the P-V curve. As with the open circuit voltage, changes in cell temperature produce equally large changes in the maximum power voltage. Changes in irradiance, although less significant also cause changes in the optimal operating voltage and thus must also be considered in the simulation. Since it is obvious that during the long periods of time the simulation will be run the cell temperature and irradiance will be constantly changing; it is important that the simulation takes into account this variation in optimal operating point in order to ensure that the maximum power is extracted.

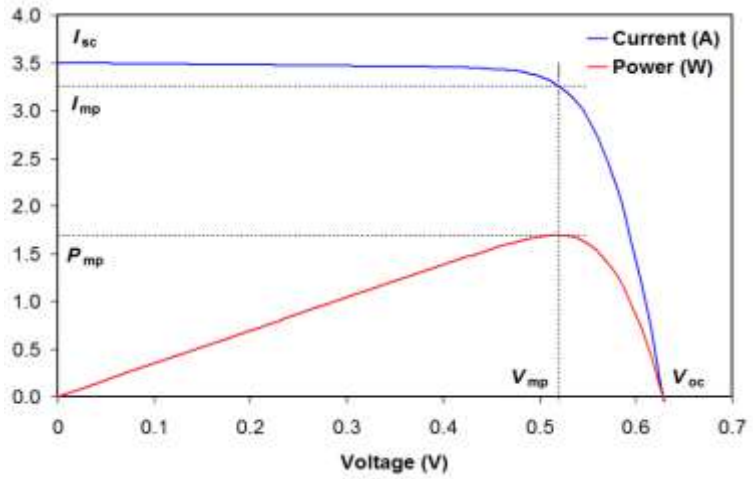

Figure 25: Solar cell I-P-V characteristic.[1]

The code seen in supplementary annexed code was used in order to calculate both the maximum power and corresponding operating voltage for the full range of combinations of cell temperature and irradiance which were likely to be used in simulation. In this case the simulation was run for 77 different temperatures ranging from -8 through to 66 Degrees Celsius and 21 values of irradiance from 0 W/m^2 through to 1000 W/m^2 in 50W/m^2 increments. The Process was to very simple, for each combination of cell temperature and irradiance, the P&O algorithm was applied and the maximum power voltage stored in an array. With the array now containing the optimal voltages for all possible climactic inputs, during long term simulations the required voltages could easily referenced and selected by the program based on the irradiance and temperature values received at the

input. Using this array to store the optimal voltages in advance removed the need to carry out the P&O algorithm during run time, for every time interval at which new inputs were received. The consequence of this in terms of reduced simulation time was immense.

The importance of this feature of the simulation is summarized below, showing the potential production deficit from the simulation, in the absence of the feature. When simulating the effect of changing temperature the irradiance was fixed at 1000W/$m^2$and when simulating the effect of changing irradiance the temperature was fixed at 25 Degrees Celsius.

Table 2: Variation in maximum power and maximum power point voltage with irradiance (fixed temperature).

Irradiance (W/m^2)	Vmpp (V)	maximum power (W)
0	0	0
50	0.36	0.078516294
100	0.39	0.171702412
150	0.41	0.270636638
200	0.42	0.372998563
250	0.43	0.478262067
300	0.44	0.585926155
350	0.45	0.695365235
400	0.46	0.805798293
450	0.46	0.918549964
500	0.47	1.031465242
550	0.47	1.146679988
600	0.47	1.261894699
650	0.48	1.378548502
700	0.48	1.496229556
750	0.48	1.613910567
800	0.49	1.732801869
850	0.49	1.8529533
900	0.49	1.973104677
950	0.49	2.093255999
1000	0.5	2.214989441
1050	0.5	2.33761626
1100	0.5	2.460243011
1150	0.5	2.582869694
1200	0.5	2.705496308

Table 3: Variation in maximum power and maximum power point voltage with Temperature (fixed irradiance).

Cell temperature (°C)	Vmpp (V)	Max Power (W)	Cell temperature (°C)	Vmpp (V)	Max Power (W)
-8	0.56	2.506243483	33	0.48	2.14419241
-7	0.56	2.497997816	34	0.48	2.135171675
-6	0.56	2.48926654	35	0.48	2.125714138
-5	0.56	2.480030027	36	0.47	2.11620197
-4	0.55	2.470479063	37	0.47	2.108000281
-3	0.55	2.462616464	38	0.47	2.099398664
-2	0.55	2.454294107	39	0.47	2.090383344
-1	0.55	2.445493627	40	0.47	2.08094017
0	0.55	2.436196081	41	0.46	2.071306481
1	0.54	2.426750339	42	0.46	2.063102772
2	0.54	2.418813489	43	0.46	2.054507124
3	0.54	2.410423883	44	0.46	2.045506264
4	0.54	2.401563791	45	0.46	2.036086566
5	0.54	2.392214933	46	0.45	2.026304053
6	0.53	2.382845308	47	0.45	2.018107164
7	0.53	2.374843421	48	0.45	2.009526414
8	0.53	2.366395939	49	0.45	2.000549021
9	0.53	2.357485744	50	0.45	1.99116187
10	0.53	2.348095201	51	0.45	1.981351499
11	0.52	2.338772794	52	0.44	1.973022225
12	0.52	2.330715029	53	0.44	1.96446528
13	0.52	2.322218972	54	0.44	1.955520335
14	0.52	2.313268104	55	0.44	1.946174769
15	0.52	2.303845414	56	0.44	1.936415636
16	0.51	2.294541538	57	0.43	1.92785688
17	0.51	2.286436995	58	0.43	1.919332633
18	0.51	2.2779016	59	0.43	1.9104291
19	0.51	2.268919412	60	0.43	1.901134142
20	0.51	2.259474027	61	0.43	1.891435312
21	0.5	2.250160214	62	0.42	1.88262026
22	0.5	2.24201794	63	0.42	1.874137606
23	0.5	2.233452377	64	0.42	1.865284448
24	0.5	2.224448149	65	0.42	1.856049115
25	0.5	2.214989441	66	0.42	1.846419647
26	0.49	2.205637447	67	0.41	1.837321752
27	0.49	2.197466436	68	0.41	1.828889602
28	0.49	2.188879816	69	0.41	1.820095794
29	0.49	2.17986276	70	0.41	1.810929117
30	0.49	2.170400023	71	0.41	1.801378084
31	0.48	2.160981833	72	0.4	1.791971065
32	0.48	2.152791031			

As can be seen above in tables 2 and 3 above, variations over the full range of temperature and irradiance values can cause significant fluctuations in V_{mpp} of up to 0.114V and 0.133V respectively for each individual cell. When then extrapolated for the whole array, failure to respond to these fluctuations in optimal operating voltage can potentially cause vast errors in the simulation production resulting in values far below what would be expected being observed. Through the iterative process observed in supplementary annexed code these errors can be removed, by calculating and assigning the optimal operating voltage for every combination of irradiance and cell temperature which may be received at the input. Whilst the combinations of G and T for which each optimal voltage is assigned contain a value of temperature for every integer value in the range, irradiance values are incremented in steps of 50 W/m^2 as mentioned previously. Therefor when inputting real data, all irradiance values must be rounded when assigning the optimal voltage. This may potentially result in very slight inaccuracies in the simulated data. However the variation in VMPP for increments of less 50 W/m^2 was concluded to be minor enough so as to be exempted from the simulation.

3. Model validation

In order to ensure that the mathematical model devised correctly described the behavior of the overall real life system the following processes discussed in this section were applied. Whilst each individual panel had already been validated, there exist many real life factors which result in the practical performance of the system varying slightly from the exact theoretical performance which one would expect. These factors will be examined in this section, and there consequences in terms of error examined. Once the average magnitude of any error is known it can be simply accounted for in any subsequent simulations in order to provide a validated system model.

3.1 climate and power logger data

When first installed the system was fitted with a series of metering and measurement devices. Measurement devices included those for measuring incident irradiance and temperature (both cell and ambient). Metering equipment logged the instantaneous power produced by each of the 6 sub arrays. Values were recorded every 15 minutes. All of this data is vitally important in order to effectively validate the software model against the behavior of the real system. Shortly after installation this metering equipment became faulty and was never replaced. This has left only 7 months of valid data, beginning in December and ending in June. This time period however was concluded to provide a large enough range of temperature and irradiance data on order for the simulation to be effectively validated. This conclusion was based on the fact that the extreme values observed during this period were equivalent to those measured at the weather station over the full course of a year. For this reason by validating the software over this time period it was possible to ensure that the model reacts accurately to any inputs over the expected range of any future simulations.

The required climactic data for simulation was all available in excel meaning with some basic manipulation it could be loaded into a format suitable to be accepted by the simulation. The array simulation was then run for the full 7 month period, taking both the irradiance and cell temperature at inputs and assigning the operating voltage as discussed previously. Code for this simulation can be seen in supplementary annexed code. The simulation would return a value of instantaneous power for every input corresponding to each of the 15 minutes intervals where data had been recorded. This allowed for easy comparison between the logged power production and that obtained by simulation. A summary of the relationship between the logged and simulated power production can be seen in table 4.

As can be seen, on average the production from the simulation is less than that recorded by the logging device (although it does fluctuate between positive and negative). Important to remember is that the simulation is very much a simplification of the real system. There are many factors not considered in the simulation, all of which may have led to slight discrepancies between the simulated and logged data. However, concluded was that there may be one significant additional reason for this deficit. Whilst for the case of this simulation it is assumed that the irradiance and temperature is constant over all panels present in the installation, this will very rarely be the case in reality (Especial when the system is expanded

over the full campus as will be seen in later sections). This can be seen in the logger data where although all 6 sub array are on a component level identical, their instantaneous production is always different. It is assumed that this is due to partial cloud cover over some sections of the array, meaning that perhaps the irradiance measured by the device at some specific point may actually be lower that received by other sections of the array. Conversely on some occasions perhaps the measurement device may be unaffected by cloud cover, whilst other sections of the array will be. This could explain the fluctuation between negative and positive for the difference between the simulated and logged productions observed during simulation. Since the average difference is negative it can be assumed that more often than not the former is the case. This idea of partial cloud cover on the overall array is further suggested by some of the data recorded by the logger, where on different occasions for the exact same cell temperature increases in the recorded irradiance results in decreases in the overall production. This suggests that the irradiance measured by the logger must not be universal for the whole array .Slight orientation differences for the individual panels as seen in figure 5 may also contribute. In addition to the factors mentioned above, inaccuracies in the measurement equipment installed in the real life system may also contribute to the error between the simulated and recorded values. This may be down to for example either simply poor accuracy equipment or perhaps drift since initial calibration.

All of the above are just a few of a wide range of factors which could have caused the discrepancy between the observed and simulated values. Whilst accounting for each of these very specific details within the model would be highly complex, analysis and further investigation into the nature of this error may allow for it to be more easily addressed. Once fully understood the error be effectively mitigated from the model helping to provide an accurate validated model of the system at present.

3.2 Error analysis

Attempting to identify and eradicate all potential causes of error from the simulation individually would be extremely difficult. It was thus concluded that understanding the nature and magnitude of the overall error and then accounting for it, could provide a simpler and equally effective solution. A summary of the error between the simulated and logged power production can be seen below.

Table 4: Summary of error in simulation instantaneous power production.

Average error
-158.9907803
Sample Standard deviation
908.4407928
Sample size
18183
Standard uncertainty
6.736958286
Degrees of freedom
18182
t-value
1.960094467
95% confidence deviation
13.20507466
upper bound of 95% error
-172.195855
lower bound of 95% error
-145.7857057

The above statistics were calculated as follows.

Instantaneous Absolute error

For each time instance (i) where the irradiance, cell temperature and logged power was known the simulation absolute error was calculated as follows.

E_i = *Simulation Power – Logged Power* (9)

Average absolute error

The average absolute error, (noted as average error above) was then calculated as follows, where n is the number of 15 minute samples in the 7 month period.

$$\bar{E} = \frac{1}{n}\sum_{i=1}^{n} E_i \quad (10)$$

Standard deviation

$$S^2 = \frac{1}{n-1}\sum_{i=1}^{n}(E_i - \bar{E})^2 \quad (11)$$

$$S = \sqrt{s^2} \quad (12)$$

Standard uncertainty

$$SE = \frac{s}{\sqrt{n}} \quad (12)$$

Degrees of freedom

Degrees of freedom = n – 1 (13)

t-value for 95% confidence interval

t = 1.96 (from look-up table)

95% confidence deviation (Absolute precision)

Absolute precision = t × SE (14)

Upper/lower limit of 95 % interval

Range = $\bar{E} \mp$ absolute precision (15)

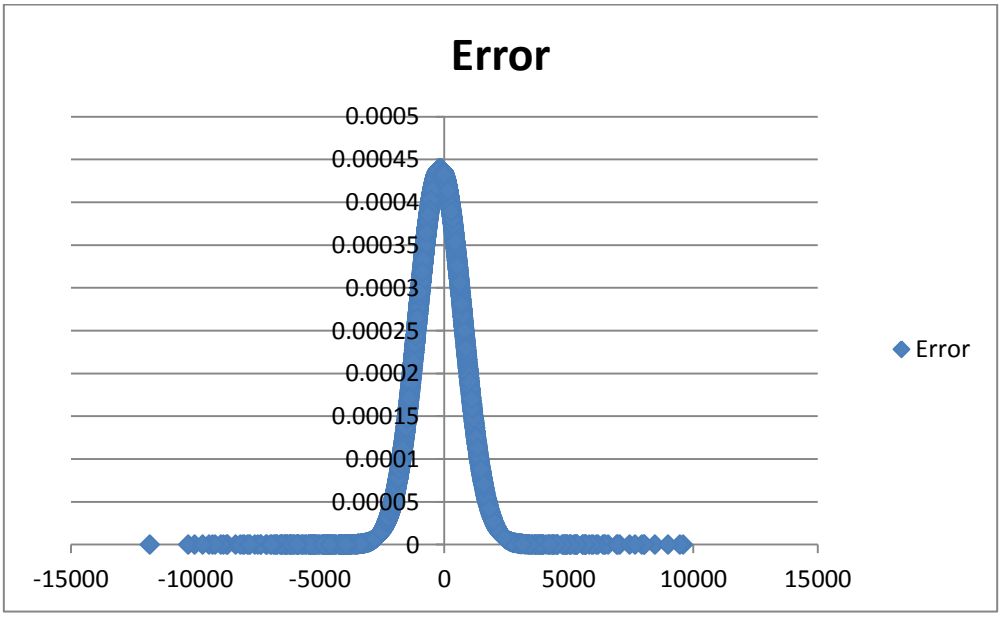

Figure 26: Simulation error distribution.

As seen in both table4 and figure 26 the error can be shown to follow a normal distribution centered on an Average value of -159. Based on the finite sample data used it can be concluded with 95% confidence that the error for any value of input will be between -145W and -172W (for the current 96 panel system).

Using this error analysis we can effectively validate the model to accurately represent the current installation as follows.

$$Validated\ production = Simulation\ production + |\bar{E}| \quad (16)$$

The above relationship will be used for all subsequent simulations, with the average error being applied as a correction factor for each value of instantaneous production. The magnitude of the error may be varied between the upper and lower bounds seen previously in order to gain an idea of the maximum and minimum expected production. Important to remember is that this value of error is based on the finite sample of data which was available from the logger (before it broke). Whilst using the above equation complete with the calculated average error in place will result in the perfect agreement for this same time period, different input values for different periods of time may still result in slight discrepancies. This is due to the finite sample size used. Using this new validated production however the difference in energy yield between that based on the simulated and logged data for a given period is now massively reduced.

Another important consideration which must be noted at this point is the following. The value recorded in table 4 above noted as "average error" is in fact the average absolute error; the average value for the difference between simulated and recorded power. Later in section 5 the possibility to expand the system over the full campus will be investigated, and the simulation altered in order to represent this newly expanded system. During the alteration process the magnitude of the error seen in equation (16) will have to be updated in order to represent the increase in the number of installed panels. This is due to the fact that the original value of -159 was only valid for the initial 96 panel system. In order to cope with the expansion, an additional type of error will be considered which relates the average absolute error to the total installed capacity of the installation. This is known as the "relative error" and can be expressed as seen below.

$$Relative\ error = \frac{\text{Average absolute error}}{Total\ installed\ capacity} = \frac{159W}{96 \times 160W} = 1.04\% \quad (17)$$

Since the relative error is now known, during the simulation process for any subsequent expanded systems the new value of "$|\bar{E}|$" as seen in equation (16) can be re-calculated using the newly proposed installed capacity and the relative error calculated above in equation (17).

4. Current sytem Production Vs partial campus consumption

This section will analyze the relatioship between the production from the system at present and a certain portion of the overall campus consumption. The primary aim of this investiagion is to gain an insight into the extend to which the system must be expanded in order to provide a reasonable proportion of the campus's consumption. As seen before the installation is located on only a small section of the EPS P1 rooftop. This location can be seen once more in figure 27 below.

Figure 27: Current system rooftop geometry.[59]

The consumption for this site on it own however is unavailabe, therefor we shall compare production with the combined comsumptions of EPS buildings P2 and P4 as seen below. This comparison aims to provide several helpfull insights including the following.

- The percentage of consumption which is likely to be able to be provided by renewable generation.
- How monthly production varies thoughout the year.
- How monthly consumption varies throughout the year.

This understanding will be usefull when considering system expansion, an idea which will be discussed in detail in later sections.

Figure 28: P2 & P4 geometry.[59]

In this analysis, considered will be the time period spanning the entirety of 2011. Data will be analysied on a monthly basis in order to see how the relationship between generation and consumption varies thoughout the year.

As mentioned in a previous section the data logging equipment located on site became faulty within the first year of installment and was never fixed. For this reason in 2011 Cell temperature data is no longer availbe. There is however ambient air temperature data made available by the university weather station. The following section will explain how this along with some key properties of the panel materiel (all available through panel data sheet) can be used in order to calculate the corresponding cell temperature. This process is vital since the cell temperature acts as one of the key inputs to the simulation model

4.1 Cell temperature calculation

The relationship between the ambient air temperture and the cell temperture is well know and is documented in [16]. The Key equation used to relate the two variables can be seen below.

$$T_{cell} = T_{air} + \frac{NCOT-20}{80} \times G \quad (18)$$

As seen previously G is the incident irradiance. NCOT is is the Nominal Cell Operating Temperature and is comonly given in the panel data sheet. In the case of the panels used in the UDG installation the value is as follows:

$$\text{NCOT} = 47 \pm 2\ ℃$$

Using the equation seen in (18) along with the irradiance and ambient temperature data recorded at the weather station it was possible to then obtain all of the required inputs to the simulation seen in the annexed code, which as seen previously can be used to determine the power output from the array.

The next section will provide an analysis of how the production over the year 2011 compares to a subsection of the overall consumption onsite. This will provide usefull insite into the potential self sustainability of the campus. This information will also be usefull for a parallel study, which will investigate the finacial benefits of system expanision

4.2 Monthly variation in production

Due to the obvious nature of the solar resource there is likely to be a definate variation in the array production throughout the year, with varying climatctic conditions. The exact nature of this variation will be studied here. Results obtained from the simulation show the monthly energy yields for the current 96 panel system installed at the UDG. Also note that seen in the supplementary annexed code, is how the correction factor is applied made in order to ensure that the error found in the validation process has been accounted for. The simulated average monthly energy yields can be seen below using the average error calculated previously.

Table 5: Simulation monthly energy yield for current system (using average error).

Month	Energy Yield kWh
January	862.1426925
February	1179.085869
March	1546.399722
April	2301.507987
May	2771.203841
June	2524.624322
July	2347.121651
August	2574.468054
September	2010.921439
October	1506.863123
Novmeber	731.1199534
December	833.9864662

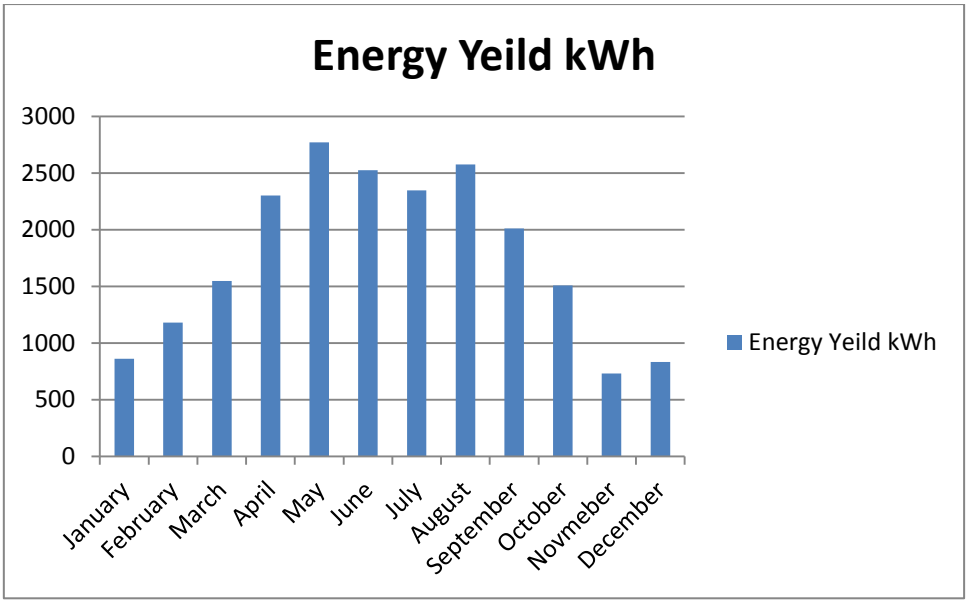

Figure 29: Average error monthly energy yields.

4.3 Monthly Variation in consumption

In addition to monthly variations in production, there are several factors which result in monthly variations in consumption. These include for example, terms dates resulting in long periods where vast sections of the university will be empty. Another important factor to consider is how the use of "heavy loads" will vary throughout the year. For example highly rated air conditioning systems are unlikely to be unused durring the winter. Conversely however perhaps heating devices drawing high currents may be used in these period. Using the metering data for both P4 and P2 this exact relationship can be understood. The consumption trend can be seen below in figure 30.

Table 6: Monthly consumption data for EPS buildings P2 and P4.

Month	Consumption kWh
January	91357.2105
February	88740.415
March	99041.1085
April	77364.32925
May	77479.475
June	77442.31075
July	81161.02475
August	55127.848
September	77387.471
October	74248.37425
November	72653.05025
December	70922.2695

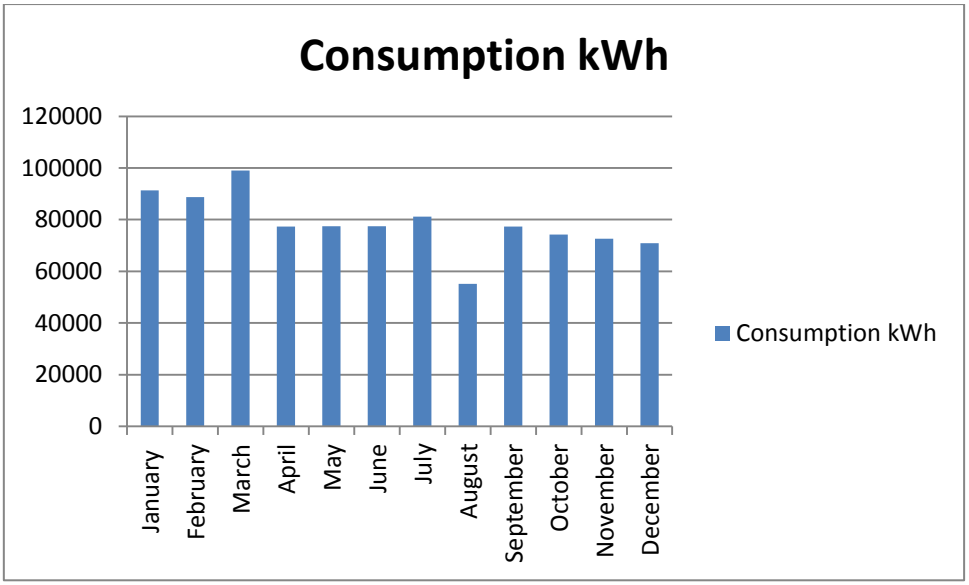

Figure 30: P2 & P4 monthly consumption.

Result here show that whilst there is some variation in comsumptiopn throughout the year it is not quite as clear as one may have predicted. It is certainly not as clear as that seen in figure 29 for the Photovoltaic production over the same period. With only really August showing a reasonable decrease in consumption compared with all other months, likely due to non use of many university facilities during the period.

4.4 Production Vs Consumption

Results from sections 4.2 and 4.3 show that Production is always in deficit of consumption for the proposed comparson. The magnitude of this deficit is seen below.

Table 7: Monthly variation in production deficit (current system production Vs P2 &P4 consumption).

Month	Production deficit kWh
January	90495.06781
February	87561.32913
March	97494.70878
April	75062.82126
May	74708.27116
June	74917.68643
July	78813.9031
August	52553.37995
September	75376.54956
October	72741.51113
November	71921.9303
December	70088.28303

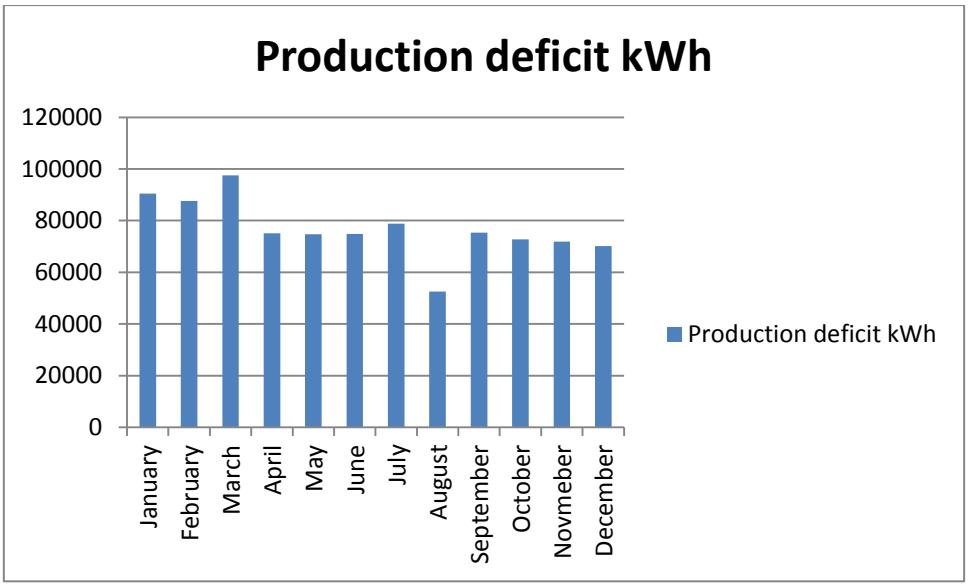

Figure 31: Monthly Energy production deficit.

Both Table 7 and Figure 31 Show that here, Production is far less than consumption. This analysis however is not truly meaningful for the following reasons.

As seen previously in Figures 27 and 28, the building on which the current solar array is placed contributes a far smaller proportion of the total EPS than do the buildings for which the metering data is recording consumption. In fact the P2 and P4 consumption contributes a vastly higher percentage of the overall campus consumption, than the installation does overall campus rooftop surface area. Whilst one may imagine it may be possible to extrapolate these findings for the full campus by simply taking the values of consumption and production used here and multiplying them by some factor based on the percentage surface area of the overall campus they account for, this aproach would result in many inncauracies. Whilst the approach may be more plausable for the production since climactic conditions will be assumed constant over the full campus, for consumption rooftop surface area does not provide any real indication of magnitude. This is primarily down to the fact it does not take into consideration the number of stories high or the typical loads in the buldings.

Another important important factor which must be considered is as follows. Although the overall monthly yield in kWh may be less, the instantaneous power production at certain points in the day may in fact be greater than the instantaneous consumption. This may perhaps not be the case for this analysis for the reasons discussed in the previous paragraph however when considering production and consumption over the full campus this analysis will be vital in order to help a parallel study to this which will be considering the Finanacial benefits of system expansion, as well as different methods of utilising production. This will be necesaryl as it is likely to provide usefull information into the periods in the day when production is most likely to sway from being in deficit into being in excess of consumption.

This analysis can be seen in the later sections an is pivotal as constantlaly varying import and export prices mean that the instantaneous deficit must be known.

5. Potential for installation expansion

This section will investigate the possibility of extending the existing system to all other possible rooftop surfaces available at the Montilivi campus. Based on the current installed capacity and the land mass assigned at present, it will be possible to gain an accurate estimate of the potential production capacity across the whole university. Based on this along with the data relating to full campus's consumption, the benefits of expansion will be examined.

5.1 Current installation

As seen previously, currently 96 modules occupy a small section of the roof of the P1 building. A schematic of this configuration can be seen below.

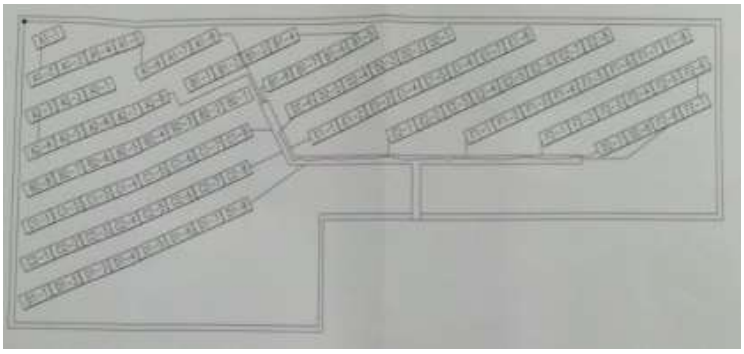

Figure 32: Current system geometric schematic.

Satellite data can provide an estimate of the dimensions for the building. The area of P1 was thus calculated as follows.

Figure 33: Current system mapping for area calculation. [59]

$$\text{P1 surface area} = (20m \times 10m) + (15.7m * 15.7m)$$

$$= 446.49\ m^2$$

The individual panel dimensions as provided in the manufacturer data sheet are as follows, where the un-bracketed terms are the dimensions in millimeters [13].

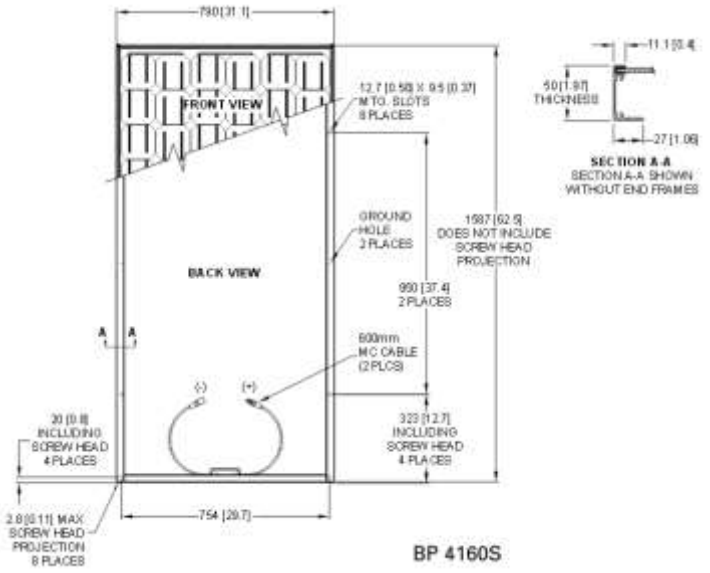

Figure 34: Pannel technology dimensions.

The surface area of each panel is thus.

$$\text{Panel surface area} = 0.79m \times 1.59m$$
$$= 1.256\ m^2$$

Intuitively one might consider that in order to calculate the potential production capacity for each building on site, the total number of panels would simply be surface area of the roof divided by that of the individual panel as calculated above. However it would be unrealistic to assume that the full surface area of every building would be available for use. Shading, among other reasons including allowing for optimal tilt make this is unfeasible in reality. For this reason, instead the percentage of available roof top surface area which the current installation occupies shall be calculated; and it will be this percentage that shall be applied to all subsequent surface areas when calculating the total number of panels which can be installed on site during system expansion.

- P1 surface area = 446.49 m^2
- Total surface area of panels = 96*1.256 m^2 = 120.58 m^2
- Percentage Cover = 27%

5.2 Remainder of EPS P1

Whilst it may not be possible to obtain a 100% accurate value for the available surface area on the roof of P1's remaining sections, by breaking down the overall area into smaller subsections as seen below an estimate to the available land mass can be calculated.

Figure 35:P1 geometry. [59]

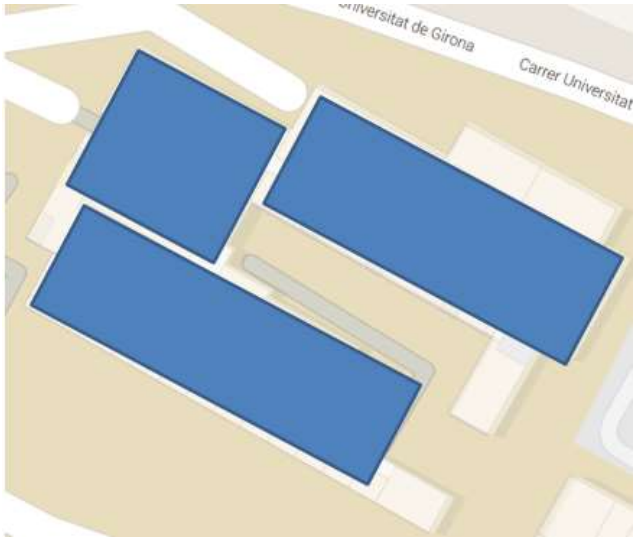

Figure 36: P1 geometry used for area calculation. [59]

$$\text{Surface area} \approx (78.3m \times 20m) + (32.2m * 28.7m) + (60.9 * 22.6m)$$

$$\approx 3866.48\ m^2$$

5.3 EPS P2 and P4

For both EPS P2 and remainder of the buildings on campus, the same approach as seen in section 5.2 has been used for calculating an estimate of the overall surface area available.

Figure 37: P2 & P4 geometry. [59]

$$\text{P2 and P4 surface area} \approx (83.5m \times 16.5m) + (83.5m * 20.4m) + (83.5m * 13.9m) + (63.9m \times 25.7m) + (15.2m * 52.2m) + (28.3m * 10.4m) + (7.8m \times 20.9m) + (11.3m * 11.3m) + (16.5m * 7.4m)$$

$$\approx 7384.6m^2$$

5.4 Moduls centrals

Figure 38:Moduls Centrals geometry. [59]

Moduls centrals surface area $\approx (82.6m \times 14.8m) + 3 * (16.5m * 11.3m) + 2 * (9.6m * 9.6m) + (13.9m \times 12.2m) + (16.5m \times 9.6) + (36.5m \times 9.6m)$

$\approx 2644.53m^2$

5.5 Biblioteca

Figure 39:Biblioteca geometry. [59]

Biblioteca surface area $\approx (28.7m \times 81.7m)$

$\approx 2344.8\ m^2$

5.6 Facultat de ciencies

Figure 40:Facultat de Ciences geometry. [59]

Facultat de Ciencies surface area $\approx (72.2m \times 26.1m) + (69.6m * 13m) + (13.9m * 13.9m) + (13.9m \times 4.4m) + (7m \times 8.7m) + (71.3m \times 10.4m)$

$\approx 3846m^2$

5.7 Facultat de Dret

Figure 41: Facultat de Dret geometry. [59]

Facultat de Dret surface area $\approx 3 * (47.8m \times 14.8m) + 6 * (7m * 7m) + (47.8 * 6.1m)$

$\approx 2707.9m^2$

5.8 Facultat de Economiques

Figure 42: Facultat de Economiques geometry. [59]

Facultat de Economiques surface area $\approx (45.2m \times 13.9m) + (5.2m * 37.4m) + (7.8m * 9.6m) + (27m \times 17.4m) + (36.5m \times 14.8m) + (47.8m \times 9.6m)$

$\approx 2366.5m^2$

6.Monthly Production energy Yield Vs Energy Consumption Across whole campusn

As mentioned previously, in consdering expansion of the current system over the full rooftop surface area available at the montilivi campus it will be possible to understand if there exist periods in the day where the university can become a self sufficnet energy provider. It may also be found that there exist periods when production is in excess of consumption leading to exportation of electrical power not required to be consumed directly on site. As mentioned before these findings will be of great benefit to a parallel study to this, which will investigate the financial benefits of system expansion.

Important to note is that at present the system is configured such that 100% of all production is exported deirectly back into the distribution grid. For this proposed scenario where the system is now expanded over all available rooftop surface area, the nature of the system will be considered to be as follows. All production is ordinarily consumed on site; when production is less than consumption, grid export is used to fill in the deficit. Conversly then production is grater than consunption excess will be exported to the Grid or harnessed by battery storage. Whilst this may be the asumed utilisation of production for this report, as mentioned previoulsy there shall be a parallel study to this which will use real time market costs in order to asses the most effective method of dealing with production in terms of financial benefits.

6.1 Total installed capacity

In previous sections the total available rooftop surface area was calculated. Also noted were the dimensions of the 160W solar panels used in the current installation. What will now be considered is the total installed capacity if the system were to be expanded over the full Montilivi campus. What is vital to remember however is that for reasons previously disucssed one can not simply devide the rooftopsurface area by the panel dimensions in order to obtain the number of panels which may be assigned for each building. Instead a more measured approach must be taken. In this study we shall continue to use the percentage cover calculated for the current installation for the remainder of the buildings on the campus. Whilst this may be a conservative estimate and perhaps more pannels could me assigned to each rooftop, it ensures consistancy with the installation at present.

6.1.1 Remainder of EPS P1

$$rooftop\ Surface\ area = \ 3866.5\ m^2$$

$$total\ panel\ coverage = \ 3866.5\ m^2 * 0.27 = 1044\ m^2$$

$$number\ of\ panels = 1044\ m^2\ \div 1.256 m^2 = 832$$

6.1.2 EPS P2 and P4

$rooftop\ Surface\ area = 7384.6m^2$

$total\ panel\ coverage = 7384.6m^2 * 0.27 = 1993.8\ m^2$

$number\ of\ panels = 1993.8\ m^2\ \div 1.256m^2 = 1588$

6.1.3 Moduls centrals

$rooftop\ Surface\ area = 2644.53m^2$

$total\ panel\ coverage = 2644.53m^2 * 0.27 = 714\ m^2$

$number\ of\ panels = 714\ m^2\ \div 1.256m^2 = 569$

6.1.4 Biblioteca

$rooftop\ Surface\ area = 2344.8\ m^2$

$total\ panel\ coverage = 2344.8\ m^2 * 0.27 = 633.1\ m^2$

$number\ of\ panels = 633.1\ m^2\ \div 1.256m^2 = 505$

6.1.5 Facultat de ciencies

$rooftop\ Surface\ area = 3846m^2$

$total\ panel\ coverage = 3846\ m^2 * 0.27 = 1038.4\ m^2$

$number\ of\ panels = 1038.4\ m^2\ \div 1.256m^2 = 827$

6.1.6 Facultat de dret

$rooftop\ Surface\ area = 2707.9m^2$

$total\ panel\ coverage = 2707.9m^2 * 0.27 = 731.1\ m^2$

$number\ of\ panels = 731.1\ m^2\ \div 1.256m^2 = 583$

6.1.7 Facultat de economiques

$rooftop\ Surface\ area = 2366.5m^2$

$total\ panel\ coverage = 2366.5m^2 * 0.27 = \ 639m^2$

$number\ of\ panels = 639m^2 \div 1.256m^2 = 509$

6.2 New Array configuration

As seen previously in section 1 the original installation consists of 6 subarrays, each consisting of 16 solar panels (2 parallel connected strings of 8). To repeat this exact configuration for all subsequent arrays which will now be added to the simulation may be a little difficult for several reasons. For example many arrays contain certain numbers of panels which result in 6 equal sub arrays not being achievable. Furthermore even when division into 6 equally sized sub arrays is possible sometimes further division into same length parallel strings cannot be achieved. The exact configuration however for the case of this simulation is not important. This is because only the instantaneous power and energy yield will be given as output. The power is the product of the current and the voltage at any given point in time. Since the total number of panels is fixed, connecting more parallel strings would mean reducing the string length, thus increasing current but decreasing voltage. Thus the overall effect has no consequence on the power output which would remain unchanged. The importance of array configuration is really only a practical consideration where voltages must remain within statutory limits for the inventor and currents must remain low enough so as not to exceed the working limit of the conductor material. Panel configuration was for this reason not considered in great detail in the simulation, with only the total number being of importance to the simulation output.

6.3 2011 Energy Yield after system expansion

Important to note here is one key assumption which has been made regarding the incident irradiance and panel temperature across all panels throughout the campus. Since the only climactic data which is available for the site is that obtained for the weather station, it will be assumed that both the irradiance and panel temperature values are identical for all panels used in the expanded installation. In reality this is unlikely to be the case. However this is an inaccuracy which this simulation must accept, as there is no other measurement devices installed at present to provide this information. It has been concluded that the data provided from the weather station is an accurate enough generalisation for the whole campus to provide valid results. The results for the 2011 energy yield across the new expanded system are given below. Important to note is that the value of instantaneous power error correction included in the simulation code was updated as seen in section 3.2. This was in order to account for the expansion of the system. The error now takes a value of -9124W compared to the value of -159W seen previously.

Table 8: Monthly variation in Average Energy yield (full campus).

Month	Production kWh
January	49474.34159
February	67662.25595
March	88740.69567
April	132072.8867
May	159026.5644
June	144876.4945
July	134690.427
August	147736.8026
September	115397.4613
October	86471.87534
November	41955.54697
December	47858.58542

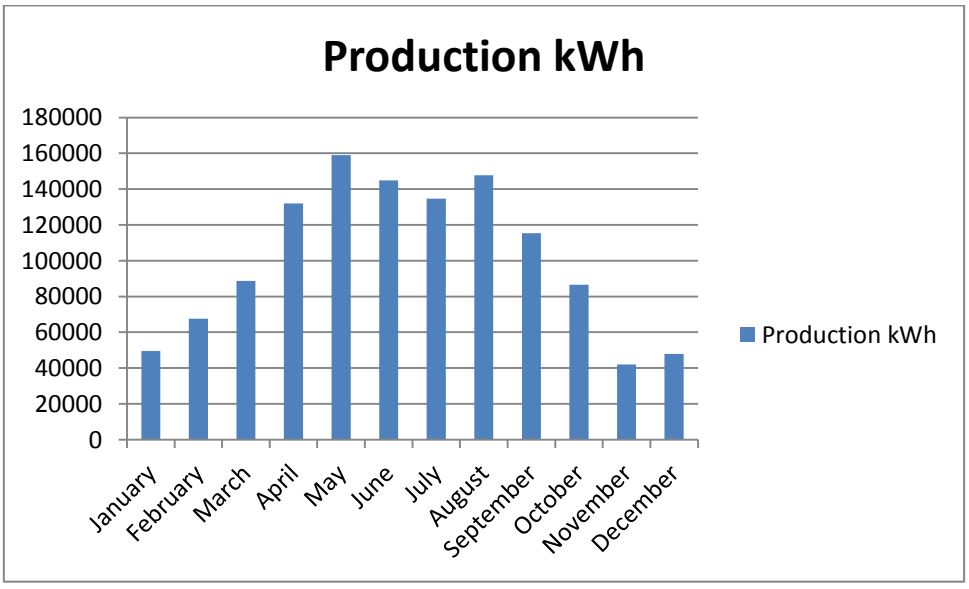

Figure 43: Monthly energy yields after system expansion.

6.4 2011 Consumption across full campus

Now that the monthly energy yields throughout the year in the newly expanded system have been calculated, the consumption across the full campus for the same time period will be examined in order understand what fraction of this could be generated on site. Consumption data for the full campus will be calculated by simple addition of the individual campus buildings consumption data; recoded by several metering devices. The buildings included in

this analysis were identical to those examined for system expansion in section 7. This makes sense and provides a fair comparison, with both the overall potential for generation and also the overall consumption being examined. The total consumption for the full Montilivi Campus recorded on a monthly basis can be seen below.

Table 9: Monthly variation in Average Energy consumption (full campus).

Month	Consumption kWh
January	453436
February	428356
March	463967
April	339822
May	393611
June	402907
July	384953
August	242615
September	374022
October	365448
November	387750
December	456849

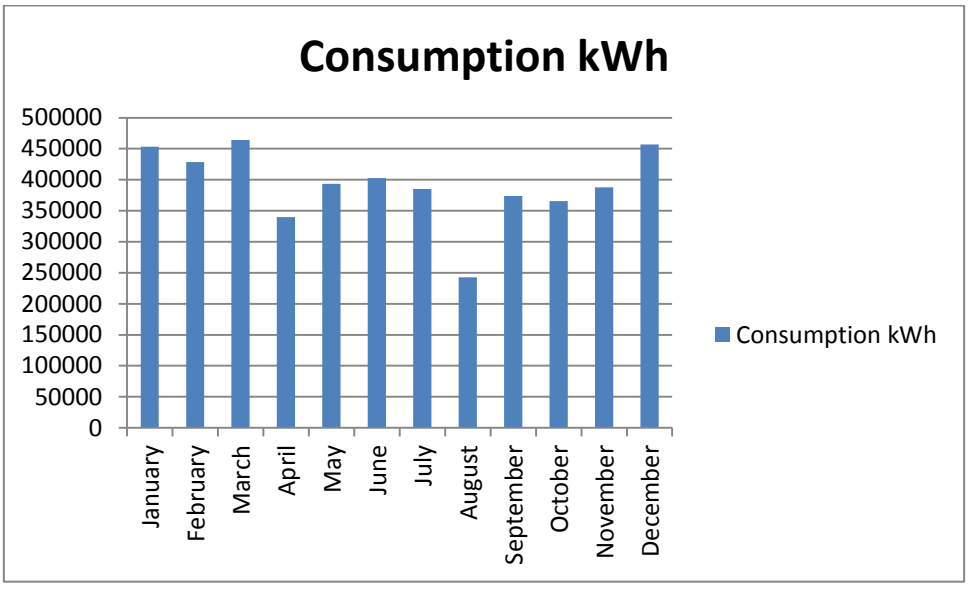

Figure 44: full campus monthly energy consumption.

What can be observed here is that when extrapolated across the full campus, consumption vastly escalates. However as does production when considering the case when the system is expanded across all available roof top surface areas. The total percentage of energy consumption each month that can be supplied by the solar installation is noted below. This percentage is denoted SS % (self-sustainability percentage) and can be seen to vary throughout the year. In August this percentage reaches a maximum in the region of 59%, showing a significant portion of the campus consumption can be provided from renewable sources. This is even more impressive considering the conservative estimate of 27% coverage which was used when calculating the potential for system expansion.

Table 10: Monthly variation in Self Sustainability Percentage (full campus).

Month	Self-Sustainability %
January	10.91098669
February	15.79579974
March	19.12651022
April	38.86531381
May	40.40196143
June	35.95780032
July	34.98879785
August	60.89351548
September	30.8531213
October	23.66188222
Novmeber	10.82025712
December	10.47579954

6.5 2011 Monthly Production Vs Consumption Comparison per Building

In previous sections of this investigation the Monthly variations in both Energy production and consumption have been examined. This analysis has considered the Full Montilivi campus as a single producer and consumer of electricity. What would also be interesting to observe however would be how these relationships between production and consumption vary across each building on campus. The results from this investigation would be of great interest when considering the utilisation of the electrical production on site and the design of the system to cope with these demands. Whilst production is directly proportional to the available rooftop surface area, due to the nature of different loads located within different departments and the number of stories in each building the variation in consumption with geometrical scaling of rooftop surface area is likely to be a more erratic. Through this investigating it will be possible to obtain an understanding of which buildings produce the largest gulf in production deficit per month, and which the smallest. This will help better

understand the required interconnected nature of the system in order to ensure that energy is utilised as effectively as possible.

As seen previously, the total rooftop surface area available on campus and thus potential installation capacity was calculated by taking the sum of the individual building surface areas as calculated in section 5. Important to note is the fact that the consumption data used previously was also obtained from several metering devices located throughout the university. The total consumption was then obtained by calculating the sum of these individual values. Using the individual building rooftop surface areas as calculated previously, production could be specified for each individual building. Conveniently there was also one single metering device within each of these buildings which allowed for comparison between individual building production and consumption to be now achieved with relative ease. The results from this analysis can be seen below. Tables 13 and 14 show the production and consumption respectively for each building in the Montilivi campus, whilst table 15 represents the self-sustainability percentage per month.

Table 11: Monthly variation in Energy production per building kWh (full campus).

Month	1	2	3	4	5	6	7	8	9	10	11	12
EPS P1	8334	11398	14949	22250	26790	24400	22690	24890	19440	14566	7067	8062
EPS P2&4	14261	19504	25580	38070	45840	41760	38830	42590	33260	24926	12094	13796
Moduls Ce	5110	6989	9166	13640	16430	14960	13910	15260	11920	8931	4333	4943
Biblioteca	4535	6202	8135	12110	14580	13280	12350	13540	10580	7927	3846	4387
Ciencies	7427	10157	13322	19830	23870	21750	20220	22180	17320	12981	6298	7184
Dret	5236	7160	9391	13980	16830	15330	14250	15630	12210	9151	4440	5065
Economiq	4571	6252	8199	12200	14690	13390	12440	13650	10660	7990	3876	4422
total	49474	67662	88742	132080	159030	144870	134690	147740	115390	86472	41954	47859

Table 12: Monthly variation in Energy consumption per building kWh (full campus).

Month	1	2	3	4	5	6	7	8	9	10	11	12
EPS P1	40588.7	38361.48	42276.68	32899.05	39487.34	39114.35	42883.41	22945.41	38959.22	35174.03	36776.95	33167.98
EPS P2&4	91357.21	88740.42	99041.11	77364.33	77479.48	77442.31	81161.02	55127.85	77387.47	74248.37	72653.05	70922.27
Moduls Ce	12602.5	11698.25	13504	8963.25	9961.75	8612.75	8381.75	4236	10201.25	13064.5	14789.75	11662
Biblioteca	73749.75	64111.75	64312.75	39242.5	51176.75	61000.5	24162.75	18624.75	28529	35889.5	46542	136502.8
Ciencies	105549.4	100839.4	111281.3	82779.24	96059.71	97966.72	99804.64	67889.29	97853.64	89496.54	95319.61	95006.8
Dret	28749	28544.5	28001.25	15794	19287	20803.25	17278	5902.5	23237.5	22568.5	26349.25	20090.25
Economiq	100839.4	96059.71	105549.4	82779.24	100159.4	97966.72	111281.3	67889.29	97853.64	95006.8	95319.61	89496.54
Total	453435.9	428355.5	463966.5	339821.6	393611.4	402906.6	384952.9	242615.1	374021.7	365448.2	387750.2	456848.6

Table 13: Monthly variation in SS% per building (full campus).

Month	1	2	3	4	5	6	7	8	9	10	11	12
EPS P1	20.53281	29.7121	35.35992	67.63113	67.84453	62.38119	52.91091	108.4748	49.89833	41.41124	19.21584	24.30657
EPS P2&4	15.61015	21.97871	25.82766	49.20872	59.16406	53.92401	47.84316	77.25678	42.97853	33.57111	16.64624	19.45228
Moduls Ce	40.54751	59.74398	67.87618	152.1769	164.9309	173.696	165.9558	360.2455	116.8484	68.36083	29.29732	42.38553
Biblioteca	6.149173	9.673734	12.64912	30.8594	28.4895	21.77031	51.11173	72.69896	37.08507	22.08724	8.263504	3.213855
Ciencies	7.036516	10.07245	11.97146	23.95528	24.84913	22.20142	20.25958	32.67084	17.6999	14.50447	6.607245	7.561564
Dret	18.21281	25.08364	33.53779	88.51463	87.26085	73.69041	82.47482	264.803	52.54438	40.54767	16.85057	25.21123
Economiq	4.53295	6.508452	7.767927	14.73799	14.66662	13.66791	11.17888	20.10626	10.89382	8.409924	4.06632	4.940973
total	10.91091	15.79576	19.12681	38.86745	40.40279	35.95622	34.9887	60.89481	30.85115	23.6619	10.81985	10.4759

As can be seen from table15 above the monthly SS% which relates production to consumption varies quite considerably from building to building. This confirms like as anticipated unlike production, consumption is not simply a function of the geometric area of the building under investigation. As can be seen above in the case of Moduls Central there exists many months of the year where production is in excess of consumption. This is likely to be down to many reasons including the fact the building is only one story high resulting in less loads within the given geometric area. Also perhaps lower rated loads than other faculties will play a part. Conversely the faculty of economics never produces a generation excess. This new understanding of the buildings which are likely to be net producers and net consumers of electricity within the overall campus will be vitally important when considering the design and interconnection of this system to ensure that production is effectively managed and utilised. As stated previously this will form a vital part of the analysis in a parallel study to this one; making this data of great importance.

7. Daily variation

This section will analyse both the production data obtained from the simulation and also the recorded consumption data over a 24 hour period. What will be obserbed here is how the daily “produtction Vs consumption” profiles for both the fully expanded system and also some individual buildings vary throughout the year.

Before observing a range of differentexamples, including average days for each of the months and individual campus buildings its is important to first look at the shape of typical consumption and production profiles for the Montilivi campus. Some of the key purposes of this examination include the following. Firstly, this will provide a very usefull insight into periods of the day when cross over between production deficit and excess is most probable; information which will be essential when considering the most efficient methods of generation utulisation. In addition to this, observing the 24 hour profiles will provide the data required in order to investigate demand side management and thus propose alternative consumption profiles which will propose maximum efficiency; both in terms of available generation as will be considered in this report but also fincacial efficency as will be considered in a parallel investigation. Typical production Vs consumption behavior for the campus is sumarised in figures 45 and 46 as seen below. The 24 hour periods seen in this case are for the average day in the month of may. Both the consumption and production data is that recorded and simulated for the full campus using the method explained previously.

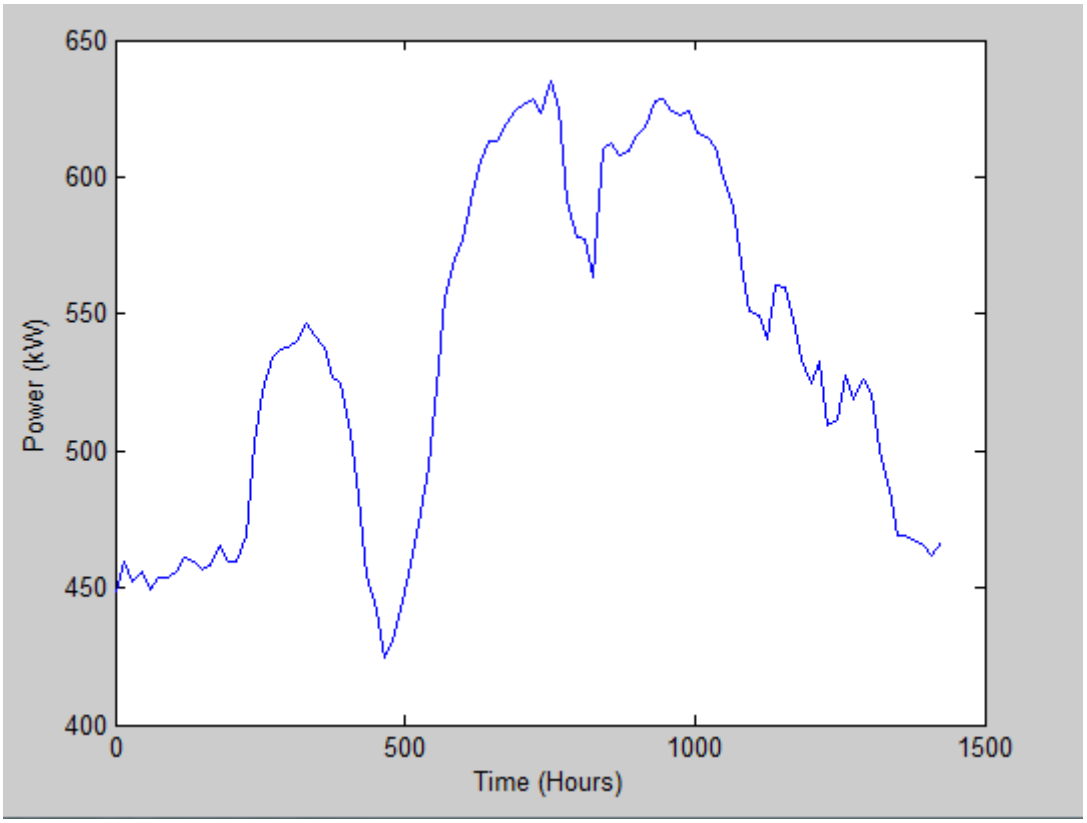

Figure 45: May full campus average daily consumption.

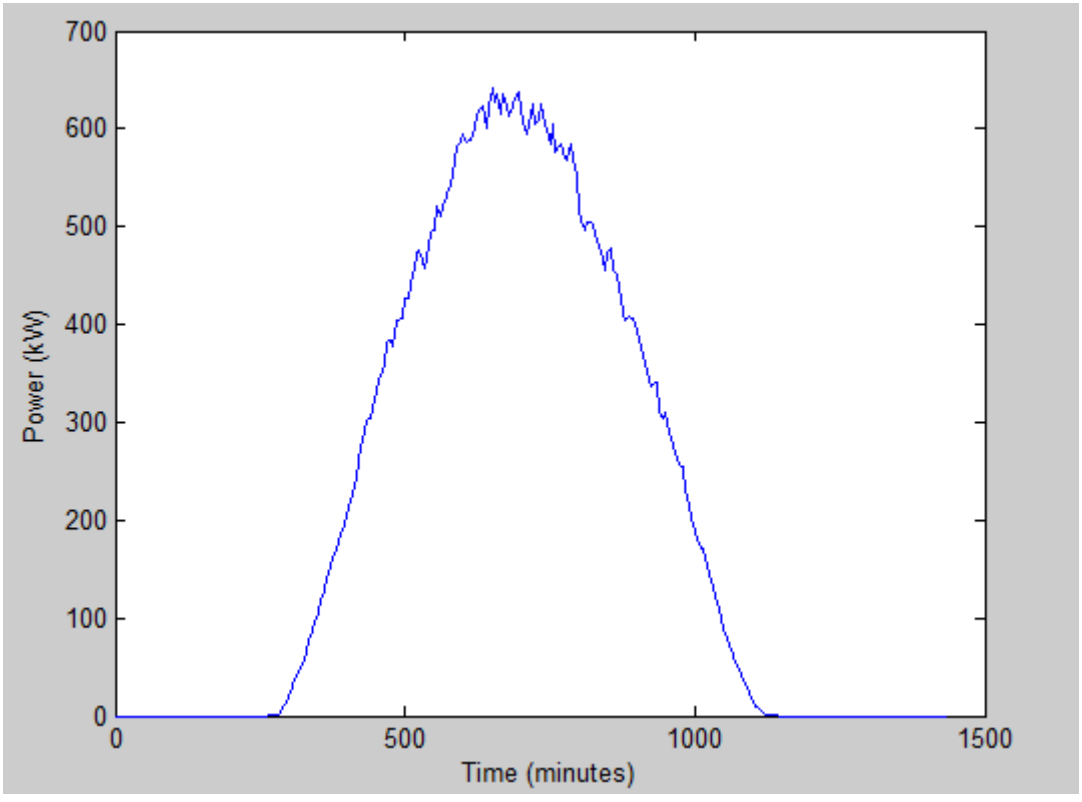

Figure 46: May average production.

Figures 45 and 46 show that the trend in consumption is is equally as distinct as that of the production. As can be seen in the consumption profile in figure 45, consumption sharply incrases around 4 Am before gradually decreasing until around half past 7. With the arrival of students on campus the comsumption then begins to increase to a maximum around midday, where whilst suffering a little fluctuation it remains high until around 2 where it again gegins to gradually decrease towards a minimum. When considering the solar production we see a profile which for the most part agrees strongly with intuition. Periods both very late at night and also very early in the morning show zero production. This is what one would imagine due to zero iraddiance being incident on the array. On the whole production increases towards a maximum output at around midday corresponding to what is known as solar noon: the time when the sun is at its highest point in the sky. After this the output gradually decreases at a similar rate. The very slight flucuations which can be seen in the profile are likely to be a result of variations in cloud cover throughout the day.

In most solar energy systems the process of intelegent demand side management is incredibley important, where user consumption profiles must be outlined in order to accommodate the periodic availability of the solar resource throughout the day. What can now be understood based on the trends seen in figures 45 and 46 is that fortunately periods of maximum consumption and production align during the day. This is incredibley helpful as it means that storage is not required to offset the time difference between peeks in both trends. Whilst in purely electrical terms the current consumption and production profiles propose and ideal solution where peaks in campus consumption can be simply supplied by peaks in solar genration, financial factors may in fact propose alternatives in order to maximise the system revenues. The hourly variation in the cost of grid purchased electricity may perhaps suggest alterations to the consumption profile such that the peak demand be shifted to a different hour in the day reducing the monthly expendature on electricity bills. At the same time hourly variations in the exportation tarrif may suggest that peak production be better stored on sight for release suring hours of typical peak demand and thus increased feed in tarrif. To conclude, this section will be of vital importance in order to provide a better understanding of the relationship between intantaneous campus generation and demand and thus better understand how to most effectively utilise all energy production. This will be investigated in a parallel study.

Noted in previous sections was that there exists large variations in energy production and consunption throughout the year due to changes in climactic variables and usage profiles. The effects of changes in these variables on instantaneous consumption and porduction will now be observed for all months in the year .

7.1 Monthly variation in instantaneous Production Vs Consumption

As mentioned previously it is very important to not only observe the relationships between the monthly energy consumption and production yields, but also the variation in

instantaneous production and consumption over the course of a day. This is extremely important as the relationship must be well understood in order to effectively and efficiently manage the production on site. Effective management will result in decreased losses and also increased revenues. This section will consider the instantaneous production and consumption across the full campus over a 24hour period. Both the mean and the mean $\pm 3\sigma$ data will be considered for each month throughout the year. Important to note in this case is that the value for standard deviation, σ is different for each month under examination. The value for σ is calculated as follows. For each day of the month and each time interval over the period of a day where the instantaneous power was recorded (every 5 minutes for production and every 15 minutes for consumption). The standard deviation across every day in each month was recorded for each of these individual time intervals in the day. The procedure was then repeated for each separate month giving traces seen below.

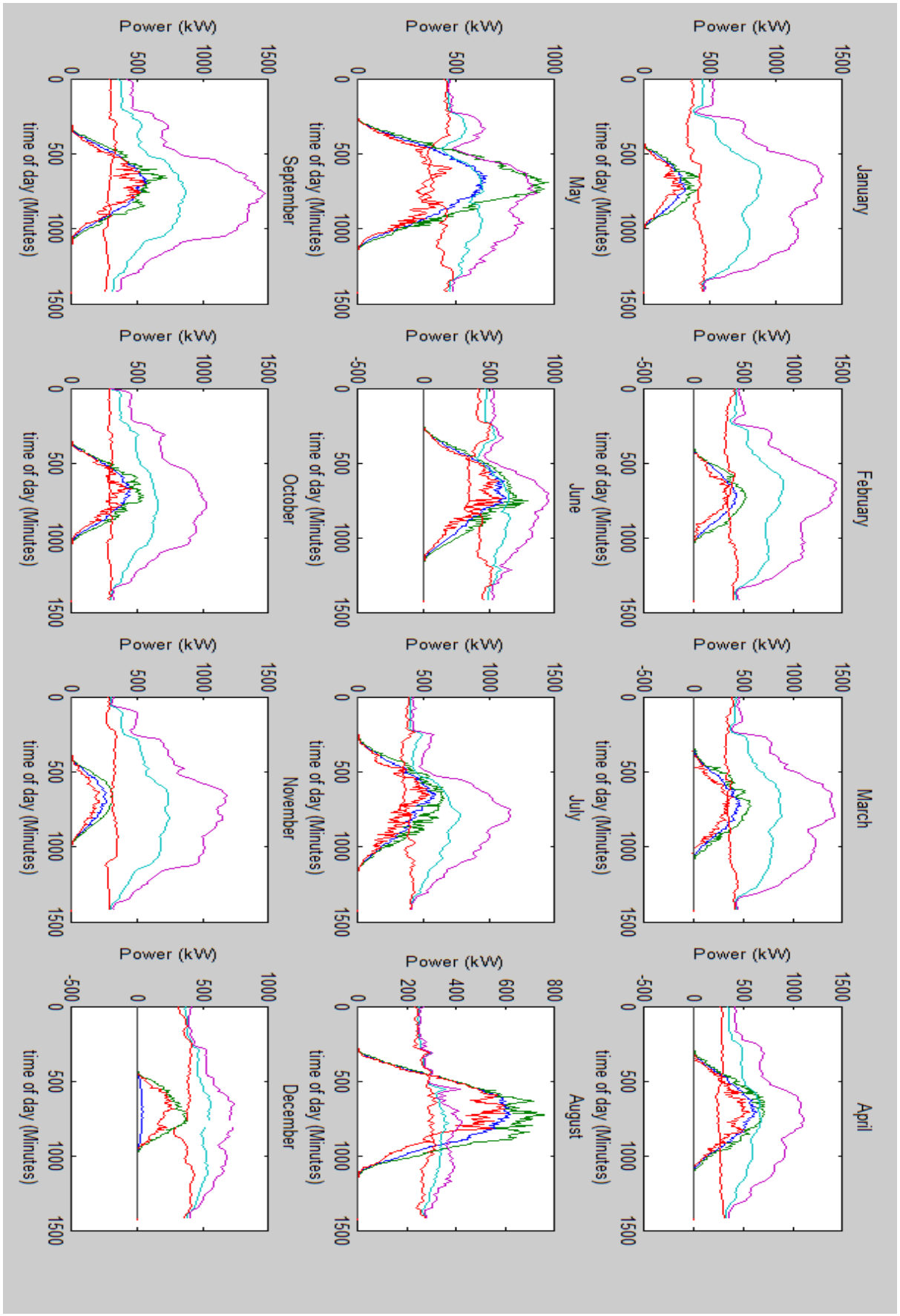

Figure 47:Monthly variation in average daily Production Vs consumption.

As can be seen the figure above over the course of the year there are quite considerable variations in both the electrical consumption and production seen on site. In August it can be seen that there exist large periods in the day when production is in significant excess of consumption. This is somewhat remarkable considering the very conservative estimate of total roof surface coverage which was discussed earlier. Conversely there are many other months where the productions in always in deficit of the consumption.

The findings of this analysis will be very important with regards to both a later section of this investigation but also for the parallel financial assessment of the installation discussed previously which will investigate utilisation methods including battery storage and grid export. Now the a better understanding of the variation in both consumption and production over the course of a day is known, methods of reducing university consumption and increasing production will be investigated. In many systems studies are carried out in order maximise efficiency in demand side management to ensure that nature of consumption over the course of the day is such that it is well aligned with production. Fortunately in the case of this system this is not required as seen previously, and instead what must solely be studied is the range of different ways in which the overall consumption can be lowered. Later sections will introduce two keys areas which must be addressed in order to optimise the benefits of a large scale PV system at the UDG. The first of these is the range of technical developments in the field of PV systems which have been made in recent years since the current systems initial construction. The second area includes examples of methods used to reduce overall consumption on university campuses.

7.2 Working Vs Holiday period analysis

One very important aspect which needs to be considered during system design is the effect of university holidays and weekends on consumption. As one would likely assume, during these periods consumption is likely to be far less than that of the working week, specifically during typical peak consumption hours. Decreased consumption during these holiday periods where large sections of the university are closed propose the following scenarios. Consider winter months where over the course of a typical working day, production never tends to be in excess of consumption due to the alignment of peak production with peak consumption. During holidays however this peak production may be high enough so as to exceed the now largely decreased consummation during peak hours. Additionally in months where peak periods already tend to produce production excess, the duration of this excess will now be increased during holidays. All in all the effects of this variation in the Production Vs Consumption deficit profile mean than the system must be designed in order to be flexible, so as to easily adapt between being the sole provider to the university campus and also working in tandem with grid bought electricity. Key system design parameters such as battery array capacity all depend on the relationship between production and consumption. Whilst the production will bear no relationship to whether the university is open or not, it will be important to observe how these holiday period's consumption typically varies from the working weeks for each month of the year. Especially weekends due to their cyclical re-occurrence every week. The following graphs were simulated in order to observe how the monthly average Production Vs Consumption profiles for both weekdays and weekends vary.

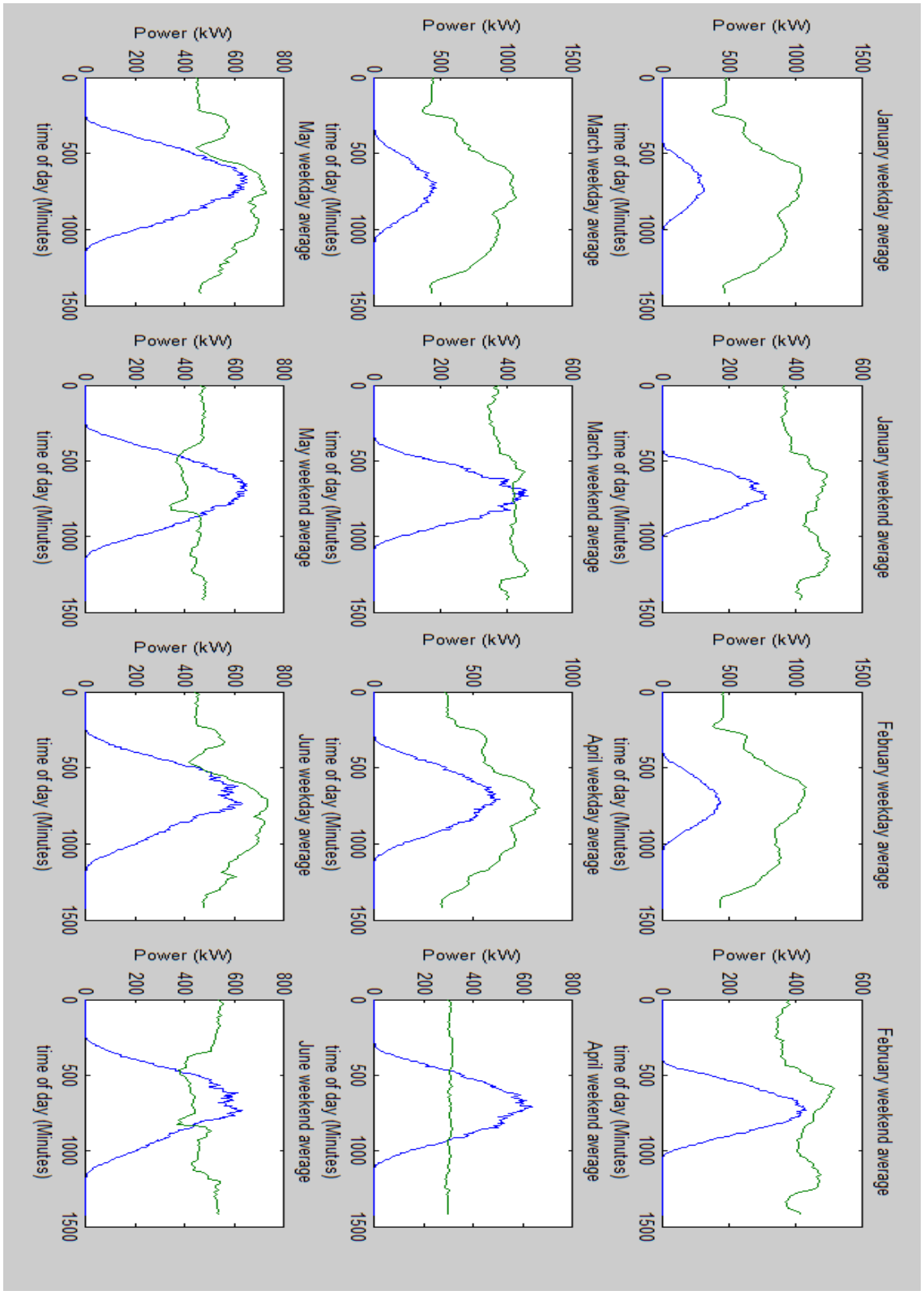

Figure 48: "Production Vs Consumption" months January to June "Weekday Vs Weekend" comparison.

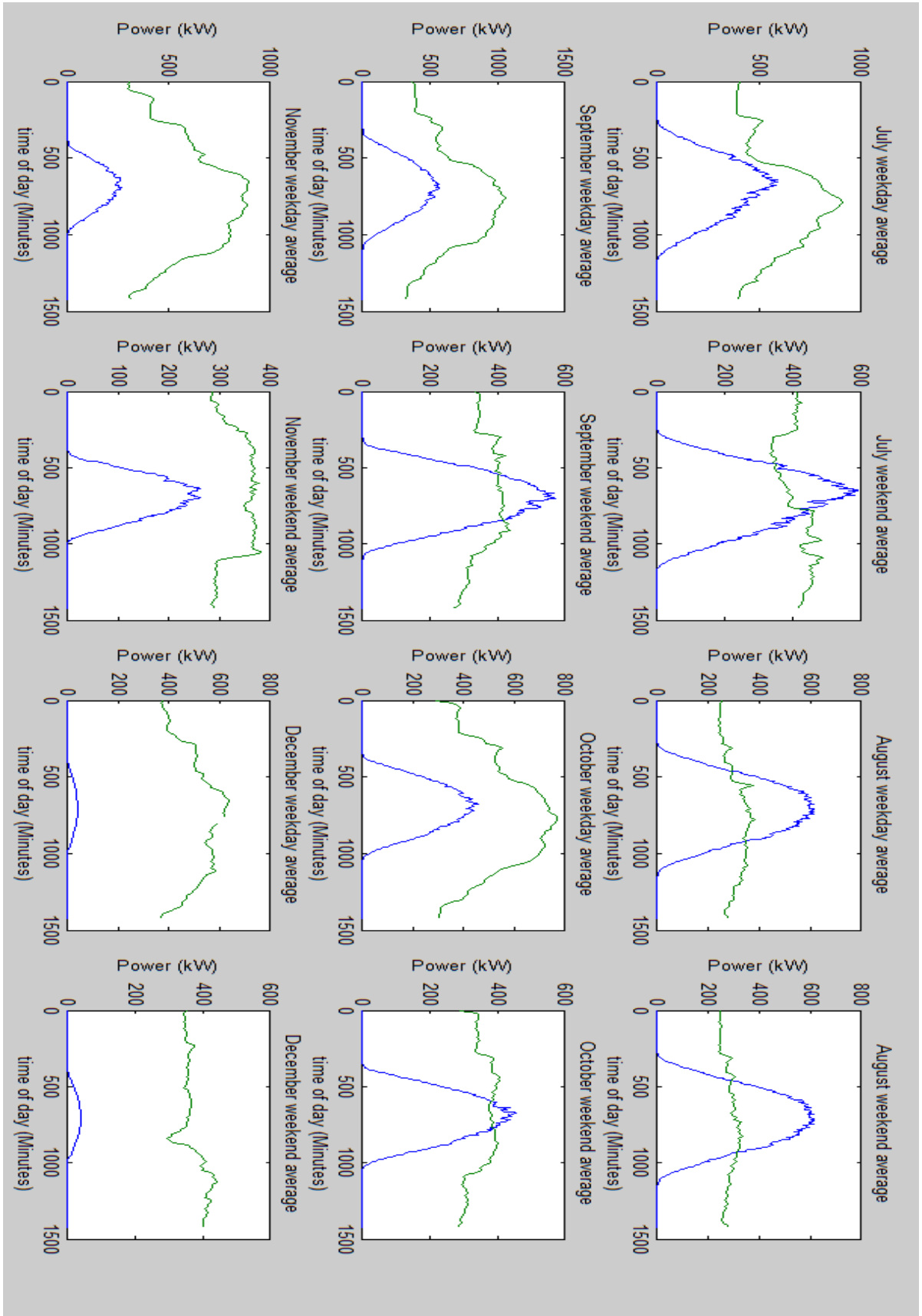

Figure 49: "Production Vs Consumption" months July to December "Weekday Vs Weekend" comparison.

Both of the above figures confirm the hypothesis that the decrease in consumption from weekdays to weekends is maximized during periods of typical peak consumption. As can also be seen during months such as August, where ordinarily production during the week is in excess of consumption for certain periods, what can now be seen at the weekends are longer periods where the production is greater. Figures 50 and 51 further demonstrate these findings. The traces seen represent difference between production and consumption. Positive values represent production excess and negative for production deficits.

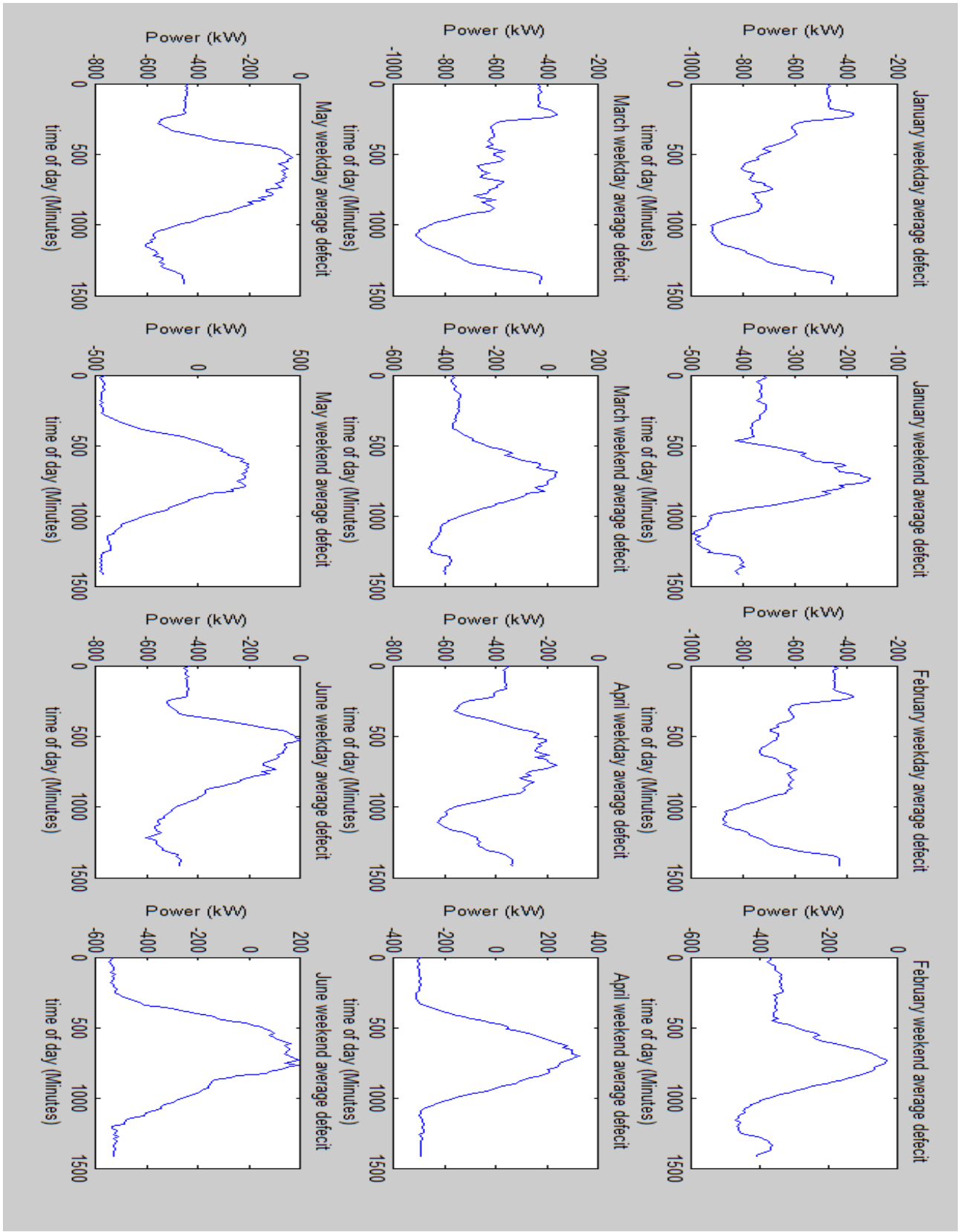

Figure 50: On sight generation excess months January to June "Weekday Vs Weekend" comparison.

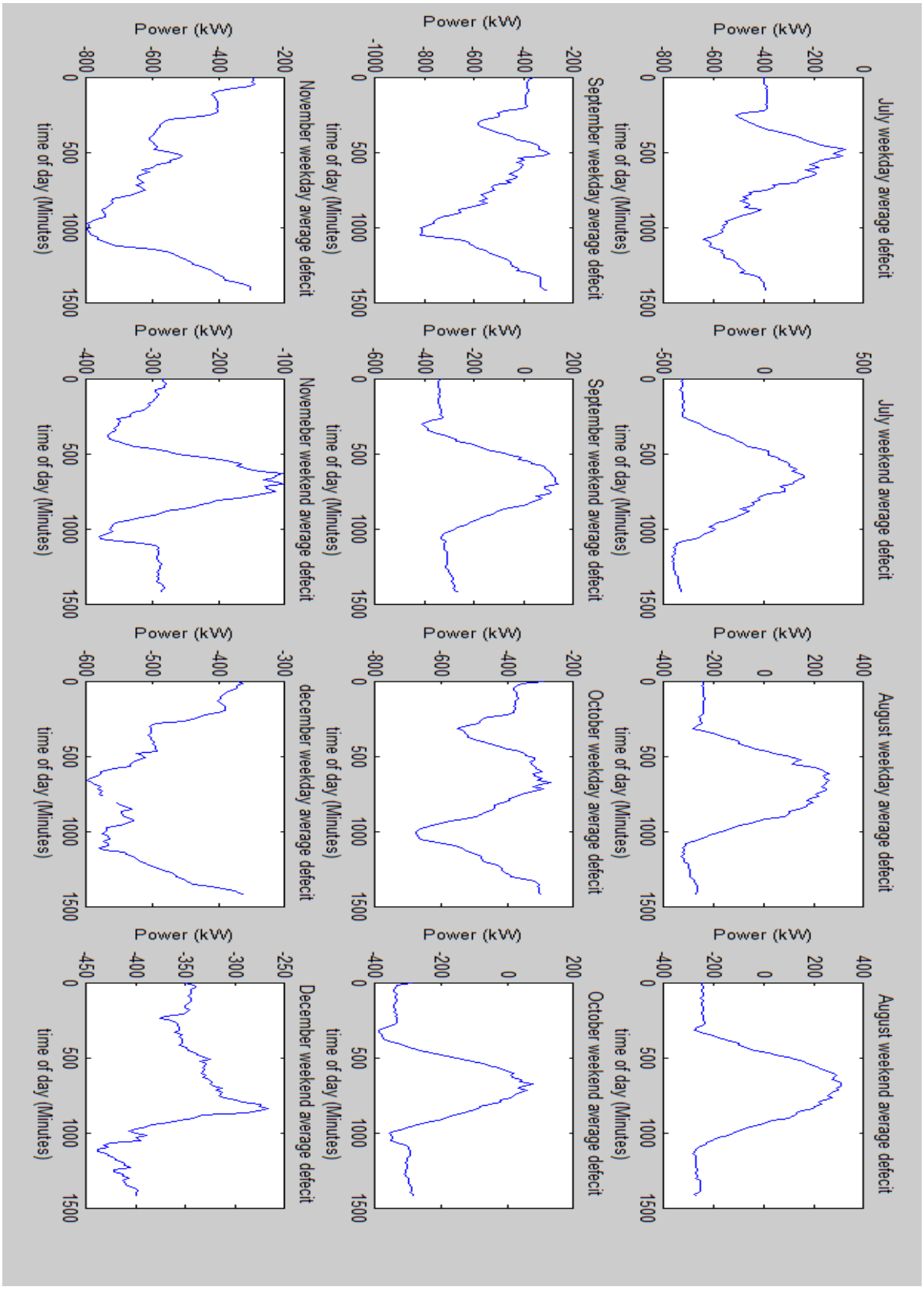

Figure 51:On sight generation excess months July to December "Weekday Vs Weekend" comparison.

The above results show that during holiday periods, specifically in summer months such as august despite the alignment of peak production with peak demand there are likely to be periods of time when production is in excess of the consumption on campus. Important to remember is that this is for the expansion of the system based on extremely dated inefficient technologies. As will be seen in section 8 below , when updated to use state of the art panel technologies and tracking systems production can be expected to massively increase. For this reason even if financial factors insist the primary intention is for all production to be directly consumed on site, there will exist periods where significant excesses in generation must be dealt with. There will be a parallel study to this one which will investigate the financial benefits of the different utilisation methods which could be used to address this excess, be it battery storage or grid export. Important to bear in mind is that the above analysis is taken as an average for the production and consumption over the full campus. Different grid connection points for different campus buildings are likely to lead to complications regarding system design when it comes to utilising excess and buying in electricity in periods of deficit. For these reasons it may well be useful to observe the relationships on an individual building basis.

7.3 Extreme of Production Vs Consumption Per Building

Table 15 shows that magnitude of the difference between consumption and production varies largely from building to building across the campus as well as throughout the year. This is largely down to the fact that whilst production is purely a based on the available roof top surface area, consumption is in fact a function of several factors. These may include for example the number of floors in the building and also the typical loads which it may serve. As can be seen in table 15 Moduls central represents the case for maximum production with minimum consumption, whilst the faculty of Economiques represents the opposite. For this reason these two examples will be examined in more detail in order to better understand how the relationship between supply and demand varies throughout the day for individual buildings in comparison to that of the full campus seen previously. The results of this examination can be seen below. Important to note that is that as well as showing the extremes, in terms of the building on campus, average daily generation and consumption profiles are shown for the extreme months throughout the year. The month of January represents that of maximum consumption and minimum production and August that of maximum production and minimum consumption.

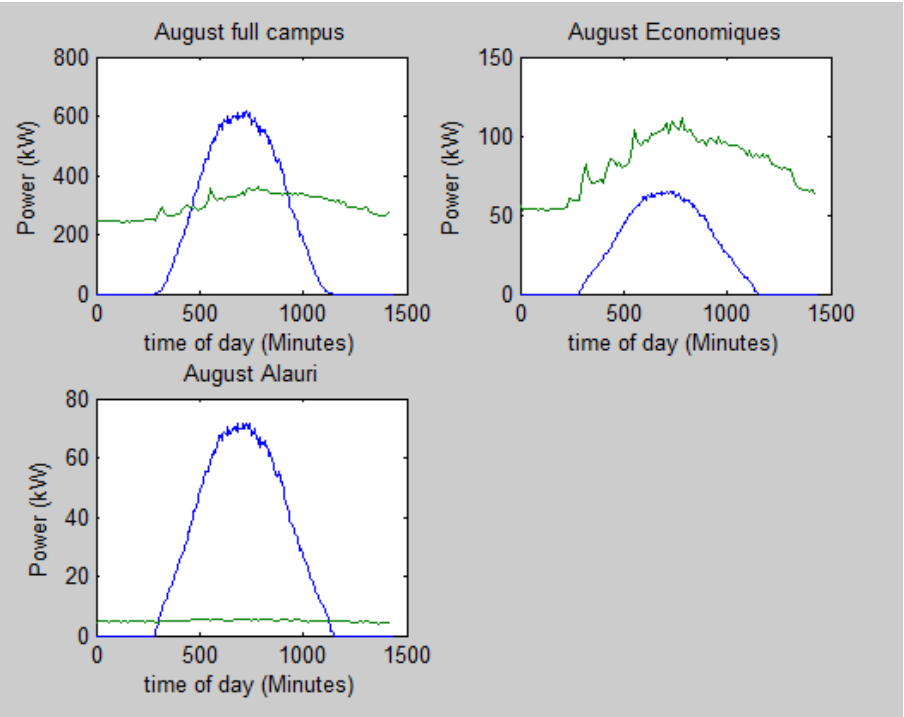

Figure 52: Extremes of individual buildings daily "Production Vs Consumption" for August.

.

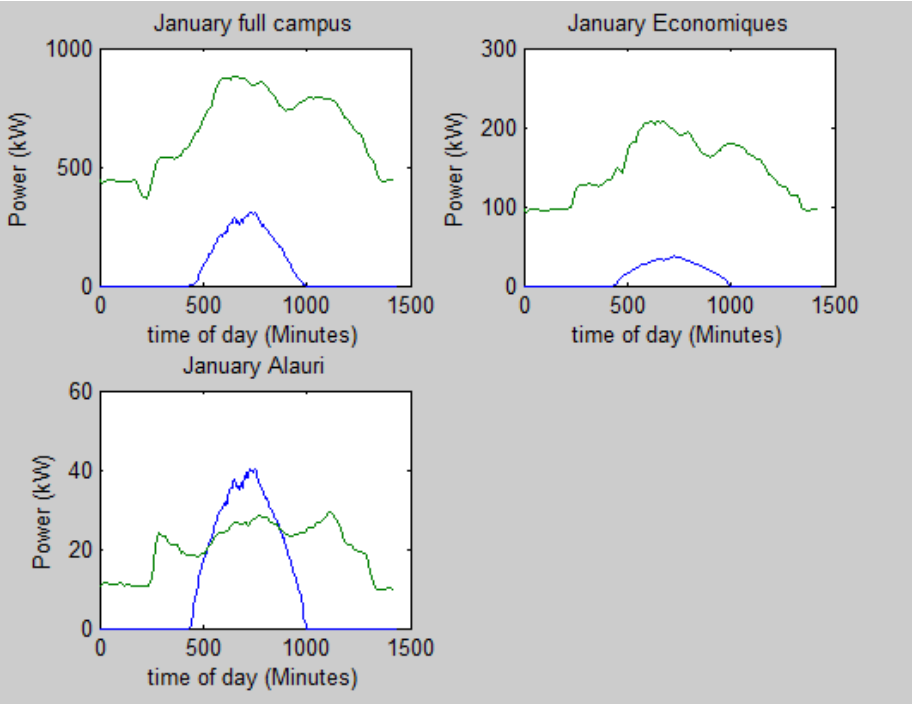

Figure 53: Extremes of individual buildings daily "Production Vs Consumption" for January.

Both figures 52 and 53 above represent that throughout all periods of the year, there are significant variations in relationship between production and consumption for different buildings on campus. Whilst at least for expansion using the current technology, the faculty of economics is never capable of producing enough power to cope with consumption, during summer specifically the modul centrals (Alauri) is capable of producing significant excesses. What can also be seen, like in previous sections is how these relationship average out when extrapolated over the full campus. The above results provide useful insight, to consider in the stage of system design, as the interconnection of arrays and connection points to both the utility grid and university load centres must be flexible such that production can be utilised as cost efficiently as possible. For example generation from an array at one side of the campus may need to be able to supply a different building during periods of significant excess generation.

8. Maximising Campus self-sustainability

8.1 State of the Art Commercial Technologies

In the years that have passed since the system at the UDG was installed, there have been major progressions in the field of PV technology. Whilst many advances exist in present commercial technologies some are still only in the R&D stage. This section will summarise developments in two key areas of commercial PV; solar tracking and cell efficiency. Using this newly gained understanding of the benefits proposed by these technologies, the simulation will be updated and the benefits in terms of enhanced energy yield observed. Seen in appendix 1 are additional examples of PV technologies which are still in development, whilst at present it is not possible to incorporate these technologies in the software simulation these provide a useful insight into how PV efficiency is likely to improve in the future.

8.1.1 Key trends in solar generation

The graphic seen in figure 54, shows 3 of the most important trends relating to Photovoltaic technology over the last 60 years. Two of these, both the reduction in panel size and also the increase in efficiency will be massively important when considering updating the hardware present in the UDG installation. Reduction in panel size for a fixed wattage will mean the same capacity can be installed over a smaller area. This will result in the ability to fit more panels onto a given roof surface resulting an in increase in the potential production of each building on campus. Increases in efficiency allow a higher percentage of the suns incident solar power to be converted into electrical power. In order to better understand the concept of cell efficiency one can consider the following equation. Efficiency is evaluated as seen below where the variables are defined as follows.

$$\eta = \frac{P_m}{E \times A_c} \quad (19)$$

- P_m = cell maximum power point (W)
- E = Incident irradiance from sun (W/m^2)
- A_c = Cell area (m^2)

Re-arranging equation 19 above reinforces the idea that for fixed cell dimensions and incident irradiance, increased efficiency will result in a greater power output. For this reason the combined effect of these two developments could result in significantly increased outputs from the system if updated to contain state of the art technology. As can be seen in figure 54 in the time period from 1953 to the present day, for a fixed wattage the required size of solar

panel has been reduced to an incredible 1/27th of its former size. This is primarily due to the huge increase in panel efficiency which has been observed over the same time period. Far apart from the pioneering technology in this field which offered very low efficiencies of around 4.5%, State of the art technology today can offer up to as high as 23.5% efficiency. With this figure set to rise even higher into the next decade as a result of the series of R&D areas discussed in appendix 1.

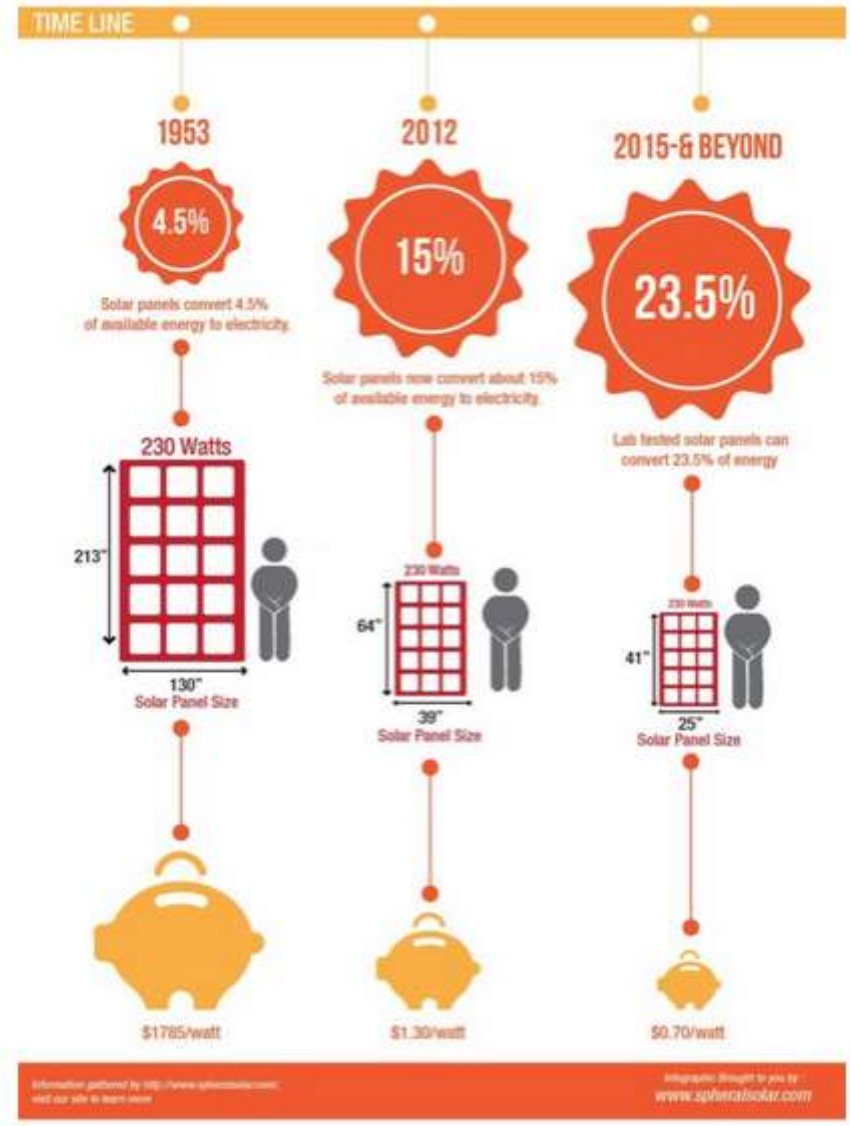

Figure 54: Summary of advances in PV technology.[21]

Two Modern State of the art solar panels from leading manufacturers will now be compared against the model used in the current installation. This comparison will help give a further insight into the technical developments which have been made since the systems inception over two decades ago.

8.1.2 BP 4160

The panel used in the current installation is the BP Solar 4160. A breakdown of the key panel characteristics is given below.

- Construction: monocrystalline silicon
- P_{max} = 160W
- Area = 1.256m^2
- Efficiency = 12.7%

8.1.3 Sunpower X-series

- Construction: Maxeon Silicon [22]
- P_{max} = 345 W
- Area = 1.631m^2
- Efficiency = 21.5%

8.1.4 Panasonic VBHN245SJ25

- Construction: Amorphous silicon
- P_{max} = 245W
- Area = 1.261m^2
- Efficiency = 19.4%

Both technologies seen above represent the huge advances which have been made in the field of PV generation since the UDG systems construction over 2 decades ago. In the case of the Sunpower X-Series module, performance has increased to the extent that an installation over the same surface area could now produce more than double the energy yield than that of the current installation for an identical time period.

8.1.5 Solar tracking

A Solar Tracker is a device which is used to automatically alter the orientation of the solar panels so as to ensure that the panel's surface is where possible to always perpendicular to the oncoming solar irradiation. Incident direct beam radiation can be more efficiently absorbed when the radiation striking the panel becomes progressively more perpendicular to the panels surface. This is well documented in the investigation seen in [27]. A brief summary of the findings of this report can be seen below, where an identical solar cell was rotated through the range of angles under identical conditions of irradiance. As can be seen, power output is at a maximum when the cell surface and solar irradiance are perpendicular and at a minimum when parallel. This again reinforces the potential benefits of solar tracking.

Solar cell angle to sunlight	Voltage (Volt)	Current (ampere)	Power (watt)
90° to sunlight	0.450V	1.80A	0.810W
75° to sunlight	0.437V	1.75A	0.765W
60° to sunlight	0.425V	1.70A	0.722W
45° to sunlight	0.400V	1.60 A	0.640W
30° to sunlight	0.362V	1.45 A	0.525W
15° to sunlight	0.325V	1.30A	0.422W
0° to sunlight	0.287V	1.15A	0.330W

Figure 55:PV Output variation with angle of incident light.[33]

For solar PV applications the most common method of solar tracking is what is known as "moving collector" where the panel surface area moves progressively throughout the day in accordance with the suns location in the sky. Moving collector technologies can be further classified further as either single or dual axis trackers. The differences as one would imagine is that the later allows for rotation in more than one direction. It is capable of tracking both the movement of the sun in the sky throughout the day, and also its movement in the opposite axis throughout the different seasons. The former however, only follows the primary motion of the sun throughout the day. Both of these are as opposed to what is known as fixed mount installations. These are those as seen in the current UDG installation where the rotation of all panels is fixed. Studies have shown that for single axis trackers significant increases in annual yield of around 30% have been observed. For dual axis trackers furthers increases of around 36% have been observed. Figure 56 below shows a simple graphical representation of how solar tracking may benefit the output from a single solar cell.

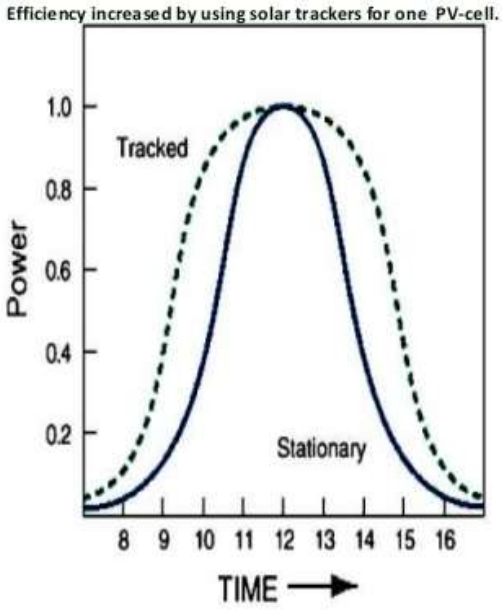

Figure 56:Typical benifits of solar tracking technology.[33]

Examined below are two examples of typical modern day solar tracking systems. These examples further describe the functionality of this technology and also the benefits it could bring to the installation at the UDG.

Example (A) Wattsun Duratrack dual axis tracker

The Wattsun Duratrack device is capable of holding up to 12 panels and provides extensive dual axis tracking. The manufacturer claims that the product is capable of obtaining 40% higher production than using the same generation with a fixed axis. Below are some of the key parameters relating to the product obtained from the manufacturer data sheet.

System Installation and Specifications	
Racking/Tracking Type	Dual Axis Tracker
Tracking range East – West	+/- 120°
Tracking range North – South	5° to 60°
Energy Gain vs. Fixed-Tilt Rack	Up to 40%, site specific
Module Configuration	9 – 12 standard 60 cell modules in landscape
Modules Supported	Most commercially available

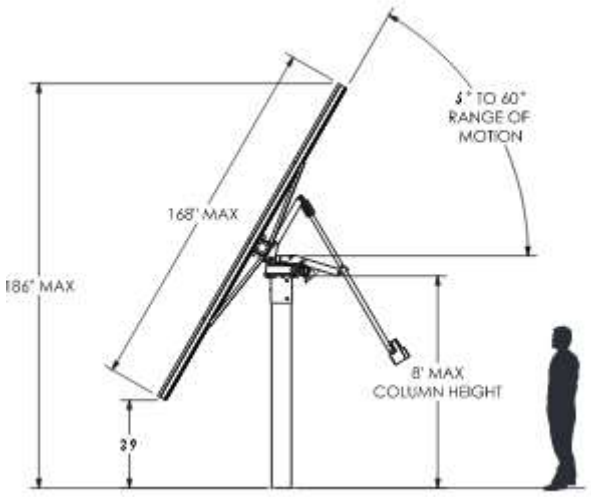

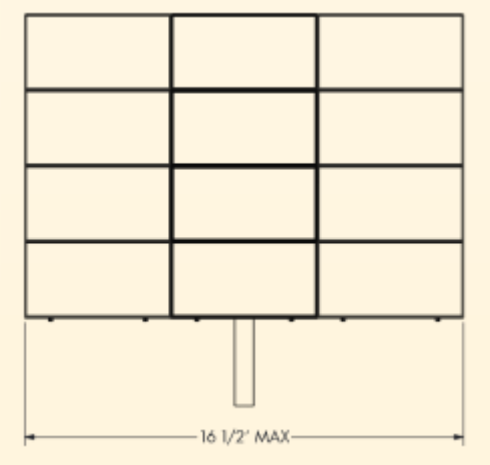

Figure 57: Summary of Dual axis tracker technology.[29]

Example (B) Wattsun Duratrack single axis tracker

This is a single axis product from the same leading manufacturer as seen previously. It is capable of holding up to 48 modules however proposes a lesser percentage increase in output as expected due to the single axis of rotation. Again some of the key parameters can be seen below.

System Installation and Specifications	
Racking/Tracking Type	Horizontal Single Axis Tracker
Tracking range East – West	45° – 45°
Tracking range North – South	Fixed
Energy Gain vs. Fixed-Tilt Rack	Up to 25%, site specific
Module Configuration	24 – 48 single standard 60 cell modules in portrait
Modules Supported	Most commercially available

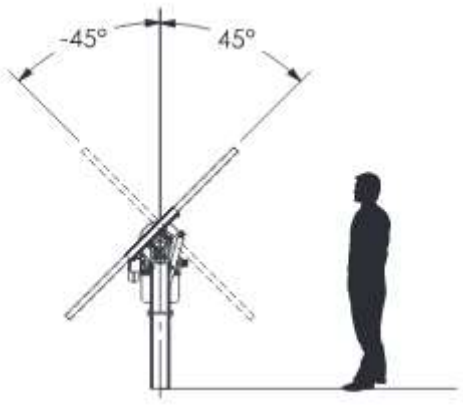

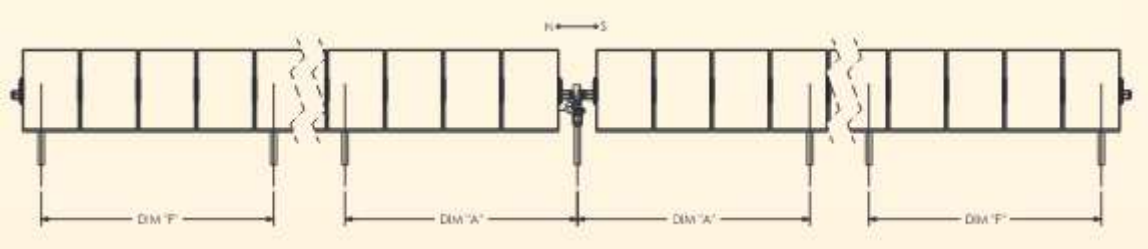

Figure 58: Summary of single axis tracket technology.[30]

Again, like with the two panel technologies seen previously this highlights another commercial product which could propose considerable increases to the electricity production on campus. Whilst all would require significant capital investment, perhaps exportation or energy savings based enhanced production within the system lifetime would result in a net saving in the period. This will all be examined in a parallel study to this one which will be investigating the financial implications of system expansion.

9. Updated simulation for modern PV technology.

Detailed in the last section were just a few of the key advances which have been made in the field of PV technology since the UDG installation was commissioned roughly 2 decades ago. This section will analyse the potential benefits in terms of energy yield which could be achieved if the system technology was updated to include the state of the art discussed above. Other advances which have been made in this period and could provide much benefit include the move towards Microinverter technology as opposed to the conventional string converter approach. For these advances however it would be difficult to determine the exact magnitude of the benefits as often yield increases arise from factors such as shading and individual panel malfunction as will be explained in appendix 1: these are all factors which are very difficult to include in the current model as Microinverter technologies provide maximum benefits when high levels of irradiance and temperature variation across the array are observed leading to panel output mismatch. When little mismatch is observed, the benefits are somewhat lessened in terms of percentage increase in system efficiency. For this reason the inclusion of this technology in the newly updated system will be given exemption.

The consequences however of changes in panel and racking technology are well known (And also constant) and can be simply entered into the existing simulation. In doing so, the benefits of upgrading the system technology to "state of the art" can be observed. In this case the panel technology will be changed to the Sunpower X-series panel seen previously, and the conventional fixed racking of the current system altered to the Wattsun dual axis tracker. These two technologies are the very best which is currently on the market and will thus provide the maximum benefits to system output. The important alterations made to the code can be seen in separately annexed code. The following section details the new relationship between monthly generation and energy consumption for this updated system.

9.1 Alteration in panel dimensions

In a previous section the available roof top surface area and existing panel dimension were used in order to calculate the total number of panels which would be installed. When upgrading to the new technology it is important to notice that the individual panel dimensions have since changed. It is important therefor to re-evaluate the total number of panels which can be installed across the full campus. In order to ensure consistency, again the same percentage coverage as used previously will be implemented. The calculation process can be seen below.

9.1.1 Number of panels adaptation

Remainder of EPS P1

$rooftop\ Surface\ area = 3866.5\ m^2$

$total\ panel\ coverage = 3866.5\ m^2 * 0.27 = 1044\ m^2$

$number\ of\ panels = 1044\ m^2 \div 1.63 m^2 = 641$

EPS P2 and P4

$rooftop\ Surface\ area = 7384.6 m^2$

$total\ panel\ coverage = 7384.6 m^2 * 0.27 = 1993.8\ m^2$

$number\ of\ panels = 1993.8\ m^2 \div 1.63 m^2 = 1223$

Moduls centrals

$rooftop\ Surface\ area = 2644.53 m^2$

$total\ panel\ coverage = 2644.53 m^2 * 0.27 = 714\ m^2$

$number\ of\ panels = 714\ m^2 \div 1.63 m^2 = 438$

Biblioteca

$rooftop\ Surface\ area = 2344.8\ m^2$

$total\ panel\ coverage = 2344.8\ m^2 * 0.27 = 633.1\ m^2$

$number\ of\ panels = 633.1\ m^2 \div 1.63 m^2 = 388$

Facultat de ciencies

$rooftop\ Surface\ area = 3846 m^2$

$total\ panel\ coverage = 3846\ m^2 * 0.27 = 1038.4\ m^2$

$number\ of\ panels = 1038.4\ m^2 \div 1.63 m^2 = 637$

Facultat de dret

$rooftop\ Surface\ area = 2707.9m^2$

$total\ panel\ coverage = 2707.9m^2 * 0.27 = 731.1\ m^2$

$number\ of\ panels = 731.1\ m^2\ \div 1.63m^2 = 449$

Facultat de economiques

$rooftop\ Surface\ area = 2366.5m^2$

$total\ panel\ coverage = 2366.5m^2 * 0.27 = \ 639m^2$

$number\ of\ panels = 639m^2\ \div 1.256m^2 = 509$

Current installation

$rooftop\ Surface\ area = = 446.49\ m^2$

$total\ panel\ coverage = = 446.49\ m^2 * 0.27 = \ 120.55m^2$

$number\ of\ panels == \ 120.55m^2\ \div 1.63m^2 = 74$

Now that the total number of panels has been calculated taking into account the new hardware dimensions, the code which details the total number of installed panels in the system was updated to account for this. What must now be altered are the specific electrical properties relevant to the new panel technology. These adaptations will be discussed in the following section.

9.2 Alterations to relevant panel parameters

Now that the total number of panels has been updated in order to account for the new panel dimensions, what must also be considered are the different electrical parameters relevant to the new hardware. As seen previously, the panel technology is defined on an individual cell level. Parameters such as the short circuit current, open circuit voltage and current/temperature coefficient are used in order to describe the exact behavior of the PV generator. The exact parameters relevant to the new hardware examined in this analysis can be seen below, taken directly from the manufacturer data sheet. The modular nature of the system simulation allows for these parameters to be very easily altered, for the full system under examination. Newsinglecell.m shows how these new parameter alterations are set

within the code compared to the original technology in singlecell.m. Again like seen in section 5, the error correction associated with the simulation was altered in order to cope with the change total installation capacity. Important to note is that whilst the same roof top area is being used as in section 5, the updated panel technology and consequent increase in efficiency will likely result in increased total capacity per meter squared. For this reason the error correction must again be altered. Calculating the correction as in equation (17) a new correction of 15567W was applied for every value of instantaneous power.

ELECTRICAL DATA		
	X21-335-BLK	**X21-345**
Nominal Power[12] (Pnom)	335 W	345 W
Power Tolerance	+5/–0%	+5/–0%
Avg. Panel Efficiency[13]	21.1%	21.5%
Rated Voltage (Vmpp)	57.3 V	57.3 V
Rated Current (Impp)	5.85 A	6.02 A
Open-Circuit Voltage (Voc)	67.9 V	68.2 V
Short-Circuit Current (Isc)	6.23 A	6.39 A
Maximum System Voltage	600 V UL ; 1000 V IEC	
Maximum Series Fuse	20 A	
Power Temp Coef. (Pmpp)	–0.30% / °C	
Voltage Temp Coef. (Voc)	–167.4 mV / °C	
Current Temp Coef. (Isc)	3.5 mA / °C	

Figure 59: State of the art Panel technology data sheet.[23]

With these new parameters now applied to the simulation as seen in newsinglecell.m both the I-V and P-V characteristics could be observed. Important to note is that these value for open circuit voltage and short circuit current are for the overall panels and not the individual cells. Since each panel consists of 96 series cells, conversion to the individual cell equivalence can be easily achieved, as seen previously with series combinations increasing the output voltage.

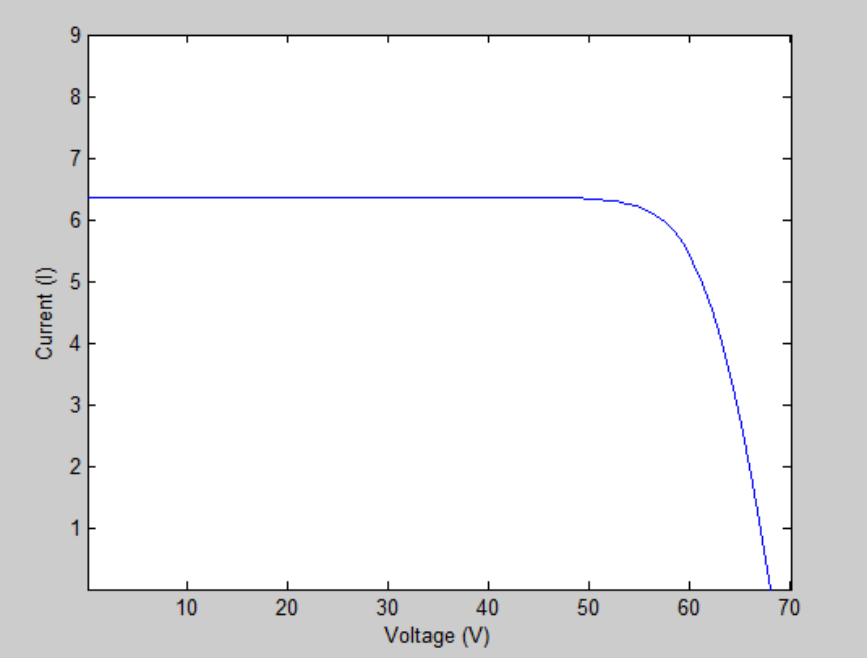

Figure 60: New technology I-V curve.

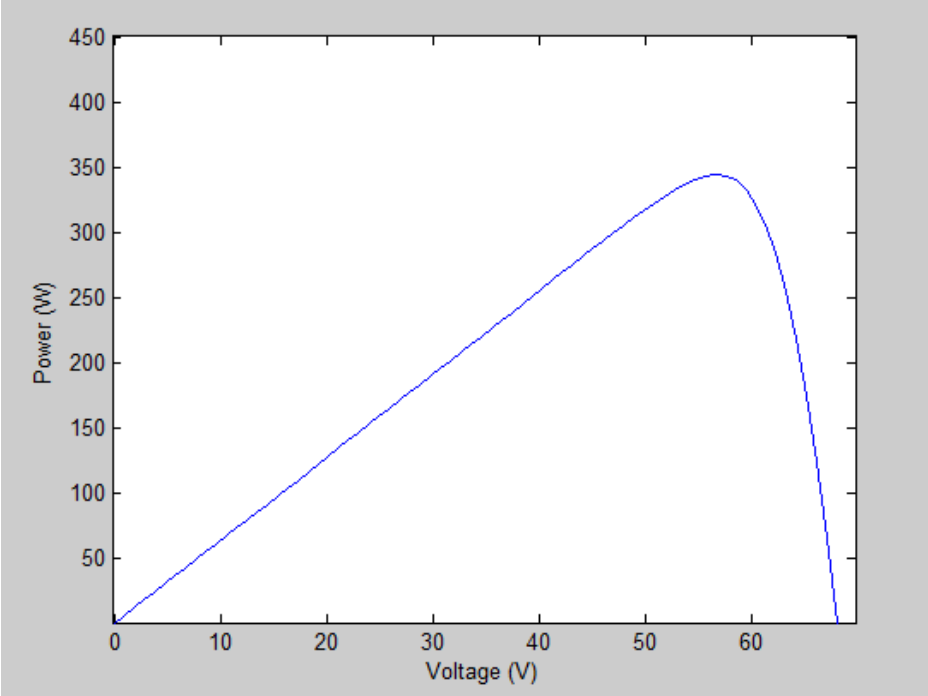

Figure 61: New technology P-V curve.

Both the I-V and P-V characteristics of the new software can be seen above. Important to note is that both the temperature and irradiance behavior could also be easily observed but have been left out of this analysis in order to avoided repetition (same relationship as previously discussed was again used). Both the Theoretical and simulated values of the maximum power and maximum power voltage can be seen below for standard test conditions. Like in the initial panel confirmation the % error was again noted. This serves as

confirmation that the newly simulated panels again accurately represent the real life hardware.

Table 14: Simulation error for new technology.

	V_{MPP}	P_{MPP}
Data sheet	57.3V	345W
Simulation	56.6V	345.2W
% error	1.2%	0.06%

These values of error were again decided to sufficiently accurately describe the hardware which is here been proposed to be installed at the university.

With this now confirmed, the analysis will be extended to production over the full campus accounting for the inclusion of dual directional solar tracking.

9.3 Updated system monthly energy yields

With the simulation now altered to account for the inclusion of state of the art PV panels the monthly energy yields were now re-evaluated and again compared to the full campus consumption. What was also considered in this analysis of the newly updated system was the inclusion of the dual directional solar tracking technology as discussed previously in section 10. As Justified by extensive manufacturer testing, use of dual direction solar tracking can provide up to 40% increases in energy yields when compared to fixed racking installations. A simple multiplication factor of 1.4 can thus be applied in order to obtain the maximum yield which could be expected from the system. The results are summarised below showing the comparison in monthly energy yield for the newly updated system, with the full campus consumption data as seen previously.

Table 15: Monthly variation in Energy consumption, production and SS% (full campus).

Month	Production no tracking kWh	Production with tracking kWh	Consumption kWh	Self-Sustainability % no tracking	Self-Sustainability % with tracking
January	93514.57053	130920.3987	453436	20.62354346	28.87296085
February	126264.1817	176769.8544	428356	29.47645923	41.26704292
March	164522.3846	230331.3384	463967	35.45993241	49.64390537
April	243661.9936	341126.791	339822	71.70283077	100.3839631
May	292814.9323	409940.9052	393611	74.39195864	104.1487421
June	268341.5541	375678.1758	402907	66.60136313	93.24190838
July	250717.0217	351003.8304	384953	65.12925518	91.18095726
August	274864.2958	384810.0141	242615	113.2923751	158.6093251
September	215745.9743	302044.364	374022	57.68269629	80.7557748
October	162574.1463	227603.8049	365448	44.4862597	62.28076357
November	80047.0681	112065.8953	387750	20.64398919	28.90158487
December	91010.77308	127415.0823	456849	19.92141234	27.88997728
Annual	2264078.896	3169710.455	4693736	48.23617894	67.53065052

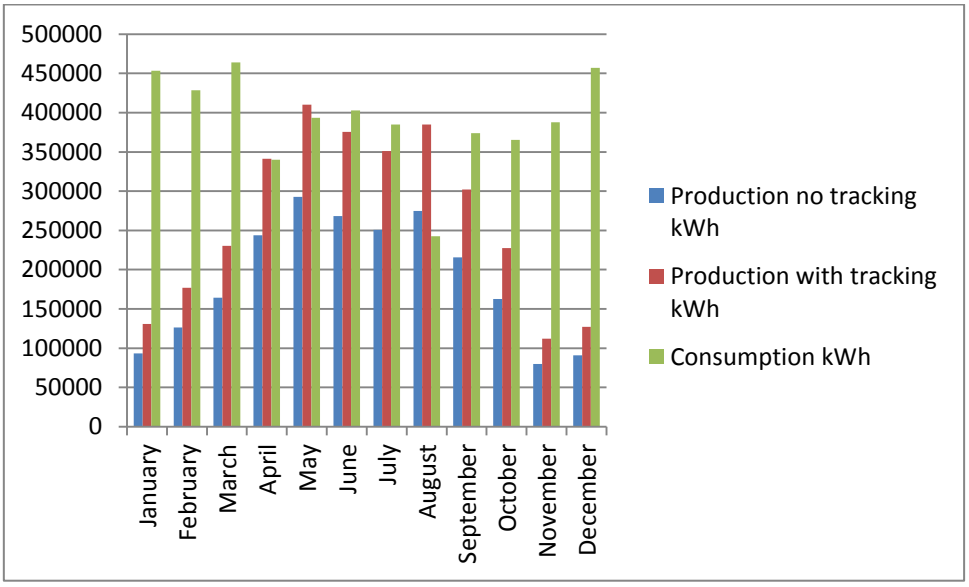

Figure 62: Proposed full system monthly energy yields with technology upgrade.

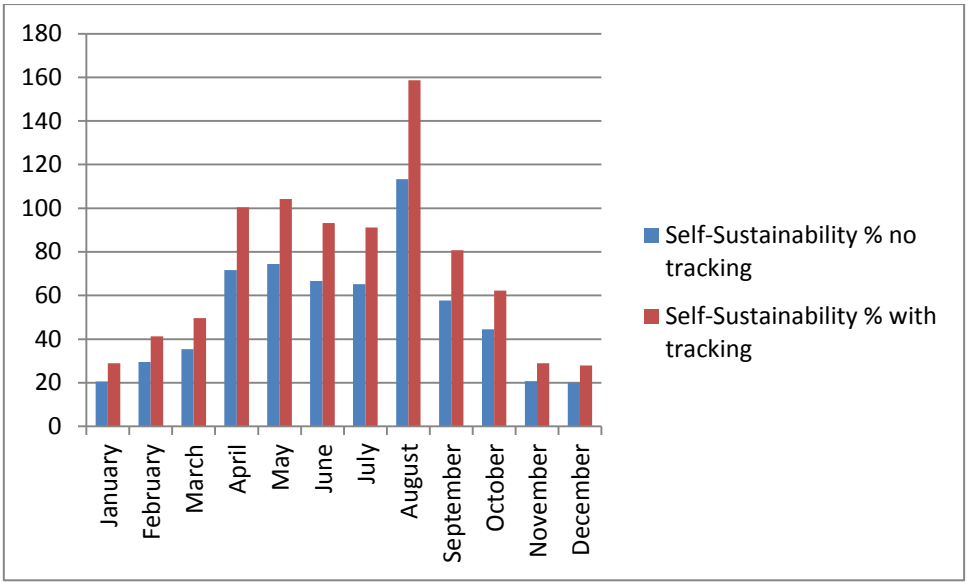

Figure 63: Monthly self-sustainability percentage with and without Solar tracking technology.

Seen in table 63 above are both the upper and lower Self-sustainability percentages. These represent the maximum and minimum percentage of full campus consumption which can be provided by an installation using both state of the art PV panel technology and solar tracking. What can be observed is that these percentages are now roughly twice as large as those seen previously for the system containing fixed racking and older, inefficient panel technology. This statistic provides a very clear representation of the significant increase in the monthly energy yield which could be achieved through updating the hardware used in the installation. As can be seen in figure 62 above, for August the monthly yield is greater than the monthly consumption. Although in analysis of the previous system there were periods in the day when the instantaneous production was greater than consumption, the accumulated yield over the course of a month was never in excess of consumption. When considering the instantaneous production verses consumption over the course of an average day in each month it is likely now that there will now be long periods of time when production surpasses consumption. This will be analysed in the next section. By gaining a clearer idea of the lengths of these periods throughout the day and also the variation throughout the year, it will be possible to better understand and analyse the most effective methods of utilising the production. Again this will be in terms of both financial and electrical benefits.

9.4 Instantaneous daily Production Vs Consumption for Upgraded System

As seen in previously sometimes it is not suffice to analyse the behavior of the system only in terms of the monthly energy yield. In order to gain a better understanding of the typical relationship between supply and demand it is required that the variation in production and consumption over the course of a typical day is observed. Like seen previously the average daily consumption and production profiles will now be assessed for each month throughout

the year. Again the average and the average $\pm 3\sigma$ values are observed in order to gain an appreciation of the possible variation in both production and consumption even throughout days of the same month. The traces for months, January through to December can be seen in the figures below.

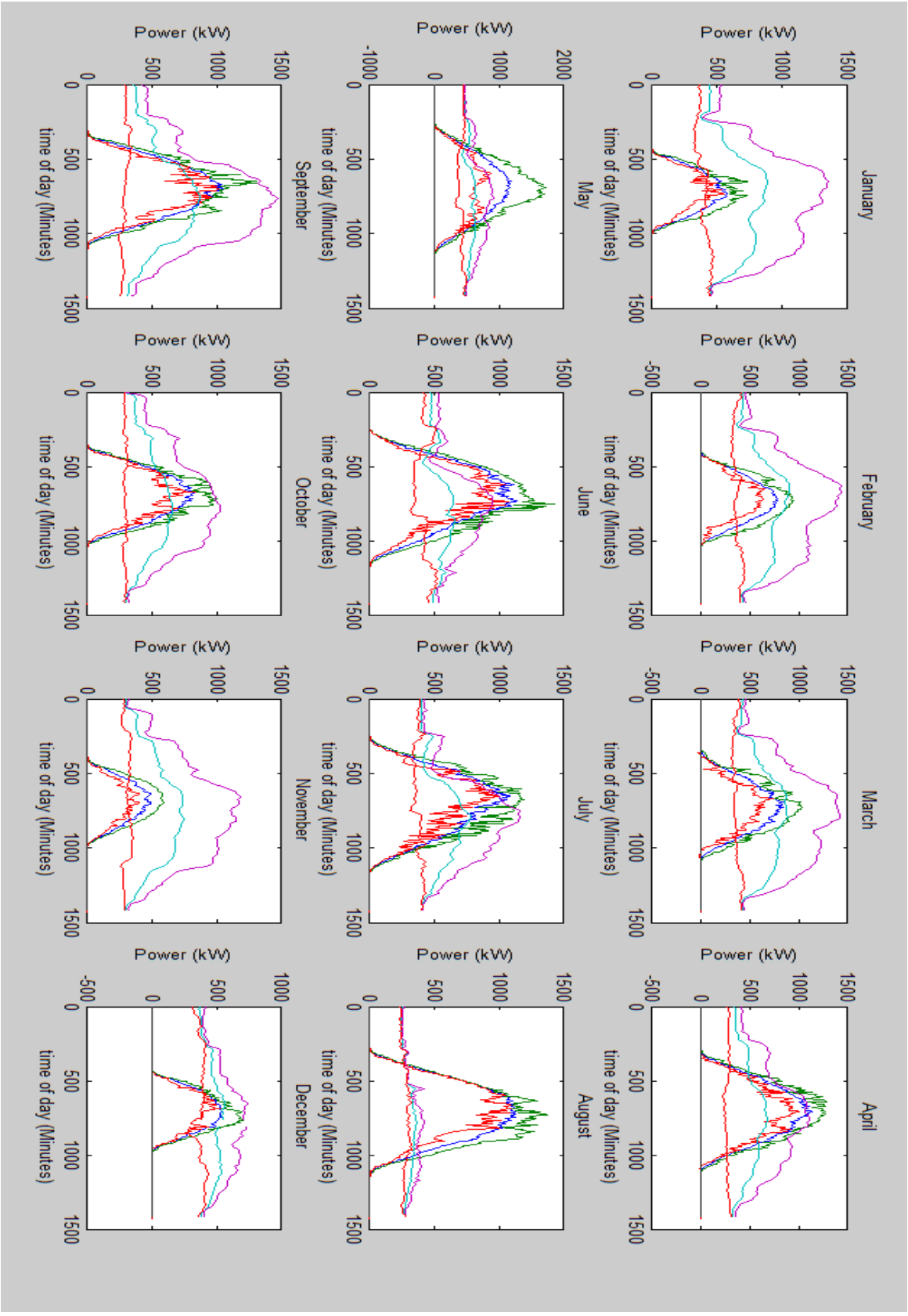

Figure 64: Monthly variation in average daily Production Vs consumption with new PV technology (No solar tracking).

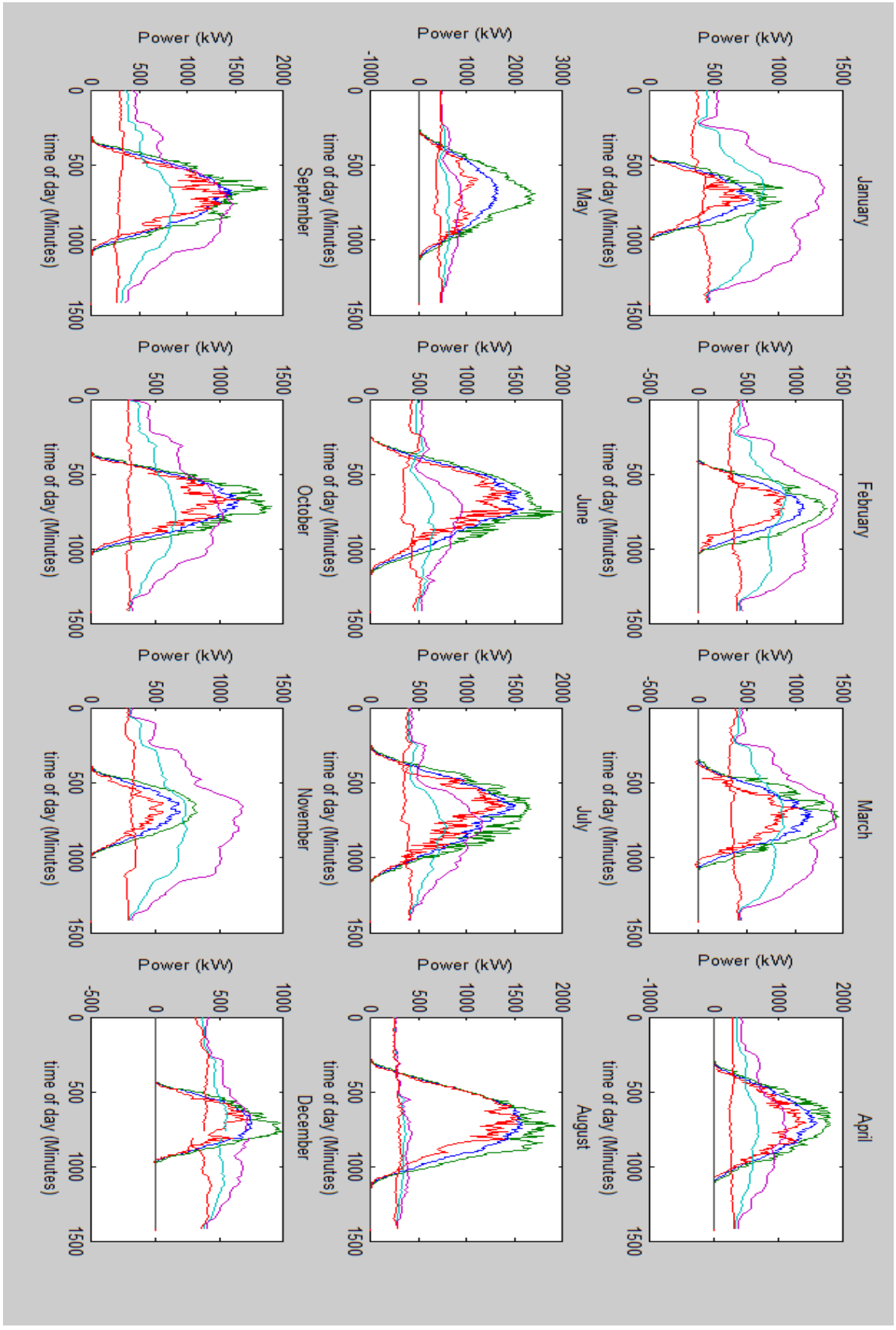

Figure 65: Figure 75: Monthly variation in average daily Production Vs consumption with new PV technology (solar tracking).

The Traces observed above can be used to draw some very clear conclusions regarding the both the production potential and consumption at the Montilivi campus. As can be seen here, with this newly upgraded system, due to the significant increase in efficiency the instantaneous power production has vastly increased at all points throughout the full year. It can be now seen that for many months of the year there exists large periods in the day where the production is in excess of consumption. In addition to this even for months where on average the production never exceeds consumption, the percentage of consumption which must be drawn from expensive grid based electricity has been reduced.

These trends will be very useful for analysing how best to utilise the power which has been produced. As can been seen here there exist periods in the day where production is zero and consumption is still relatively high corresponding to hours of darkness. Conversely there exist hours when production exceeds consumption .This data will be used to allow the parallel study to investigate the financial benefits of different utilisation methods including battery storage and direct exportation during hours of production excess. This analysis will be used in order to help provide insight into the financial feasibility of this system upgrade. As although reduced spending on electricity purchase and revenues from exportation may be significant, they may not be so significant so as to overcome the required capital investment within the expected lifetime of the system.

10. Achieving campus Self-sustainability for grid Independence

In the previous section it was seen that by utilising state of the art PV panel technology and dual axis solar tackers the monthly energy yields from the installation could be dramatically increased. With both technologies in place and the installation expanded across all possible roof area, it was seen that a maximum of 158% and a minimum of 28% of consumption could be accounted for by solar production. These values were observed in the months of August and January respectively. Whilst some months come very close, only 2 months throughout the year are capable of providing production in excess of the current consumption. In order to achieve grid independence and a campus capable of 100% Self-sustainability, other untapped sources of generation must be considered. Some of these potential methods will be discussed below.

10.1 expansion of PV over all campus land mass

As seen previously the current installation at the Montilivi campus consists of 96 fixed rack panels located on the roof of a small section of EPS P1. For this reason initial expansion only considered the idea of expanding over all available roof top surface area. There is however in fact much more university property which with slight alterations to the current infrastructure could be utilised in order to further enhance production, and thus move the campus ever closer to the possibility of grid independence. The primary source of university property which could be exploited in order to increase production would be car parking areas. Whilst the infrastructure at present is not currently capable of providing a means for extending the installation with relatively small investment, shelters could be added to the car parks capable of providing a base for mounting additional PV. Due to the extent of the land available, investment in shelters could be paid back as a consequence of energy savings or generation export within an acceptable time period. The available area for expansion will be summarized below. The following satellite image shows clearly university parking lots.

Figure 66: university parking areas satellite view. [60]

Figure 67: university car park areas with scale for mapping. [60]

Using the same simple geometric estimation seen in previous sections the total available land mass could be calculated.

$$\text{Total available area} = (50\times50) + (25\times30) + (60\times40) + (40\times50) + (70\times40)$$

$$= 10450m^2$$

Total panel coverage = $10450m^2 * 0.27 = 2821.5m^2$

Total number of panels = $2821.5 \div 1.63m^2 = 1731$

Adding this new potential installation capacity to that seen previously for the system expanded over the full Montilivi roof top area the following monthly energy yields were simulated in Matlab, for the cases both with and without solar tracking. Again the simulation error was adapted accordingly (see equations 16 & 17).

Table 16: Monthly variation in Energy consumption, production and SS% (full campus including car parks).

Month	Production no tracking kWh	Production with tracking kWh	Consumption kWh	Self-Sustainability % no tracking	Self-Sustainability % with tracking
January	130650.1422	182910.199	453436	28.81335893	40.3387025
February	176404.934	246966.9076	428356	41.18185201	57.65459281
March	229855.8434	321798.1807	463967	49.5414207	69.35798898
April	340422.5448	476591.5628	339822	100.1767234	140.2474127
May	409094.5894	572732.4251	393611	103.9337288	145.5072204
June	374902.603	524863.6443	402907	93.04941414	130.2691798
July	350279.2044	490390.8861	384953	90.99271972	127.3898076
August	384015.5833	537621.8166	242615	158.2818801	221.5946321
September	301420.8076	421989.1307	374022	80.5890583	112.8246816
October	227133.9383	317987.5136	365448	62.15219081	87.01306713
November	111834.5676	156568.3946	387750	28.84192588	40.37869623
December	127152.0625	178012.8875	456849	27.83240469	38.96536657
Annual	3163166.82	4428433.549	4693736	67.39123846	94.34773384

As can be seen above in table 18 both with and without solar tracking due to the increased number of panels the production throughout all months of the year is now capable of contributing a larger percent of the overall consumption. Even when averaged throughout the whole year, self-sustainability percentages of 65% and 91% can be observed. It is noted that there exist many months when production is in significant excess of consumption meaning that some form of battery storage may be useful in order to store this excess for use in less plentiful months. However, ultimately winter periods of low solar insolation and high consumption lead to an overall SS% less than 100%. Despite this, perhaps a more detailed investigation of the available rooftop area could allow for a higher overall percentage cover than the 27% elected previously. This increase in installation capacity may facilitate a breakthrough of the 100% Self-sustainability barrier seen in table 18.

The next section will assess the feasibility of utilising a different natural energy resource in the form of micro wind power. The primary reason here being to boost production in these low insolation periods and thus help the campus become self-sustainable, allowing for independence from the conventional electricity grid.

10.2 Micro-wind power installation feasibility analysis

As seen above, as a result of utilising the majority of viable university land for PV installations it is possible to almost achieve campus self-sustainability. However ultimately, winter periods of low solar insolation halt the system's ability to break the 100% barrier. One potential method to help overcome this is to combine solar with other renewable sources in order to provide a hybrid solution.

By using wind power alongside the solar array seen previously, winter periods of low insolation as well as period of autonomy such as hours of darkness could perhaps be utilised in order to enhance production. Before considering the hardware requirements and potential locations for this wind installation it was important to first analyse the wind resource available in the area and its variation throughout the year. This will be important as perhaps the wind available may be either insufficient for any installation at all, or perhaps too low as to produce sufficient enough energy to payback capital investment within a required time period. The later will be examined in the parallel financial investigation to this study.

Two important factors relating to the wind which must be considered are the local wind speed and direction respectively. Both of which are important for determining the size, axis type and orientation of the wind turbines. Seen in Table 19 are the maximum, minimum and average wind speeds and directions as recorded by the campus weather station for the 6 year period between 2009 and 2015. Table 20 and figure 68 represent a statistical break down of the monthly wind speeds throughout 2011 representing the average, maximum, minimum and quartile data.

Table 17: Local wind data from Montilivi weather station.

	Maximum	Minimum	mean
Wind speed m/s	13.96	0.309	1.180081
wind direction degrees	360	0	151.2573

Table 18: Local wind speeds breakdown from Montilivi weather station.

Month	1	2	3	4	5	6	7	8	9	10	11	12
Median	0.3320	0.7220	0.7210	0.5565	0.7100	0.7185	0.9810	0.7750	0.5790	0.3835	0.3290	0.3220
Quartile 1	0.3090	0.3090	0.3090	0.3090	0.3090	0.3110	0.3280	0.3110	0.3090	0.3090	0.3090	0.3090
minimum	0.3090	0.3090	0.3090	0.3090	0.3090	0.3090	0.3090	0.3090	0.3090	0.3090	0.3090	0.3090
maximum	11.6000	8.8100	12.5300	8.2800	10.7400	8.1900	7.9600	8.0100	6.3790	9.2400	7.4200	12.0400
Quartile 3	1.3180	1.9503	2.1315	1.8100	1.8520	1.8330	2.1120	1.9170	1.6830	1.6193	1.0195	0.9300

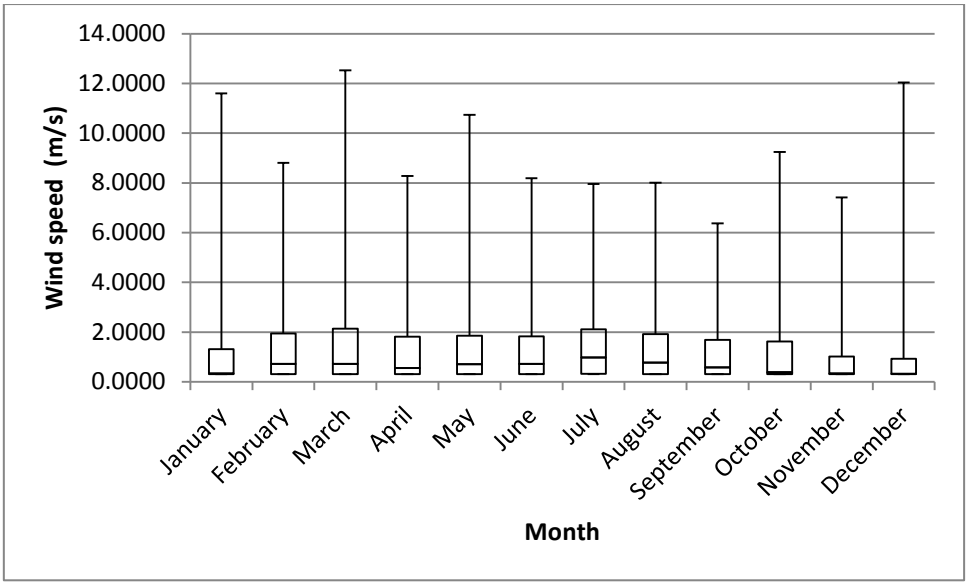

Figure 68: weather station wind speed boxplot [61]

As mentioned above the average wind speed at the intended sight is essential in determining the size of the installation. Small scale wind turbines are defined as those capable of producing anything in the range of 300 to 10,000 watts [62]. In order to provide a financially viable source of energy [63] claims that a minimum average speed of 5 m/s is required. This point is further backed up by the report seen in [64] which proposes technical hardware solutions for micro wind projects in areas with low average wind speeds. Even these special turbines specifically designed to cope with low wind speeds have zero output below 5mph (2.24m/s) as seen below.

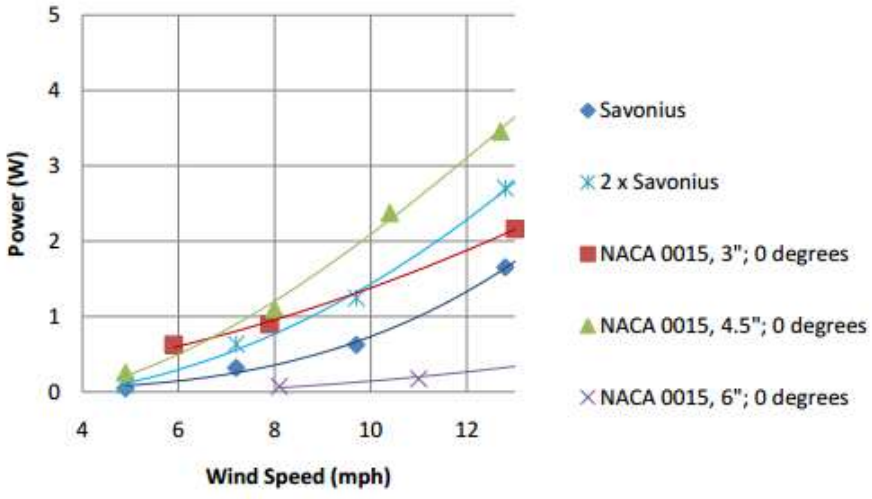

Figure 69: Power Vs Wind speed for small scale low speed turbines. [64]

Figure 68 and table 19 both show that for Girona the average wind speed is below this feasibility threshold. Figure 68 shows that for the local area wind speeds for 2011 varied between a maximum of roughly 12.5m/s in March and a minimum of roughly 0.3m/s throughout the year. However the average wind speed throughout the year is 1.18m/s over the 6 year period .The conclusion based on [63] and [64] is thus that the location may not be financially viable for the deployment of a small scale wind installation and perhaps a different method of increasing campus generation would be better considered.

10.3 Concentrated Photovoltaics

Having concluded that even after expanding over all possible campus rooftop areas (both those which exist at present and those which could be potentially constructed) it would still not be possible to achieve 100% campus self-sustainability, it was clear that an additional method of renewable production would have to be considered. In section 10.2 it was found that the wind resource available was not significant enough so as to prove financially beneficial, due to the low average wind speeds available throughout the year.

As seen previously however the solar resource available on site is significant. In fact it may even have been possible to reach this 100% SS mark with only the use of PV as important to remember is that a very conservative value for roof top percentage coverage was used based on the current installation. In fact, in reality perhaps many more panels could actually be installed allowing the 100% threshold to be passed. Nevertheless in order to try and combat the problem of limitation of available land mass a technology known as Concentrated PV could perhaps hold the answer. This section will outline the key advantages of this technology, how exactly it operates, any increases in yield which could be expected and its feasibility for the site under investigation here.

The basic principle of concentrated photovoltaics is that a large area of sunlight is focused using a standard optical device onto a small area. One benefit of this is that it reduces the amount of PV cells that are required for the same power output. This reduction in the amount of PV material required per Watt could prove beneficial for the case of UDG allowing higher yields to be achieved for the available land on site; so long as the concentrating equipment is suitable for the location and also doesn't take up large amounts of surface area. Outputs are further increased through the use of high efficiency Multijunction cells those properties are described in appendix 12.1. One downside to the technology is that unlike the standard PV seen previously which still provides some output for diffuse generation (during cloud cover), Concentrated PV requires direct sunlight to operate. This will potentially provide negative consequences in winter months which contribute greater proportions of cloud cover.

CPV systems can be further defined by their degree of concentration. This is the number of times higher the intensity of the light is than it would be in the absence of the concentrator [65]. The key differences between categories is summarised below, detailing the differences in hardware required for each. Also seen is a generic diagram for CPV system, although the exact architecture can take many different specific forms.

	Low concentration	Medium concentration	High concentration
Degree of concentration	2 - 10	10 - 100	> 100
Tracking?	No tracking necessary	1-axis tracking sufficient	Dual axis tracking required
Cooling	No cooling required	Passive cooling sufficient	Active cooling reuqired in most instances.
Photovoltaic Material	High- quality silicon		Multi-junction cells

Figure 70: Typical degrees of concentration. [65]

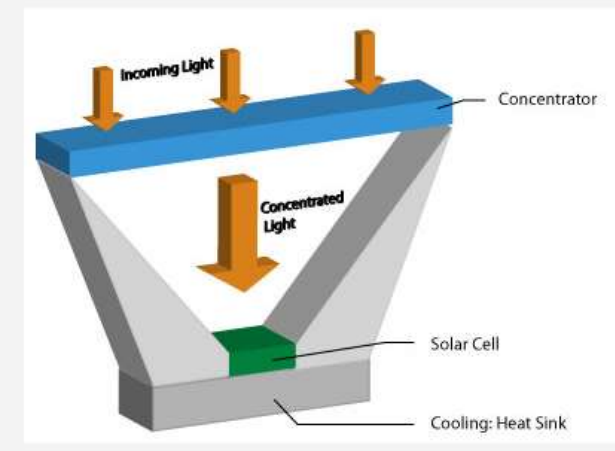

Figure 71: Key components in CPV systems. [65]

Some of the most common CPV architectures include the Fresnel lens, parabolic mirror, reflector and luminescent concentrator. A diagrammatic summary of the differences in these architectures can be seen below.

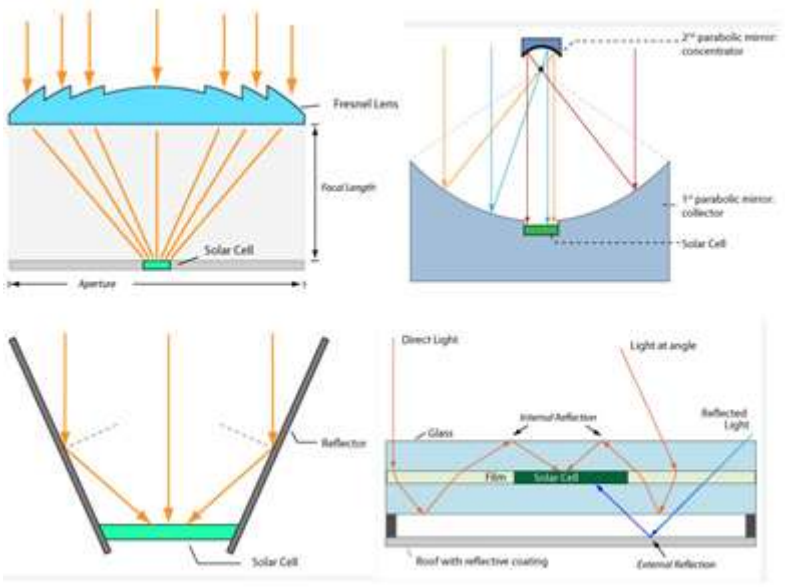

Figure 72: Fresnel, parabolic, reflector,and concentrator (reading left to right, top to bottom). [65]

Now that some of the typical architectures available within CPV systems have been seen, some examples of real life commercial installations will be observed in order to better understand the feasibility of such systems for the site available at the Montilivi campus.

Investigation into the market has shown that the deployment of CPV systems tends to be predominantly limited to large utility scale installations. This is predominantly down to the extremely high complexity, and initial costs of such systems. The largest system in 2011 was a 5MW installation in New Mexico USA, which made use of a Fresnel lens as seen above and complex Multijunction cells as seen in appendix 1. According to the NREL [67] around 471MW of CPV projects are now currently in development including a single 30MW installation in Colorado, requiring around 90.6 million pounds worth of investment. Despite even these anticipated significant increases in CPV deployment over the next few years, further increases and continued mass manufacturing will still be required in order for drive down the costs of this technology in order to make it competitive with traditional PV for smaller scale applications (Kurtz 2011 [67]).

From this it is possible to conclude that whilst in the future perhaps CPV could provide a cost effective solution for Grid independence at the Montilivi campus, there is sufficient evidence to suggest that at present for an installation of this scale traditional PV is more suitable. This is due to several different factors including the following. CPV systems require complex mechanisms which are not feasible for construction on the specific land available on sight (rooftops). Also high capital investment due to immaturity of the technology and size of the required installation are important considerations which enhance the opinion that a traditional PV system may be more suitable for the site proposed at the UDG. A comparative assessment of both PV and CPV technologies seen in [68] confirms this opinion stating that only for installations in excess of the 10MW does CPV become financially beneficial and also that the rooftop surface area on sight is not suitable for such an installation. A summary of these findings can be seen below.

Characteristics	PV	CSP
Use	Direct and diffuse sunlight	Direct sunlight
Size	from Watt to MW	10 MW to a few hundred MW
Installation:	everywhere (roof etc.)	flat unused land
Capacity:	700 – 2000 full load hours	2000 – 7000 full load hours
Reserve capacity:	External	Internal (fossil operation)
Proofed life time:	> 20 years	> 20 years
Annual production (2004)	>25 000 GWh	> 2 500 GWh
LEC (today)	0,20 – 0,35 €/kWh	0,15 – 0,25 €/kWh

Figure 73: PV Vs CPV. [68]

11. Conclusions, collaborations and Future work

In recent years the erratic nature of the energy market has been highlighted. Instability in energy prices and uncertainty over the long term future of fossil fuels have contributed to a surge in the uptake of PV energy projects. Factors such as concerns for the environment, government financial incentives, hardware cost reductions and advances in technology have further highlighted the attractiveness of such ventures for both large and small scale deployments. This report details through the use of a validated software model and an investigation into state of the art technologies, that using the rooftop surfaces available on the university campus, the UDG could dramatically reduce is spending on grid purchased electricity whilst at the same time reduce its carbon footprint. Investigation has shown that for certain months of the year without making any amendments to consumption at present, a fully expanded system would be capable of becoming the sole provider of electricity for the full campus. Additionally, in other months the proportion of grid purchased electricity could be greatly reduced. The findings of this report clearly show how typically the relationship between consumption and production on site varies throughout the day, these findings will be used by a parallel study which will assess economically how best to utilise the production on sight from this newly proposed system. Also assessed will be the financial feasibility of the upgrade in terms of financial savings over the expected life time of the system. Over this period, in order to justify the investment the combination of energy bill savings and grid export revenue must outweigh the required capital investment.

For the case of this investigation, case studies were carried out in order to examine how best to maximise production and also reduce consumption. Whilst the effects of updating to modern panel and dual axis tracking technologies were included for the updated system simulation, other methods of increasing generation as well as those for reducing consumption which were investigated were not included. These further methods of increasing production and reducing consumption can be seen below in appendices 1 and 2 respectively. Important to note is that these methods could propose massive increases in production and cost savings for the system at the UDG. Their inclusion in the model however would require the transition of these technologies through from the R&D stage to commercial products and also a significantly more detailed analysis of the exact loads used on sight to be carried out. Both of these areas would be interesting branches for future work relating to this project. However even without these further advances included in the campus design, the results were extremely positive in terms of the ability of the system to dramatically increase the self-sustainability of the campus.

This study provides an overview of the estimated potential PV capacity which the campus can accommodate based on the current installation and does not in fact consider in detail the exact nature of the rooftop surface area. Closer inspection of the sight could lead to far larger volumes of PV being able to be installed. Investigation of the exact rooftop areas available could unlock larger volumes of PV capacity for installation, far above the 27% estimate

adopted previously. This could be vital in allowing for the 100% self-sustainability barrier to be surpassed, making a closer analysis of the land mass a very interesting area for further studies relating to this project. Once the most efficient method of utilising the generation produced on site is known another area for potential instigation would be to propose a component level design of the system. This would be massively important in order to better understand the true initial financial costs of implementing this expanded system rather than very basic estimates based purely on the panel costs. Investigating in detail the heavy loads present at the campus could lead to the identification of any reasons for vast levels of consumption, with old inefficient technology and low levels of operational control likely to be the cause. Implementing a detailed system level investigation like that seen in appendix 2 would be another fantastic investigation to lead on from this in order to propose innovative ways of driving down campus consumption. This would be another hugely important stage in moving the campus ever closer to a self-sustainable future.

This investigation provides an insight into the magnitude of the universities consumption which could potentially be provided by PV on campus. It also provides essential data in order to assess the financial feasibility of such an upgrade. There remains however fantastic scope for further research into the proposal in order to better understand how to efficiently implement a system which could maximise the self-sustainability of the UDG campus, taking advantage of the fantastic solar resource available on sight.

12. Appendices

12.1 Appendix 1: future advances in PV investigation

12.1.1 Driving the trend in increased efficiency

It was seen previously in figure 54, over the past few decades there have been significant increases in the efficiency of commercial Solar panels with current state of the art technologies capable of producing efficiencies of around 22%. In recent years there have been a wide range of advances in research based technologies which are capable of producing efficiencies as high as 51% in 2013 [25]. Whilst at present some advances have not been concluded to be financially viable enough so as to be rolled out on a large scale these represent the exciting future in store for PV technologies. Detailed below are some areas of research which have led to the production of the high efficiency cells discussed above as well as some other technologies within the broader field of Photovoltaics.

12.1.2 Multijunction Photovoltaic Cells

In comparison to traditional PV cells which contain only one P-N junction fabricated using a single type of material, Multijunction cells contain multiple P-N junctions each created using different semiconductor materials. By increasing the number of P-N junctions within each cell it is possible to increase the percentage of incident sunlight which can be absorbed by the cell, thus increasing the efficiency. This is because cells with multiple different P-N Junctions can absorb light from a wider range of wavelengths; with each specific junction type dedicated to a specific range in the light spectrum. There exist both experimental lab based examples of this technology as well as some rare commercial applications both of which offer enhanced conversion efficiencies in the region on 30-44%. Commercial products have been limited to a few very specific applications including space based solar and also large scale concentrated PV. In the future large scale manufacturing is expected to drive down prices allowing for the technology to enter the wide scale commercial market more competitively.

The underlying principle behind the technology is as follows. Electrical current is generated when photons with energy greater than the band gap energy (conduction band – valence band energies) of the semiconductor material are incident on the P-N junction. This theory can be visualised on the band diagram seen below.

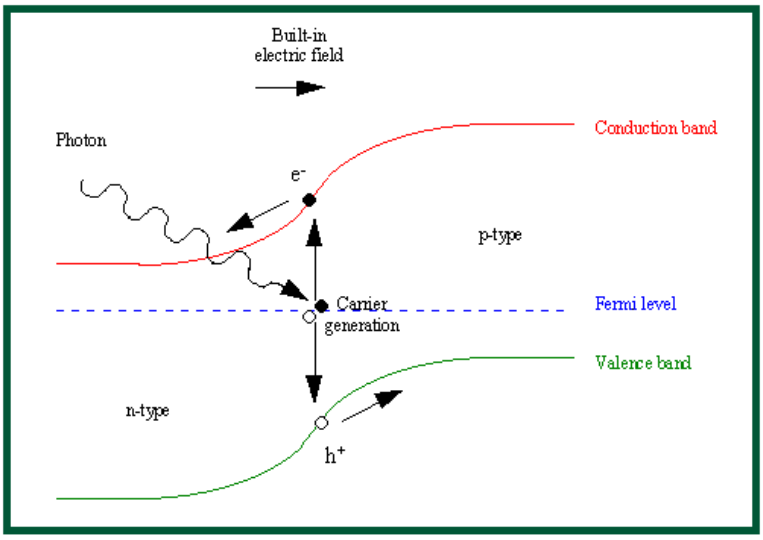

Figure 74: PV cell energy band diagram.[46]

Whilst there exist certain losses which cannot be overcome, leading to a fundamental efficiency limit for all solar cells there are many factors which can be mitigated. The Multijunction cell is one such method for removing these inefficiencies.

Consider the following scenarios. Suppose that the incident photons are of a wavelength such that their energy is less than that of the material band gap. In this case the photon is not absorbed and no current is produced. Conversely for photons with wavelengths such that the photon energy is greatly in excess of the band gap energy, this excess serves to produce no additional current and incident energy is effectively lost to heat which in fact further reduces cell efficiency. The consequence of both of the above is that for the one single material only a small portion of the suns incident wavelengths can be absorbed efficiently (or at all). This results in a dramatic decrease in the theoretical maximum efficiency. Multijunction cells aim to solve this problem though the use of multiple junction materials each with a different Bandgap. This allows certain wavelengths to be absorbed by each junction. The effect is to dramatically increase the maximum theoretical efficiency for the cells by increasing the overall range of wavelengths which may be absorbed. The cells are designed so as to have the multiple junctions' layers one on top of the other with decreasing bandgap as shown below. Each junction designated a specific section of the suns light spectrum.

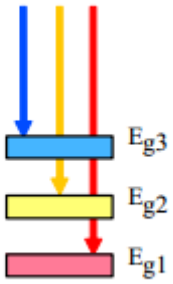

Figure 75: multijunction PV cell showing absorption of different wavelengths.[47]

The figure below shows an example of one of the earlier Multijunction diodes constructed in 2002. It consists of a 3 layer solar cell and was capable of producing efficiencies of around 34% under concentration [48]. Materials were chosen as to match band gap energies with the most predominant sections of the solar spectrum.

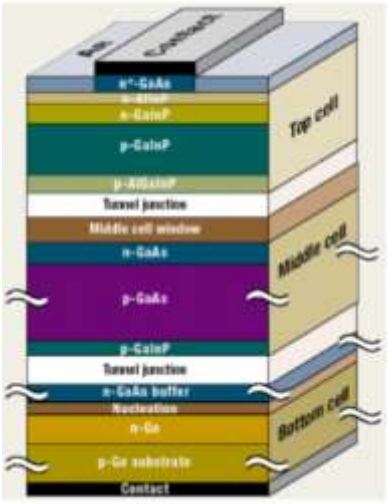

Figure 76:multijunction PV cell physical representation.[48]

In 2013 as a result of further developments in the technology this figure has further increased. Researchers at the California institute of technology recorded performance in the region of 51.8% using a 4 layer cell, greatly surpassing the previous record of 43.5%. These results show the massive potential of solar power in the future. For now however these technologies will remain predominantly for scientific applications until the manufacturing processes catch up with research allowing for mass production.

12.1.3 Textured Solar Cells

One major problem which can lead to decreased efficiency in PV applications is reflection. Reflection causes light which does have sufficient energy to produce electron hole pair to be reflected by the material surface, resulting in decreased short circuit current. This phenomenon can be seen below.

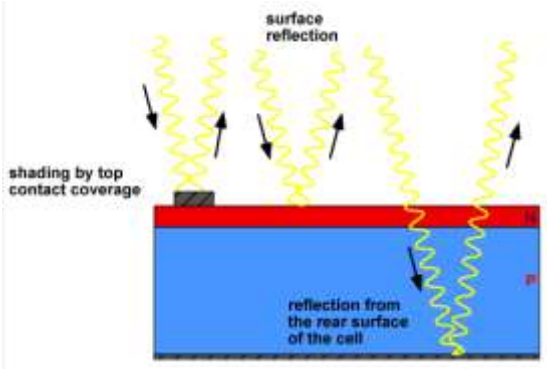

Figure 77:reflectionin PV cells.[49]

One method of reducing this problem is to manufacture cells with a textured surface. Surface texturing results in a larger percentage of the reflected photons being picked up by another surface as opposed to simply returning into the atmosphere. The figure below shows how using textured surfaces a smaller portion of the incident light will be reflected back, allowing for higher absorption and thus the creation of greater numbers of electron hole pairs.

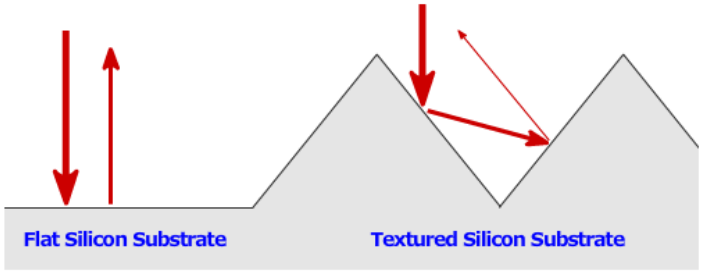

Figure 78: Textures cell theory graphical representation.[50]

The figure below shows a cross sectional image of the textured silicon as implemented by a team at the University of Seattle. The team were able to produce a 17% efficient single layer panel by utilising the geometric benefits discussed above.

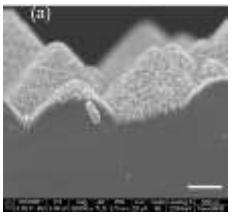

Figure 79: Textured PV cell surface.[51]

12.1.4 Lambertian Rear Reflector

This device uses a rear mirrors behind the solar cell in order to reflect light back onto the cell which would otherwise have been transmitted straight through the cell or absorbed by the metal contacts. This special type of rear reflector adds a random element to the direction of the reflected light. This increases the chance of absorption with reflected rays suffering total internal reflection being reflected once more but this time with a different angle of incidence. This behavior is visualised below along with the benefits of such a design. As can be seen using such a device can increase production for a given thickness of Silicon. The result being thus decreased cost for a given power output, a very important factor in PV installations. Important to note is that for thin film devices the benefits of the technology are increased due to more likely transmission through the cell.

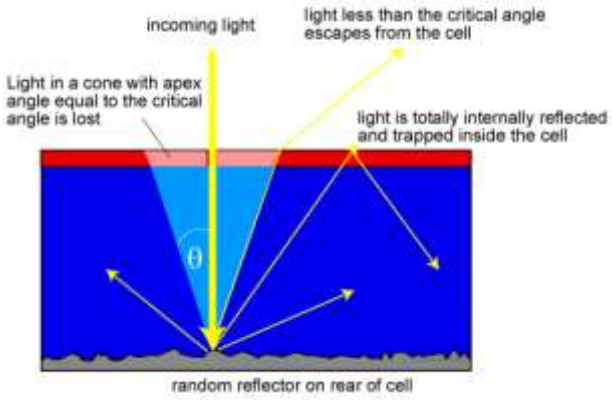

Figure 80: Lambertian Rear Reflector theoretical diagram.[53]

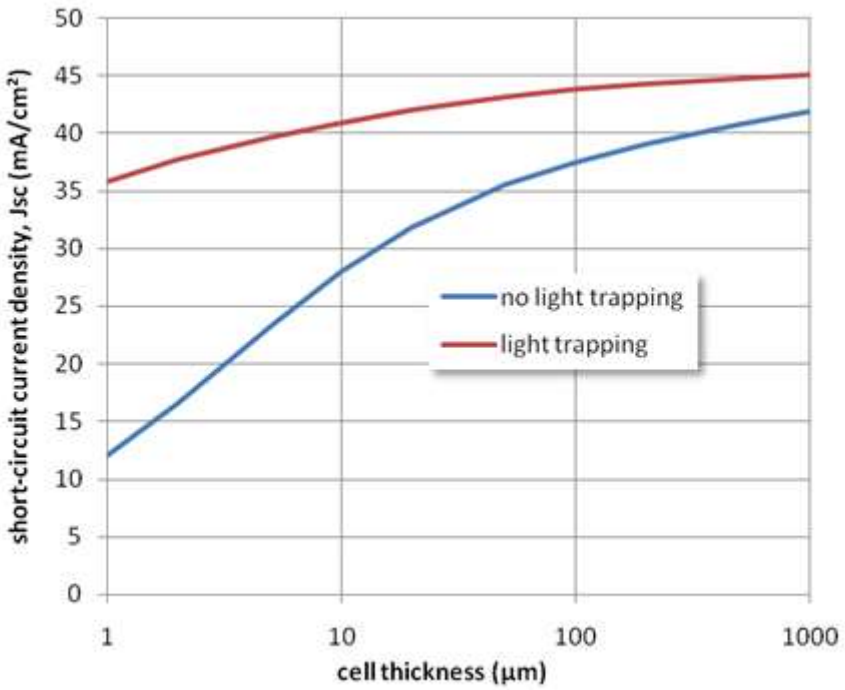

Figure 81: Benifits of Lambertian Rear Reflector.[53]

12.1.5 Anti-reflective coating

As we have seen previously, one major problem which leads to a reduction in PV cell efficiency is reflection. With bare silicon over 30% of incident light is reflected [54]. In addition to surface texturing as seen previously one other method which is commonly adopted to reduce this reflection coefficient is to apply what is known as an "anti-reflective coating". A dielectric coating of a specific thickness is applied such that the reflected waves from both the silicon and dielectric surfaces destructively interfere. The consequence is zero net reflected energy [54]. This principle can be seen graphically in figure 84 below.

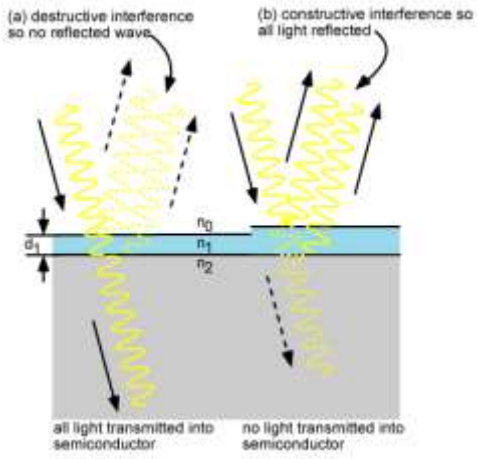

Figure 82: Constructive and deconstructive interference of reflected waves.[54]

Almost all modern panels utilise this technology and there have been a wide range of investigations into the benefits in terms of increase in panel efficiency which can be consequently achieved. The findings of two such studies are summarised below.

The first study conducted at the Hong Kong University of Technology and science (HKUTS) identifies and aims to correct two fundamental issues associated with traditional anti reflective coatings. These are that they typically only work for a small fraction of the solar spectrum and also because they are ineffective for light striking the cell at acute angles. This is often the case during hours close to sunrise and sunset. The team of researchers came up with an anti-reflective coating technology which effectively combines both AR coatings and also textured cells. By using the lithography process the team was able to apply a textured "silicone" coating to the cells. In using the lithography process they were able to ensure that the bumps in the texture were in the nanometre scale and thus the problem of dirt filling the cavities was avoided. This "silicone" layer; similar to the material used in the contact lenses, ensured that a larger fraction of the suns irradiance could be affected. At the same time the texturing solved the problem of acute angle rays. The results were extremely positive, with the reflection losses being halved [55]. The power output increased at all points during the day and an increase in daily energy yield of roughly 7% was observed. A graphical representation of the technology as well as a summary of the benefits can be seen below in figure 83.

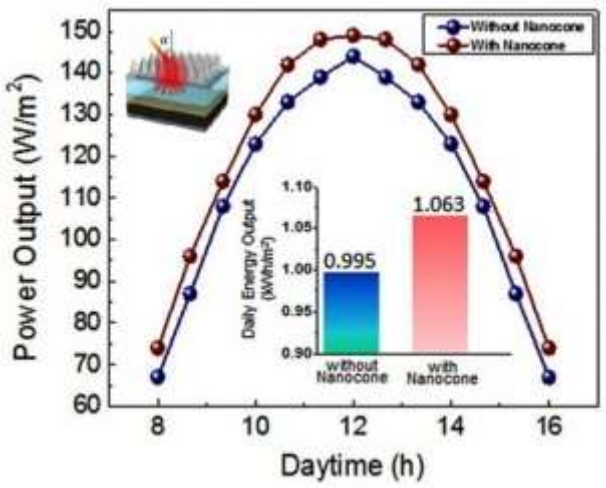

Figure 83: Power output benifits of AR technology developed at HKUTS.[55]

Using a different approach with utilises a multi-layered AR coating, the University of Loughborough was able to increase module efficiency by 4%. This increase in panel efficiency was achieved by reducing reflection by around 70% for all wavelengths in the solar spectrum commonly accepted by PV panels. The multilayer coating consisted of four alternate layers of zirconium oxide and silicon dioxide deposited using an inexpensive, well known method similar to that used in the manufacture of spectacles.

Both of the above case studies represent different ways in which the advances AR coatings can provide increases in efficiency for PV applications. Deployment of these developments within the commercial technologies of the future will result in further increases in panel efficiency, one of the key drivers for increasing global PV uptake.

12.1.6 Glass sphere concentrator

The majority of the methods seen previously in this section have aimed to improve efficiency either by geometric, material or manufacturing alterations. This is commonly the approach adopted by many researchers in the field; however there are sometimes slight variations from this. As seen previously there is a field known as concentrated photovoltaics (CPV) which uses mirrors and complex tracking systems with the aim of focusing the suns light in order to achieve greater power output with less PV material. These technologies are very expensive, heavy and complex and are typically limited to utility scale projects. A German researcher in 2014 however proposed an innovative and relatively low cost adaptation of the typical CPV model which utilises a water filled glass sphere in order to achieve increased efficiency. The sphere automatically focuses the light onto a cylindrical arm containing the PV cells which rotates throughout the day. This light, cheaper approach to CPV has been found to be capable of producing increases in cell efficiency of around 35% compared with an un-concentrated equivalent system [57]. A graphic of these spherical concentrators can be seen below.

Figure 84: Glass sphere concentrator physical representation.[57]

12.1.7 'Smartwire' interconnection technologies

This is a revolutionary new technology which claims to reduce cell costs whilst at the same time providing improvements in efficiency. The company claims that reductions in cost of around $0.25 per cell are possible by altering the way in which individual cells are connected. Typically millimetre wide silver bus bars located on the top of the cell are used to interconnect individual cells. Alternatively here, sheets of micrometre wide copper wires are used to make the connections. Whilst providing the same conducting properties as the previous approach. The cell now benefits from reduced shading and thus produces greater electrical power output. A graphic of this technology can be seen below. Seen here are multiple connection points between cells which again can lead to increases in cell performance via decreased resistance [58].

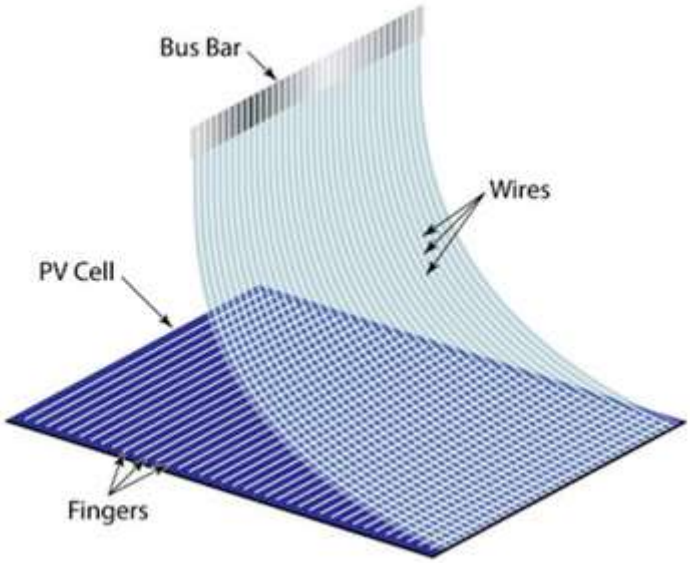

Figure 85: Smartwire technology physical representation.[58]

12.1.8 Solar Microinverter

Often not given much thought, however vitally important in all solar energy systems is the role the solar inverter. Whilst its primary role is to convert DC power produced by PV generation to AC power which can either be consumed or exported back to the grid, the inverters themselves play a hugely influential role in the quantity of power which can be extracted.

One Major advance in this field which has been made since the systems initial construction is the development of Microinverter technology. Whilst traditionally sections of series connected panels known as “strings” are connected to one single inverter; with Microinverters each individual panel has its own separate inverter. The benefits of this technology are very clear and very simple to understand. Consider the case as seen below in figure 55 where either a single panel or a group of panels within a full array have been shaded for some period.

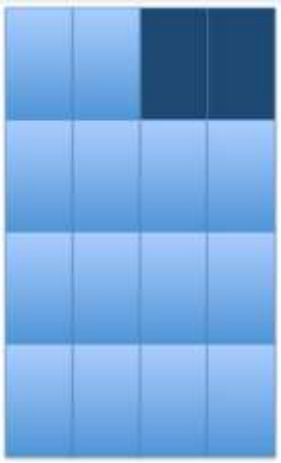

Figure 86: Pannel shading example.[25]

The main problem with the “string inverter” configuration as seen in the current UDG installation where relatively long sections of series connected panels are connected to a singular solar inverter is as follows. As seen previously connecting cells in series has the effect of increasing the overall voltage whilst maintaining the same current as for a single panel. Revisiting figure 86 what can be seen is 2 shaded panels within a larger array where the remainder is unaffected by shading. The current output from the shaded panels is reduced which results in the current output from the full series string also being reduced. Thus the performance of the full array is affected by the worst performer. However in adopting the Microinverter approach the consequences of any low performing modules due to shading or internal faults are limited to that panel with the remainder of the panels continuing to function at their maximum capacity.

In addition to this there is also another issue associated with the “string inverter” configuration which Microinverter technology helps to mitigate. Again considering the case seen in figure 86 where different panels within an overall array are subject to different levels

of irradiance the following can be understood. As seen in previous sections, different levels of irradiance and temperature lead to different operating points where the maximum power can be extracted. The Maximum power point tracking process is carried out by the solar inverter. Thus for "string inverter" configurations this operating point can only be varied for the full string and not for each individual panel. Therefor if conditions instantaneously change for one panel due to shading the inverter can only see the overall change for the full string. In making this observation the operating point will be adjusted. This adjustment now averaged across the full string is likely not only to be insufficient to make the appropriate change for the shaded panel but also implements change to the unshaded panels which required no change in operating point. Using inverters for each panel allows the maximum power operating point to be monitored on an individual basis ensuring that each panel will always be operating to its maximum potential. This can result in significant increases in energy yield.

All of the above research areas represent ways in which the advances are being made in Photovoltaics. Advances which when further developed and mass deployed will ensure that PV efficiency further increases. A combination of this alongside the reduction in manufacturing costs will see the financial benefits of solar become ever greater, making solar an even more feasible option for energy production on a wide range of scales. These advances and the consequent increases potential power output will make a system, like that proposed for the Montilivi campus even more of an attractive venture in the future.

12.2 Appendix 2: methods of reducing campus consumption investigation

Previously it was possible to observe how both the production and consumption on site varied throughout the day. One major issue which often power distribution and transmission companies have to deal with is demand side management, which relates to the aligning of periods of high demand with those of high generation. This can be a very challenging task, and in recent years the idea of smart metering and cash incentives for purchasing during low demand periods have been proposed to solve the issue. Fortunately in the case of the PV installation at the UDG campus, periods of maximum demand fall perfectly in line with those of high consumption, meaning very little alterations are required to the consumption behavior in order to maximise efficiency. What must instead be examined are possible methods to drive down the base level consumption at the university and also potential methods of decreasing the rise in consumption during peak hours.

In previous sections, detailed have been some of the key advances which have been made in technology relating to PV generation in the last decade. What must also now be considered are changes which could be made at the university in order to reduce consumption. In recent years there have been many fantastic examples across the globe of innovative changes made to university campuses in order to reduce electricity consumption, some of which showing

fantastic results. This section will analyse a few specific case studies in order to determine the level of consumption reduction which is likely to be able to be achieved at the Montilivi campus.

12.2.1 Cornell University, Green Campus

Since 1997 the University of Cornell in the United States has pioneered the concept of Campus environmental sustainability. A whole range of projects have been introduced throughout all fields relating to the reduction of carbon footprint and increasing energy efficiency. Some of the key areas include, waste, water, transportation, food, land and most important off all for this investigation; Energy both conservation and generation. A range of the key initiatives which have been introduced are detailed below.

Initiative 1: BACS

The university has installed a complex microprocessor based system referred to as "BACS": Building automation and control system. The system carries out a wide variety of roles including metering, monitoring, control and automation. Some of the key university systems which work in conjunction with the BACS system include: heating, ventilation, air conditioning, refrigeration, lighting, smoke control and elevators. Using this reliable information regarding building performance, the university is effectively able to pinpoint any inefficiency and then mitigate such issues using the BACS control and automation features. Some areas where inefficiencies were removed can be seen below, along with the percentage reduction achieved.

Initiative 2: Fume hood hibernation

The university has introduced what is known as "Fume hood hibernation technology" which allows laboratory fume hood's exhaust flow to be dramatically reduced when not in use. Controlled by the BACS software discussed previously, allows for both long and short term shutdowns as well as quick revival times permitting on demand use during periods when laboratories are normally out of use. University studies have shown that as a result of automated shut down periods such as weekends and university holidays, the energy consumption associated with this technology can be reduced by up to 40% representing significant savings in energy consumption when extrapolated across all campus laboratories [35].

Initiative 3: Langmuir chiller replacement

Within one of the university campus buildings, specifically the Langmuir Lab the air conditioning system was replaced by new equipment fitted with capacity control allowing the new system to operate in conjunction with BACS as discussed previously. A Statistical breakdown of some of the benefits of this system can be seen below.

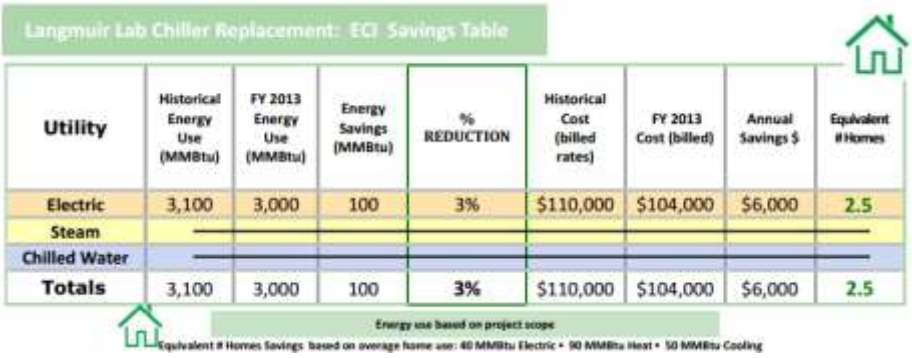

Langmuir Lab Chiller Replacement: ECI Savings Table

Utility	Historical Energy Use (MMBtu)	FY 2013 Energy Use (MMBtu)	Energy Savings (MMBtu)	% REDUCTION	Historical Cost (billed rates)	FY 2013 Cost (billed)	Annual Savings $	Equivalent # Homes
Electric	3,100	3,000	100	3%	$110,000	$104,000	$6,000	2.5
Steam								
Chilled Water								
Totals	3,100	3,000	100	3%	$110,000	$104,000	$6,000	2.5

Energy use based on project scope

Equivalent # Homes Savings based on average home use: 40 MMBtu Electric + 90 MMBtu Heat + 50 MMBtu Cooling

Figure 87: Air conditioning system upgrade related savings.[36]

Initiative 4: Air handling upgrade

This project involved an upgrade to the Malott hall air handling system. Previous inefficient piping arrangements had led to simultaneous heating and cooling resulting in decreased system efficiency. Along with rearranging of piping networks, automatic control via the BACS system allowed for the system to be managed according to building occupancy. The benefits of such alterations can be again seen below.

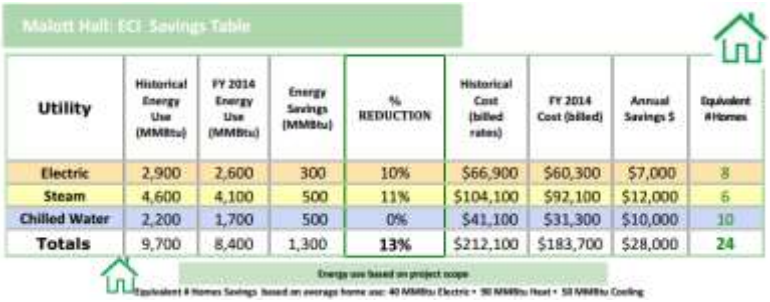

Malott Hall: ECI Savings Table

Utility	Historical Energy Use (MMBtu)	FY 2014 Energy Use (MMBtu)	Energy Savings (MMBtu)	% REDUCTION	Historical Cost (billed rates)	FY 2014 Cost (billed)	Annual Savings $	Equivalent # Homes
Electric	2,900	2,600	300	10%	$66,900	$60,300	$7,000	8
Steam	4,600	4,100	500	11%	$104,100	$92,100	$12,000	6
Chilled Water	2,200	1,700	500	0%	$41,100	$31,300	$10,000	10
Totals	9,700	8,400	1,300	13%	$212,100	$183,700	$28,000	24

Energy use based on project scope

Equivalent # Homes Savings based on average home use: 40 MMBtu Electric + 90 MMBtu Heat + 50 MMBtu Cooling

Figure 88:Air handling system upgrade related savings.[37]

Initiative 5: Mann library ventilation alteration

Alterations were made to a sequence of operations to allow for both enhanced demand and temperature control. Again utilising the remote monitoring and control the levels of outdoor air entering the building was able to be dynamically controlled. Whilst requiring high levels of capital investment of around £840,000 the benefits of the upgrade seen here are significant as can be seen in figure 89, resulting in a relatively short payback period.

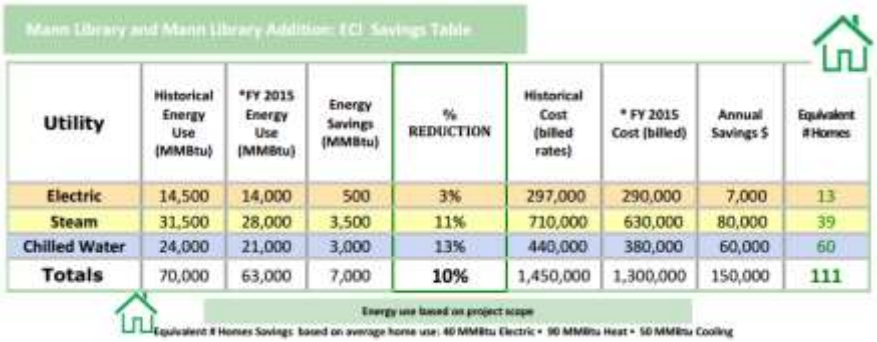

Mann Library and Mann Library Addition: ECI Savings Table

Utility	Historical Energy Use (MMBtu)	*FY 2015 Energy Use (MMBtu)	Energy Savings (MMBtu)	% REDUCTION	Historical Cost (billed rates)	* FY 2015 Cost (billed)	Annual Savings $	Equivalent # Homes
Electric	14,500	14,000	500	3%	297,000	290,000	7,000	13
Steam	31,500	28,000	3,500	11%	710,000	630,000	80,000	39
Chilled Water	24,000	21,000	3,000	13%	440,000	380,000	60,000	60
Totals	70,000	63,000	7,000	10%	1,450,000	1,300,000	150,000	111

Energy use based on project scope

Equivalent # Homes Savings based on average home use: 40 MMBtu Electric • 90 MMBtu Heat • 50 MMBtu Cooling

Figure 89:Ventelation system upgrade related savings.[38]

Initiative 6: Wilson lab Lighting

The university Physics department controls a large synchrotron located within an extensive tunnel network. Previous lighting controls required that lighting remained on 24 hours of the day. A new control system was implemented ensuring that lighting remained on only during periods of synchrotron operation reducing this percentage to 50%. With relatively low investment in control alteration, significant consumption and financial savings could be made as seen below.

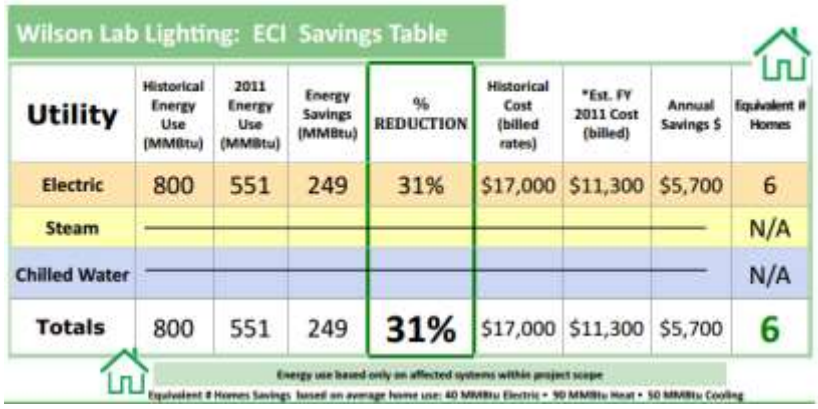

Wilson Lab Lighting: ECI Savings Table

Utility	Historical Energy Use (MMBtu)	2011 Energy Use (MMBtu)	Energy Savings (MMBtu)	% REDUCTION	Historical Cost (billed rates)	*Est. FY 2011 Cost (billed)	Annual Savings $	Equivalent # Homes
Electric	800	551	249	31%	$17,000	$11,300	$5,700	6
Steam								N/A
Chilled Water								N/A
Totals	800	551	249	31%	$17,000	$11,300	$5,700	6

Energy use based only on affected systems within project scope

Equivalent # Homes Savings based on average home use: 40 MMBtu Electric • 90 MMBtu Heat • 50 MMBtu Cooling

Figure 90: Lab lighting savings summary. [40]

Initiative 7: Ries Tennis centre lighting

Like with initiative 6, this project again was related to reduction consumption through lighting alterations. Unlike number 6 where it was simply the control of the lighting hours that was altered here the lighting technology used was also changed. The roof of the tennis centre was opened up to allow for more natural (direct) light. A combination of this alongside automatic light level sensing equipment and highly efficient multi-level fluorescent lights allowed for indirect lighting levels to be reduced when not required. This new system is capable of providing double the light intensity at full brightness. At periods of the day when natural light is abundant, lighting can be dimmed to 50 or 0 percent representing significant reductions in consumptions. The vast benefits of this upgrade can again be seen below.

Reis Tennis Center: ECI Savings Table

Utility	Historical Energy Use (MMBtu)	FY 2011 Energy Use (MMBtu)	Energy Savings (MMBtu)	% REDUCTION	Historical Cost (billed rates)	FY 2011 Cost (billed)	Savings $	Equivalent # Homes
Electric	2,312	968	1,344	58	$67,750	$28,250	$39,500	34
Gas	2,289	2,305	(16)	(1)	$27,500	$27,500	(192)	.1
Chilled Water								NA
Totals	4601	3273	1328	29	95,250	55,750	39,500	67

Figure 91: Tennis centre lighting savings summary.[39]

Summary of energy conservation

The initiatives listed above are just a few of the long list of conservation projects implemented across the campus. The above projects represent the various methods in which savings in energy consumption can be made across university campuses. These savings have been seen to come across a wide range of systems from lighting to heating systems. The complete list of projects can be found on the Cornell green campus website referenced at [34]. All of these projects were completed under what is referred to as phase one of the Energy Conservation Incentive (ECI) program which is due for completion later this year, leading onto the second phase. A summary of the benefits of these energy saving incentives can be seen below, where the university is shown to have kept a constant energy profile despite expanding headquarters by over one million square feet.

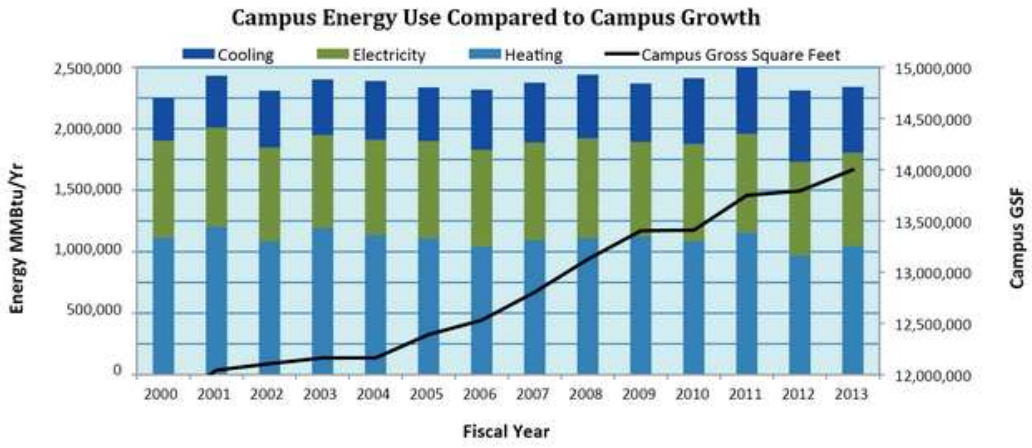

Figure 92: Campus area growth Vs Energy consumption.[41]

Cornell state that the range of retrofits, replacements, atomization and control projects introduced under phase one of the ECI phase one are expected to reduce the utility costs by over $3 million per year by 2016. With $33 million dollars allocated to projects during ECI

phase one this proposes a payback period of around 10 years. Well within the realms of what is considered to be acceptable. Investigating the range of systems used in the Montilivi campus for heating, lighting, ventilation etc. would be a very interesting study to carry on from this project. In knowing the exact hardware used and assessing the inefficiencies, new processes like those mentioned above could be proposed and the potential consumption reduction assessed.

12.2.2 Greening university campus buildings by Nader Chalfoun

This paper describes multiple methods of "greening university" campuses guilty of vast levels of air pollution, resource depletion, water consumption and of most interest to this investigation energy consumption. More specifically the university under examination here is the University of Arizona. In this study the initial university consumption was obtained through both simulation and utility bills. The results of these can be seen below.

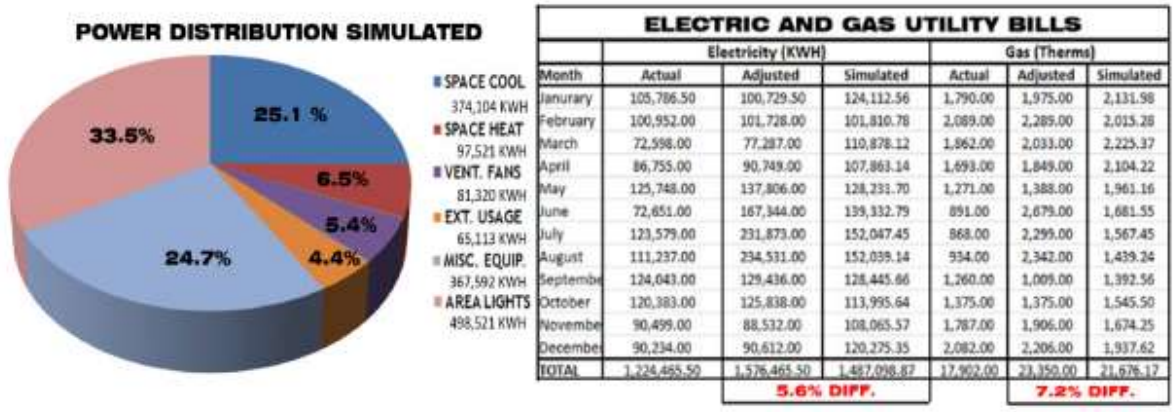

ELECTRIC AND GAS UTILITY BILLS

	Electricity (KWH)			Gas (Therms)		
Month	Actual	Adjusted	Simulated	Actual	Adjusted	Simulated
January	105,786.50	100,729.50	124,112.56	1,790.00	1,975.00	2,131.98
February	100,952.00	101,728.00	101,810.78	2,089.00	2,289.00	2,015.28
March	72,598.00	77,287.00	110,878.12	1,862.00	2,033.00	2,225.37
April	86,755.00	90,749.00	107,863.14	1,693.00	1,849.00	2,104.22
May	125,748.00	137,806.00	128,231.70	1,271.00	1,388.00	1,961.16
June	72,651.00	167,344.00	139,332.79	891.00	2,679.00	1,681.55
July	123,579.00	231,873.00	152,047.45	868.00	2,299.00	1,567.45
August	111,237.00	234,531.00	152,039.14	934.00	2,342.00	1,439.24
Septembe	124,043.00	129,436.00	128,445.66	1,260.00	1,009.00	1,392.56
October	120,383.00	125,838.00	113,995.64	1,375.00	1,375.00	1,545.50
Novembe	90,499.00	88,532.00	108,065.57	1,787.00	1,906.00	1,674.25
Decembe	90,234.00	90,612.00	120,275.35	2,082.00	2,206.00	1,937.62
TOTAL	1,224,465.50	1,576,465.50	1,487,098.87	17,902.00	23,350.00	21,676.17
		5.6% DIFF.			7.2% DIFF.	

Figure 93: Initial university energy consumption.[43]

After carrying out several different physical audits on the university campus building the following areas were concluded to be the key design issues leading to building inefficiency [43].

- Inefficient window and glazing systems.
- Poor insulation, both roof and wall.
- Building air leaks.
- Insufficient use of natural light.
- Dark, heat absorbing exterior colours.
- Exterior lighting running throughout day.
- No sets backs in thermostat.
- No window shading for periods of high temperature and sunlight.

- Over exposure of rooftop cooling systems.

By optimizing each of the design efficiencies above and re- running the initial simulation the increases in efficiency and financial savings for each individual change could be examined. The results from these optimizations can be seen below.

Replacement of inefficient rooftop heat pump systems

- Annual Energy savings : 206899kWh
- Annual financial savings: $15724

Figure 94: Heat pump replcement benifits summary.[43]

Installation of automatic light sensors and high efficiency bulbs to utilise natural daylight

- Annual Energy savings : 43417kWh
- Annual financial savings: $3299

Figure 95: Light sensors benifits summary.[43]

Solar pre heating of hot water

Important to note is that in this case it was a gas boiler system being used so savings were in terms of British thermal units, MMBTU rather than kWh as have been seen previously.

- Annual Energy savings : 2000MMBTU
- Annual financial savings: $21000

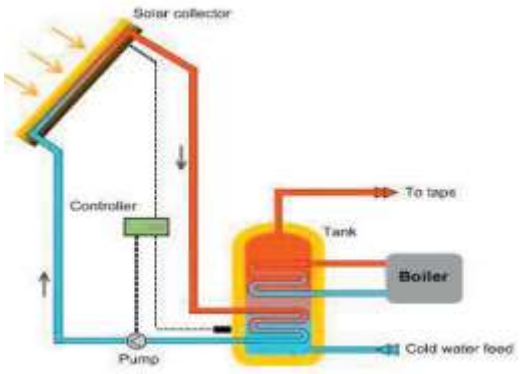

Figure 96: solar heating system diagram.[43]

Conclusions from case studies

As can be seen from both the large scale investment at Cornel and the smaller scale changes made in Arizona it is possible to significantly reduce the energy consumption of large university campuses. Previously in this investigation, it has seen how the benefits expanding and upgrading the existing solar installation at the Montilivi campus could provide significant reductions to the level of expensive grid electricity needed to be purchased. This study shows

how in fact consumption can also be greatly reduced in order to further help move the campus towards a fully sustainable future. Whilst this investigation is primarily focused on production, the potential consumption reduction which could be achieved at the UDG is another area for penitential investigation in the future.

13. References

http://pveducation.org/pvcdrom/solar-cell-operation/open-circuit-voltage [1]

http://www.amsolar.com/home/amr/page_164 [2]

http://www.mathworks.com/matlabcentral/fileexchange/46108-solar-photovoltaic-panel [3]

http://electronics.stackexchange.com/questions/23390/how-do-i-define-solar-irradiance-in-the-context-of-a-solar-cell [4]

http://sargosis.com/articles/science/how-shade-affects-a-solar-array/ [5]

http://www.pveducation.org/pvcdrom/properties-of-sunlight/solar-radiation-on-tilted-surface [6]

http://www.mathworks.com/matlabcentral/fileexchange/31305-simple-solar-cell-and-panel-model [7]

http://www.solar-facts.com/panels/panel-wiring.php [8]

http://pveducation.org/pvcdrom/solar-cell-operation/effect-of-temperature [9]

http://www.sustainabilityoutlook.in/content/want-buy-solar-panel-%E2%80%93-key-things-be-considered [10]

http://da.wikipedia.org/wiki/Maximum_power_point_tracker#mediaviewer/File:I-V_Curve_MPP.png [11]

http://www.hws.edu/fli/pdf/sma_brochure.pdf [12]

http://www.oksolar.com/pdfiles/Solar%20Panels%20bp_sm160.pdf [13]

http://calcscience.uwe.ac.uk/w2/am/ExcelTuts/ExcelDataUncert.htm [14]

http://smallbusiness.chron.com/making-normal-curve-excel-73850.html [15]

http://pveducation.org/pvcdrom/modules/nominal-operating-cell-temperature [16]

http://en.wikipedia.org/wiki/Maximum_power_point_tracking [17]

http://www.ni.com/white-paper/8106/en/[18]

http://www.seia.org/research-resources/solar-market-insight-report-2014-q4 [19]

http://cleantechnica.com/2014/04/13/world-solar-power-capacity-increased-35-2013-charts/ [20] global pic

http://cleantechnica.com/2014/02/06/technological-advancements-drove-solar-panel-prices/ [21]

http://www.sunpower.com.au/why-sunpower/high-efficiency-solar-technology/ [22]

http://us.sunpower.com/sites/sunpower/files/media-library/data-sheets/ds-x21-series-335-345-residential-solar-panels-datasheet.pdf [23]

http://eu-solar.panasonic.net/fileadmin/user_upload/downloads/technical_documents/VBHN245SJ25_PEWEU_EN.pdf [24]

http://greencomplianceplus.markenglisharchitects.com/technical/solar-technology-whats-state-art/ [25]

http://en.wikipedia.org/wiki/Solar_micro-inverter [26]

http://www.slideshare.net/harshi1990/solar-tracker [27]

http://en.wikipedia.org/wiki/Solar_tracker [28]

http://www.civicsolar.com/sites/default/files/documents/ati-wattsun-duratrack-da-datasheet-144329.pdf [29]

http://www.civicsolar.com/sites/default/files/documents/wattsun-duratrack-hzsr-datasheet-147626.pdf [30]

http://en.wikipedia.org/wiki/Solar_cell_efficiency [31]

http://physics.stackexchange.com/questions/38270/why-is-the-solar-noon-time-different-every-day [32]

http://www.all-science-fair-projects.com/print_project_1091_96 [33]

http://www.sustainablecampus.cornell.edu/ [34]

http://www.sustainablecampus.cornell.edu/pages/modal-fume-hood-hibernation[35]

http://energyandsustainability.fs.cornell.edu/file/Langmuir-Chiller-Replacement.pdf [36]

http://energyandsustainability.fs.cornell.edu/file/Malott%20Hall.pdf [37]

http://energyandsustainability.fs.cornell.edu/file/Mann.pdf [38]

http://energyandsustainability.fs.cornell.edu/file/Reis_Cons_Proj_Summary2012.pdf [39]

http://energyandsustainability.fs.cornell.edu/file/Wilson%20Lab%20Lighting.pdf [40]

http://energyandsustainability.fs.cornell.edu/em/projsum/default.cfm [41]

http://www.sustainablecampus.cornell.edu/initiatives/energy-conservation [42]

http://ac.els-cdn.com/S1878029614000371/1-s2.0-S1878029614000371-main.pdf?_tid=0a5f8412-b6b3-11e4-9713-00000aab0f26&acdnat=1424184261_141fee46bd75683ad6d5b6c3e7e425eb [43]

http://en.wikipedia.org/wiki/Multijunction_photovoltaic_cell [44]

http://pveducation.org/pvcdrom/pn-junction/band-gap [45]

http://www.liv.ac.uk/renewable-energy/about/staff/ken-durose/[46]

http://www.uotechnology.edu.iq/eretc/books/NRELokok.pdf [47]

http://phys.org/news/2013-02-multijunction-solar-cell-efficiency-goal.html [48]

http://www.pveducation.org/pvcdrom/design/optical-losses [49]

http://www.pveducation.org/pvcdrom/design/surface-texturing[50]

http://www.opticsinfobase.org/view_article.cfm?gotourl=http%3A%2F%2Fwww%2Eopticsinfobase%2Eorg%2FDirectPDFAccess%2FF2191863-A37E-C187-D866F7DDE1C12C07_300542%2Foe-22-S6-A1422%2Epdf%3Fda%3D1%26id%3D300542%26seq%3D0%26mobile%3Dno&org [51]

http://www.nrel.gov/docs/fy11osti/50707.pdf [52]

http://www.pveducation.org/pvcdrom/design/lambertian-rear-reclectors [53]

http://www.pveducation.org/pvcdrom/design/anti-reflection-coatings[54]

http://www.solarchoice.net.au/blog/news/new-silicone-based-ar-coating-promises-7-higher-pv-energy-output-180214/[55]

http://www.solarchoice.net.au/blog/news/ar-coating-improves-module-efficiency-4pc-300414 [56]

http://www.solarchoice.net.au/blog/news/glass-sphere-concentrator-creative-solution-improving-solar-pv-efficiency-210514 [57]

http://www.solarchoice.net.au/blog/news-smartwire-cell-interconnection-technology-manufactured-poland-240614 [58]

https://www.google.es/maps/search/montilivi+campus/@41.9672854,2.8053731,14z/data=!3m1!4b1 [59]

https://www.google.es/maps/search/montilivi+campus/@41.962232,2.8305738,592m/data=!3m1!1e3 [60]

https://weatherspark.com/averages/32032/Girona-Girona-Costa-Brava-Cataluna-Spain [61]

http://en.wikipedia.org/wiki/Small_wind_turbine [62]

http://www.goodenergy.co.uk/generate/choosing-your-technology/home-generation/wind-turbines/wind-turbine-faqs [63]

http://kb.osu.edu/dspace/bitstream/handle/1811/45531/Hayes_Proceedings_Paper.pdf [64]

http://www.greenrhinoenergy.com/solar/technologies/pv_concentration.php [65]

http://www.zytech.es/viewall.asp?bigid=54&smallid=84 [66]

http://www.nrel.gov/docs/fy12osti/51137.pdf [67]

http://www.geni.org/globalenergy/research/review-and-comparison-of-solar-technologies/Review-and-Comparison-of-Different-Solar-Technologies.pdf [68]